UNIVERSITY OF THE
WITWATERSRAND,
JOHANNESBURG

A Technical and Economic Comparison of Wet Milling versus Dry Milling (Vertical Roller Mill)

C Swart

A Technical and Economic Comparison of Wet Milling versus Dry Milling (Vertical Roller Mill)

MSc (50/50) Research Report

by

C Swart (1776130)

A dissertation submitted to the Faculty of Engineering and the Built Environment University of the Witwatersrand, Johannesburg, South Africa, in fulfillment of the requirements for the Degree of Master of Science in Engineering

September 2020

Declaration

I declare that this Research Report is my own work. It is being submitted for the Degree of Master of Science in Engineering (Metallurgical) to the University of the Witwatersrand, Johannesburg. This work has neither been submitted previously for the award of any degree, nor in a meeting examination requirement, at any other university.

_____

Cara Swart

Abstract

Stringent SO_2 emission regulations have placed immense pressure on coal-fired power plants to desulfurize exhaust flue gas. Wet Flue Gas Desulfurization (WFGD), using limestone with forced oxidation (LSFO), is a common FGD process where limestone reacts with SO_2 to produce gypsum ($CaSO_4.2H_2O$). Eskom's Kusile Power Station (Kusile) receives high-grade limestone (96% $CaCO_3$) from Idwala Lime's Danielskuil mine site at a top size of 19 mm and work index of 12 kWh/t. The limestone is stockpiled and conveyed to a feed preparation area where conventional wet ball milling (in closed circuit with a classifier cyclone cluster) is used to reduce the limestone particle size to 95% passing 45 µm. The Kusile ball mill specific energy is 26.5 kWh/t.

The dry vertical roller mill (VRM) is a novel grinding technology that dries, grinds and classifies ore within a single unit. Testwork was conducted using a pilot-scale Loesche VRM to determine the energy consumption required to grind 100 t/h of the Danielskuil limestone to 85% and 95% passing 45 µm. The specific energy for these two conditions is 13.7 kWh/t and 16.1 kWh/t, respectively. A wet ball mill locked cycle test was conducted at Mintek to grind the limestone to 85% passing 45 µm and resulted in a circuit specific energy of 15.4 kWh/t (compared to 13.7 kWh/t from the dry Loesche VRM testwork).

The testwork data and information received from Kusile were used to set up flow diagrams and generate mass balances for equipment sizing. Various suppliers provided budgetary quotations for the different milling technologies and ancillary equipment. The total installed power for the wet ball mill circuit (including ancillary equipment) is 3,802 kW compared to 1,893 kW for the dry Loesche VRM circuit. The absorbed power for the wet and dry circuit is 2,734 kW and 1,703 kW, respectively. The mechanical cost of the wet ball milling circuit is R48,328,000 compared to R59,185,000 for the dry Loesche VRM circuit (increase of 22.5%). The different components of the capital expenditure (CAPEX) were calculated as a percentage of the mechanical cost. The CAPEX for the wet ball milling circuit and dry Loesche VRM circuit (including ancillary equipment) is R239,960,400 and R265,042,900, respectively (10.5% increase).

A hot gas generator (HGG) is required in the dry Loesche VRM circuit if the moisture content of the limestone feed is higher than 6.0%. Data provided by Kusile indicated that the feed moisture content is less than 1.0%. Therefore, the HGG was not included in the main cost comparison. The stockpile and conveying areas at Kusile are large enough so that the maximum rainfall in Delmas (where Kusile is situated) should not increase the moisture content of the limestone feed to more than 6%. With the HGG included, the CAPEX of the dry

Loesche VRM circuit is R286,283,200, which is 8.0% more expensive than the dry circuit without the HGG, and 19.3% more expensive than the wet ball milling circuit.

No water saving is realized for this application (even though the dry Loesche VRM circuit does not require water) because a 30% solids concentration limestone slurry is required for the FGD process to be sprayed into the scrubber. The operating factor for both milling circuits is 89.8%, because the limestone consumption is dependent on the SO_2 concentration in the flue gas. Therefore, the annual raw material (limestone cost) and water cost are the same for both circuits. The annual operating cost for the wet ball milling circuit and dry Loesche VRM circuit is R254,819,200 and R238,890,700, respectively. The reduced OPEX is as a result of the reduced power consumption (decrease of 37.8%) and no grinding media used for the Loesche VRM. Revenue from gypsum sales (R267/t) is estimated to be R361,304,200 for both circuits.

The net present value (NPV) of the wet ball mill circuit is R348,407,000 based on an assumed 20-year plant life, 12% interest rate, and 35% corporate income tax. The corresponding interest rate of return (IRR) is 20.2% with a discounted payback period (DPBP) of 4.1 years. The return on investment (ROI) is 39.9%. In comparison, the NPV of the dry Loesche VRM circuit is R408,573,000 which is 17.3% higher than for the wet ball mill circuit. An increased IRR of 21.3% is observed with a slightly reduced DPBP of 3.8 years. The ROI is 8.6% higher at 48.5%.

An alternative option is for the limestone to be milled off-site (dry VRM circuit at the limestone mine) so that the dry, milled limestone is delivered to site without further grinding and/or processing required. This could result in a significantly reduced CAPEX and OPEX for the FGD process at any coal-fired power plant.

It should be noted that the results obtained from this study are specific to this project and characteristics of the Danielskuil limestone ore. The aim of the study is to compare the different circuits, and not to provide an accurate overall project cost estimate. A detailed engineering study is required to increase the accuracy of the cost estimate.

Acknowledgements

I would like to express my sincere gratitude and appreciation towards all those who provided me with the opportunity to complete this project. A special word of thanks is owed to Professor Gaylard at the University of the Witwatersrand, whose guidance, contribution and encouragement helped me to deliver this thesis. I would also like to show my appreciation to my co-supervisor, Dr Bwalya, for review of my work.

Furthermore, I would like to thank Hatch for the continued support and financial contribution towards my master's degree and allowing me to take time to conduct testwork. Hatch also provided me with technical assistance and support throughout this study.

A special thanks is owed to Idwala Industrial Holdings Ltd (Idwala Lime) for sample preparation and transportation of a bulk sample to Germany, and for providing information with regards to their limestone operations.

I would like to acknowledge Loesche South Africa (Pty) Ltd (Loesche) for the testwork conducted in Germany, and for the continued support throughout the duration of this project. A special thanks to Christian Gerhard and Jonathan Smith for meeting with me and providing relevant information.

Furthermore, I would like to thank the operations team at Eskom's Kusile Power Plant for providing me with information regarding their limestone feed preparation area and allowing us to visit their premises for a site walk.

I would also like to acknowledge Mintek for allowing me to conduct ball mill testwork at their facilities and for training me in their standard operating procedures (SOP's) for locked cycle tests. A special word of thanks is owed to Elizma Ford for organizing this testwork.

Finally, I would like to thank my parents, brother and fiancé for their continued support and encouragement throughout my studies.

Table of Contents

List of Tables

List of Figures

List of Acronyms and Abbreviations

BFD	Block flow diagram
CAPEX	Capital expenditure
CF	Cash flow
CB	Conical bottom
C	Contingency
CF	Contractor's fee
CTC	Cost to company
D	Direct cost
DCFROR	Discounted cash flow rate of return
EPA	Environmental Protection Agency
FCI	Fixed capital investment
FGD	Flue gas desulfurization
HGG	Hot gas generator
I	Indirect cost
LSFO	Limestone with forced oxidation
LCT	Locked cycle test
LM	Loesche Mill
MEL	Magnesium enhanced lime
MEL	Mechanical equipment list
MES	Minimum emission standards
NPV	Net present value
OPEX	Operating expenditure
PSD	Particle size distribution
P&ID/PID	Piping and instrumentation diagram
POD	Point of distribution
PDC	Process design criteria
PFD	Process flow diagram
E	Purchased equipment cost
ROI	Return on investment
SB	Slanted bottom
SG	Specific gravity
TCI	Total capital investment
VRM	Vertical roller mill
WFGD	Wet flue gas desulfurization
WC	Working capital
WCI	Working capital investment
XRF	X-ray fluorescence

List of Units

Am^3/h	Actual cubic meters per hour
c	Cent
c/kWh	Cent per kilowatt-hour
cm^2/g	Centimeter squared (surface area) per gram
cm^3	Cubic centimeter
m^3	Cubic meter
°C	Degree Celsius
g	Gram
g/cm^3	Gram per cubic centimeter
h	Hours
kN	Kilo Newton (force)
kN/m^2	Kilo Newton per square meter
kg	Kilogram
kg/h	Kilogram per hour
kVA	Kilo-volt ampere
kW	Kilowatt
kWh/t	Kilowatt hour per ton
kWh	Kilowatt-hour
MPa	Mega pascal
Mt	Mega tons
m	Meter
m/s	Meter per second (velocity)
m^2	Meter squared (area)
µm	Micron
mg	Milligram
mm	Millimeter
N	Newton
%	Percentage
R/a	Rand per annum
R/m^3	Rand per cubic meter
R/kL	Rand per kiloliter
R/t	Rand per ton
rev	Revolution
rev/min	Revolution per minute
R	South African Rands
t	Tons
t/a	Tons per annum
t/h	Tons per hour
v/v	Volume based
W	Watt
w/w	Weight based
wt%	Weight percentage

List of Components

$Ca(OH)_2$	Calcium hydroxide (slaked lime)
Ca^{2+}	Calcium ion
$CaCO_3$	Calcium carbonate (limestone)
$CaMg(CO_3)_2$	Dolomite
CaO	Calcium oxide (quicklime)
$CaSO_3•½H_2O$	Calcium sulfite hemihydrate
$CaSO_4•2H_2O$	Calcium sulfate dihydrate (gypsum)
CO_2	Carbon dioxide
H^+	Hydrogen ion (hydron)
H_2O	Dihydrogen monoxide (water)
H_2SO_3	Hydrogen sulfite (sulfurous acid)
H_2SO_4	Sulfuric acid
H_3O^+	Hydronium ion
HCO_3^-	Bicarbonate
$MgCO_3$	Magnesium carbonate
$Na_3(CO_3)(HCO_3)•2(H_2O)$	Trona
$NaHCO_3$	Sodium bicarbonate
NH_3	Ammonia
O_2	Oxygen
S	Sulfur
SO_2	Sulfur dioxide
SO_3^{2-}	Sulfite ion

List of Symbols

A_i	Abrasion index
A	Ampere
E_{actual}	Actual specific energy input
aq	Aqueous
W	Ball mill work input
v_{Belt}	Belt velocity
w_i	Bond work index
E_G	Bond's circuit specific energy
d	Charge diameter
E	Classification efficiency
k	Constant
D_{50C}	Corrected cut-size
C_F	Correction factor
C_n	Cost estimate
N_c	Critical speed
C_1	Cyclone correction factor for feed density
C_2	Cyclone correction factor for pressure change
C_3	Cyclone correction factor for solids specific gravity
ρ_B	Density of media
ρ_S	Density of solids

m_{Design}	Design tonnage
D	Diameter
D_{Roller}	Diameter of the roller
K_e	Empty friction coefficient
E	Energy
E_{input}	Energy input
E_{target}	Energy required to produce target undersize
$FR_{Hydraulic}$	Exerted pressure
P_{Shaft}	Fan motor power
F_{100}	Feed 100% passing size
F_{80}	Feed 80% passing size
F	Feed particle size
b	Fines present in the feed
d	Fines present in the overflow
c	Fines present in the underflow
F_{Dust}	Flowrate of the dust
μ	Friction factor or viscosity
$P_{Friction}$	Friction power
L_{Face}	Full cone face length
F_{Dyn}	Gas dynamic flowrate
g	Gaseous
F_{Roller}	Grinding force
h	Height or head
z	Height
h_b	Height of the bottom
h_L	Horizontal length
$L_{h,L}$	Horizontal loaded length
$m_{Idler\ Spacing,Carry\ Idlers}$	Idler spacing carry idlers
$m_{Idler\ Spacing,Return\ Idlers}$	Idler spacing return idlers
D_i	Inside diameter of mill
$d_{i,Nozzle}$	Inside diameter of nozzle
i	Interest rate
V_M	Internal volume of the mill
L/D	Length to diameter ratio
K_L	Load friction coefficient
$m_{Platework,Steel}$	Mass of steel for platework
m_{Belts}	Mass of the belts
M_B	Mass of the media balls
$m_{Moving\ Parts}$	Mass of the moving parts
M_R	Mass of the rocks
m_S	Mass of the solids
Q	Mill capacity
L or L_i	Mill effective grinding length
J_B	Mill volume fraction occupied by the ball charge
J_R	Mill volume fraction occupied by the bulk rock charge
M	Multiplier
$f_1,f_2,...$	Multiplying factors for piping, electrical, instrumentation, etc.
T	New feed to mill

$E_{input,new}$	New specific energy target
I	Number of rollers
ϕ_C	Percentage of the critical speed
PN_{Plies}	Polyester nylon number of plies
φ	Porosity of the bed
P	Power draw or particle product size
ΔP	Pressure drop
P_{100}	Product 100% passing size
P_{80}	Product 80% passing size
t	Project life in years
A_{Roller}	Roller surface area
FR_{Weight}	Roller weight
$m_{Rolling\ Mass,Carry\ Idlers}$	Rolling mass carry idlers
$m_{Rolling\ Mass,Return\ Idlers}$	Rolling mass return idlers
P_M	Shaft power
l_{Face}	Small cone face length
SG_S	Specific gravity of the solids
P_{Roller}	Specific grinding force
K_T	Specific roller pressure
A	Surface area
C_T	Terminal friction constant
T_{Plate}	Thickness of plate
T_{Cover}	Thickness of the cover
D_b	Top size of the grinding media
v	Velocity
V	Voltage
$V_{Full\ Cone,Steel}$	Volume of steel for conical bottom
$V_{Straight,Steel}$	Volume of steel for cylinder
$V_{Nozzle,Steel}$	Volume of steel for nozzle
$V_{Small\ Cone,Steel}$	Volume of steel for small conical bottom
W_{Belt}	Width of the belt
W_{Roller}	Width of the roller

1. Introduction

In South Africa, 83% of electricity is generated through coal-fired power plants (Pretorius, et al. 2015). Combustion of coal produces hazardous sulfur dioxide (SO_2), which is an indirect greenhouse gas. International concern about climate change has resulted in stringent SO_2 emission regulations. Moreover, SO_2 emissions result in major environmental concerns regarding acid rain and health issues.

Flue gas desulfurization (FGD) is the process of removing SO_2 from exhaust gas of coal-fired power plants. Wet flue gas desulfurization (WFGD) using finely ground limestone has been predominantly used over other FGD technologies because of its low operating cost and high SO_2 removal efficiency (Córdoba, 2015). Wet limestone slurry is sprayed counter current to the flue gas and reacts with the SO_2 to form synthetic gypsum ($CaSO_4.2H_2O$). The process removes up to 98% of the hazardous compounds (Gansley, 2008).

Eskom's Kusile Power Plant (Kusile) is the first South African power facility to incorporate an FGD plant. High-grade limestone is transported from Danielskuil in the Northern Cape to a truck offloading facility at Kusile, where it is stockpiled and subsequently conveyed to the reagent feed preparation area. The feed preparation area includes closed-circuit wet ball milling to reduce the limestone particle size to 95% passing 45 µm for FGD scrubbing.

The reagent preparation system influences the overall efficiency of the FGD process because the reactivity of limestone is increased as it is reduced in size (Cai, *et al.*, 2019). Ball milling has been predominantly used for limestone size reduction in the reagent preparation area (Hassibi, Rogers, & Yang, 1999). The advantages of ball milling include large reduction ratio capability and low maintenance requirements.

The Loesche vertical roller mill (VRM) is a dry milling technology that could be used as an alternative to the ball mill because of its lower specific energy (Jorgensen, 2005) and the advantage of drying, milling and classifying within a single unit. It also allows for the possibility of off-site milling which will decrease the power plant's operational and capital costs. The Loesche VRM has been predominantly used in the coal and cement industry with 55% market share worldwide. Since 1934, the design concepts of the VRM have been adapted to the industrial minerals industry, with more than 63 Loesche VRM's installed worldwide for the grinding of limestone.

According to Loesche, the advantages of the VRM include the simplified and robust construction, grinding and drying of ore in one machine, low operating costs, fast reaction to fluctuations in material qualities and short equipment delivery periods.

This study involves the technical and economic evaluation of both milling technologies to assess the viability of the dry Loesche VRM technology in comparison with wet ball milling as a South African option. The objectives of this study are to:

1. Compare the power required to grind 100 t/h of the high-grade (96% $CaCO_3$) limestone sample from Idwala Lime's Danielskuil site that is used in a wet ball milling circuit against a dry Loesche VRM circuit:
    - Determine the circuit specific energy requirement for the wet ball milling application at Kusile Power Station to grind the high-grade limestone (top size of 19 mm) to 95% passing 45 µm.
    - Conduct testwork to determine the circuit specific energy for a 100 t/h conventional wet ball milling application to grind the high-grade limestone (top size of 19 mm) to 85% passing 45 µm.
    - Conduct testwork to determine the circuit specific energy of a 100 t/h dry Loesche VRM to reduce the high-grade limestone (top size of 19 mm) to 85% and 95% passing 45 µm.
2. Determine the mechanical cost, total capital investment and operational cost of the 100 t/h wet ball mill circuit compared to the 100 t/h dry Loesche VRM circuit (including ancillary equipment). Generate the design criteria, block flow diagram, process flow diagram, stream tables and typical piping and instrumentation diagram for each of the two circuits.
3. Identify the most suitable and economically viable option for limestone comminution in the FGD process by comparing the net present value, interest rate of return, discounted payback period and rate of return of each circuit.

This research report covers a technical and economic comparison evaluation between the wet ball mill and dry Loesche VRM circuit for limestone grinding in the FGD process. The report includes the design criteria, flow diagrams, stream tables and equipment sizing (including installed and absorbed power) for both circuits. The capital investment, operational expenditure and revenue of gypsum are used to compare the net present value, interest rate of return, payback period and return on investment.

A presentation for this project was held at the Idwala Lime head office on the 10th of September 2019.

2. Literature Review

2.1 Background

Gaseous SO_2 emissions from coal-fired power generating plants are known to have detrimental effects on the environment and on human health. As a result, many countries have implemented stringent SO_2 emission regulations for fossil fuel power plants (Srivastava and Jozewicz, 2001). According to the International Energy Clean Coal Centre, the SO_2 emission limits in South Africa for new and existing plants are 500 mg/Nm^3 and 3500 mg/Nm^3, respectively. The Minimum Emission Standards (MES) of South Africa apply to Eskom's coal-fired power generating plants, such as Kusile and Medupi, that are fitted with Wet Flue Gas Desulfurization (WFGD) processing plants.

2.1.1 Flue Gas Desulfurization (FGD)

Flue gas desulfurization is the process of extracting hazardous SO_2 from exhaust combustion flue gas generated by coal-fired utility boilers (Gaigward & Boward, 2003). FGD can be classified as a wet (wet scrubbing), semi-dry or dry process. Even though there is a large variety of commercial FGD processes available, the wet limestone FGD process constitutes more than 80% of the total installed worldwide FGD processes (Córdoba, 2015). According to Córdoba, this is because of its high desulfurization performance, low operating cost and simplicity of design and operation. Wet limestone FGD is a non-regenerable process where SO_2 is bound in the sorbent and utilized as a byproduct (synthetic gypsum). Conversely, in regenerable technologies, SO_2 is released from the sorbent and processed to yield sulfuric acid (H_2SO_4), elemental sulfur (S) or liquid SO_2 (Srivastava & Jozewicz, 2001).

In the wet limestone FGD process, limestone ($CaCO_3$) is milled and mixed with water to form a slurry, which is sprayed countercurrent to the flue gas flowing upward in the absorber. The spray liquor droplets absorb the SO_2 gas which facilitates gypsum formation (Gaigward and Boward, 2003). Two regions can be identified in the absorber; (1) the gas-to-liquid contact zone and (2) the reaction tank (Córdoba, 2015). In the FGD process where limestone is used with forced oxidation (LSFO), slurry is aerated in the reaction tank of the absorber. Conversely, a separate tank for slurry aeration is required when magnesium enhanced lime (MEL) is used as the sorbent. Figure 2-1 illustrates an overview of the LSFO WFGD process.

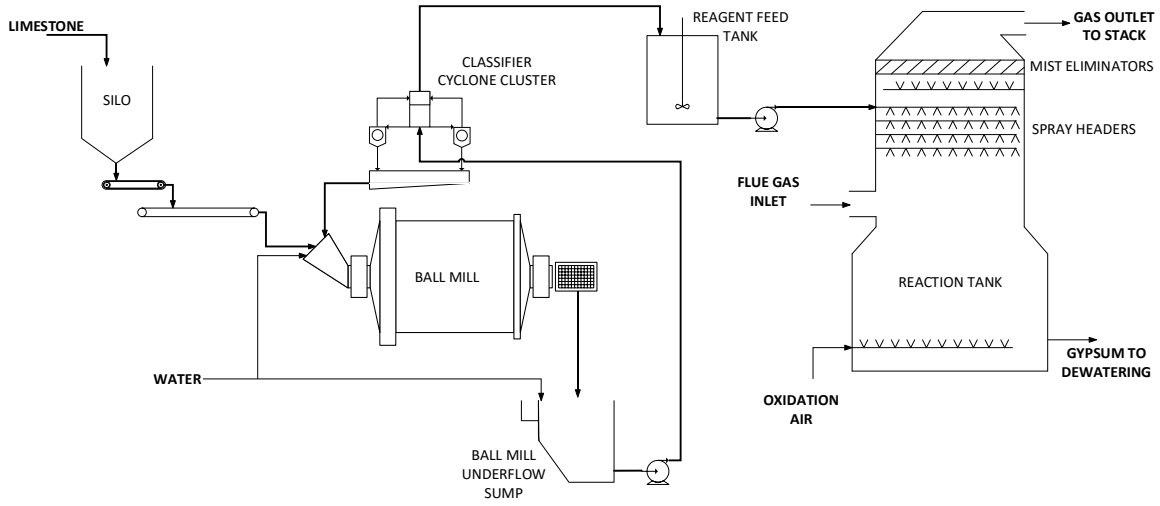

Figure 2-1: Flow Diagram of LSFO Process

Limestone slurry is prepared in a closed ball mill circuit. The fine limestone is discharged into an agitated preparation tank before it is pumped to the reaction tank of the scrubber in a controlled regime to maintain the pH (Córdoba, 2015).

The LSFO process (Córdoba, 2015) is based on complex acid-base reactions (Equation 1 to 7). Aeration in the reaction tank (LSFO) allows calcium sulfite hemihydrate ($CaSO_3$•½H_2O) to be oxidized to calcium sulfate dihydrate ($CaSO_4$•2H_2O), or gypsum (Equation 8).

SO_2 Dissolution:	$SO_2(g) \leftrightarrow SO_2(aq)$	1
Hydrolysis of SO_2:	$SO_2(aq) + H_2O \leftrightarrow H_2SO_3(aq)$	2
H_2SO_3 dissociation:	$H_2SO_3(aq) \leftrightarrow H^+(aq) + HSO_3^- \leftrightarrow 2H^+(aq) + SO_3^{2-}(aq)$	3
Limestone dissolution:	$CaCO_3(s) + H_3O^+(aq) \leftrightarrow Ca^{2+}(aq) + HCO_3^-(aq) + H_2O(aq)$	4
Acid-base neutralization:	$HCO_3^-(aq) + H^+(aq) \leftrightarrow CO_2(aq) + H_2O(aq)$	5
Overall gas-to liquid:	$CaCO_3(s) + SO_2(g) + \frac{1}{2}H_2O(aq) \rightarrow CaSO_3 \bullet \frac{1}{2}H_2O(aq) + CO_2(g)$	6
Oxidation and sedimentation:	$CaSO_3 \bullet \frac{1}{2}H_2O(aq) + \frac{1}{2}O_2(g) + \frac{3}{2}H_2O \rightarrow CaSO_4 \bullet 2H_2O(s)$	7
Overall chemical reaction:	$2SO_2 + 2CaCO_3 + O_2 + 4H_2O \rightarrow 2CaSO_4 \bullet 2H_2O + 2CO_2$	8

According to the United States Environmental Protection Agency (EPA), the stoichiometric ratio of limestone ($CaCO_3$) to SO_2 employed in commercial FGD systems is 1.1 and 1.4 for new and older designs, respectively (Burnett, et. al. 1984). According to Eskom (Chang, et al. 2018), the WFGD scrubber is fed with 1.02 to 1.05 moles of limestone per mole of captured SO_2.

2.1.2 FGD Sorbents

The fundamental concept of FGD is that SO_2 and SO_3 are acidic and can therefore be removed by reacting with a suitable alkaline component (Carpenter, 2012). The efficiency of SO_2 removal is dependent on the nature of each sorbent. Common sorbents used for FGD include:

- Calcium-based components: limestone, quicklime (CaO), slaked lime ($Ca(OH)_2$) and dolomitic lime ($CaMgO_2$)
- Sodium-based components: sodium bicarbonate ($NaHCO_3$), and trona ($Na_3(CO_3)(HCO_3)•2(H_2O)$)
- Magnesium carbonate ($MgCO_3$)
- Ammonia (NH_3)

Sodium-based sorbents tend to have a high SO_2 removal efficiency. However these are much more expensive than the calcium-based sorbents (Ramsaroop, 2012). Moreover, the sodium-based sorbents produce hazardous wastes (Kohl and Nielsen, 1997).

Limestone is the most commonly used sorbent in WFGD because of its high availability and low cost. Calcination of limestone results in the formation of quicklime (Equation 9), which reacts with water to form slaked lime (Equation 10). Both lime components could be used as sorbents for FGD.

$$CaCO_3(s) \rightarrow CaO(s) + CO_2(g) \quad 9$$

$$CaO(s) + H_2O \rightarrow Ca(OH)_2 \quad 10$$

Quicklime has a higher surface area and porosity than limestone and is thus more reactive. Slaked lime has an even higher reactivity than quicklime. According to Carpenter (2012), the reactivity and performance of the calcium-based sorbents can be improved by adding fly ash. However, in the wet FGD LSFO operation, fly ash reduces the quality of gypsum. Thus, WFGD plants have ash removal prior to the Absorber.

According to KC Cottrell (2016), limestone makes up 55% of reagents used in the FGD processes compared to 33% as lime reagents.

2.1.3 Limestone

2.1.3.1 Limestone Deposits in South Africa

Limestone is a carbonate sedimentary rock which occurs naturally as calcite or occasionally as aragonite (Harrison, 1993). Carbonate sedimentary rocks are predominantly formed during biogenic processes; however, in some cases they form during chemical precipitation.

According to Harrison, approximately 20% of all sedimentary rocks are limestone, dolomite or a combination thereof.

Three major sub-basins were formed in South Africa during the early Proterozoic era (Altermann & Wotherspoon, 1995) approximately 2,500 million years ago (Evans & Newell, 2013), namely; (1) the Transvaal basin, (2) the Griqualand West basin and (3) the Kanye basin (Botswana). During this time, clastic and chemical sediments and igneous rock accumulated. The dominant lithologies in these basins consist of carbonates. The largest continuously outcropping basin is the Griqualand West basin (Altermann & Wotherspoon, 1995) and this supplies the largest quantity of carbonates for the limestone industry of South Africa.

According to Altermann & Wotherspoon (1995), 20 million tons of limestone is produced every year, of which the Chuniespoort Group deposit and the Ghaap Plateau deposit (in the Campbell group) contribute the largest part. Both groups are in the Griqualand West basin. Figure 2-2 depicts the approximate location of limestone deposits in South Africa.

Limestone and dolomite are considered low-cost, high-bulk commodities. In South Africa, the market driver for limestone is the cement industry. A study conducted in South Africa during 2015 indicated that 75% of the annual mined limestone was utilized in the cement industry, while the metallurgical and agricultural industries used 9% and 5%, respectively (Bekker, 2017). Uranium and gold operations are also strongly dependent on lime products (Agnello, 2005). According to Agnello (2005), South Africa's high-grade limestone deposits are isolated, therefore only a few processing plants with high-rate lime production have been constructed.

Limestone is mined in open-cast quarries using drilling and blasting. It is then crushed and stockpiled, before being transported to site. According to Eskom (Haripersad and Swart, 2015), one of the highest cost drivers of limestone is the transportation component.

Impurities that are commonly found in limestone deposits include silica, organic matter and iron minerals. Eskom (Haripersad and Swart, 2015) investigated the impact of using a lower quality limestone during FGD, which resulted in an increased limestone consumption and a lower quality gypsum production.

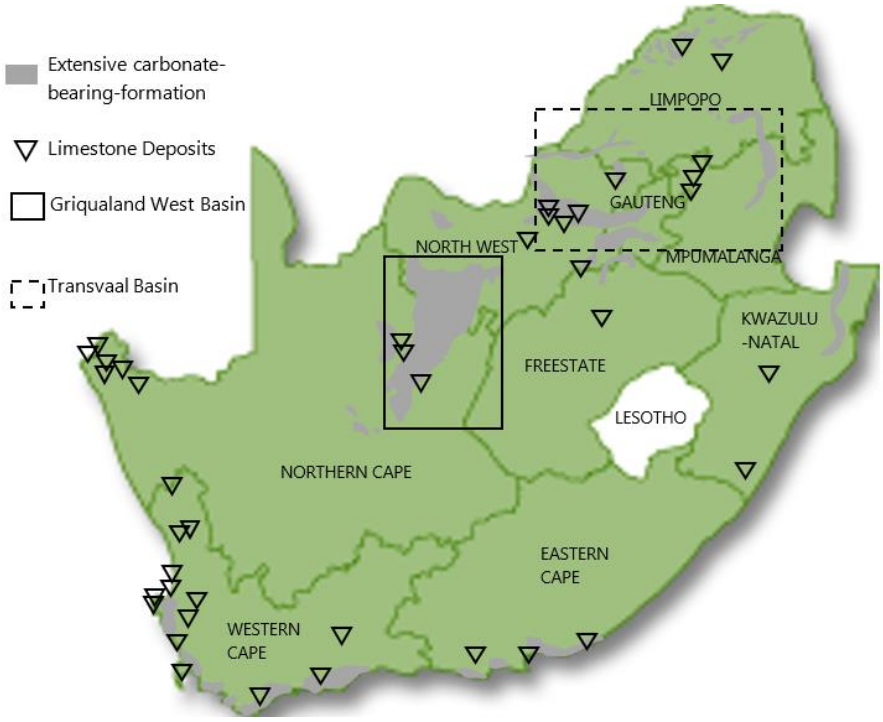

Figure 2-2: Limestone Deposits in South Africa (adapted from Agnello (2005))

2.1.3.2 Limestone Properties

The properties of limestone typically found in South Africa are listed in Table 2-1 below (Ozkahraman, 2010).

Table 2-1: Breakage Mechanisms and Properties of Limestone (Ozkahraman, 2010)

Parameter	Unit	Value
Unit Weight	g/cm³	2.67
Uniaxial compressive strength	MPa	54.95
Bond Work Index (Doering International)	kWh/t	14

2.2 Wet Milling

The comminution of ore is generally a feed preparation step for subsequent processing stages. Mills used for fine and ultra-fine grinding require a large capital investment and incurs high operational expense due to high power usage and consumption of wear resistant materials. Rotating drums are most frequently used for grinding; these utilize a charge of loose grinding media (ore itself, pebbles or manufactured steel balls) which is lifted by the rotating drum to break the ore through impact, attrition and abrasion.

2.2.1 Ball Mill Introduction and Mechanism

A finer limestone particle size provides an increased surface area and thus improves the reactivity of limestone. The typical limestone FGD feed particle size to the reagent preparation

section is minus 19 mm from which a product P_{95} of 45 µm is expected (Hassibi et al., 1999). Others specify a limestone FGD feed size between P_{90} and P_{94} minus 44 µm (Gansley, 2008) or an average limestone FGD feed particle size between 5 and 20 µm (Córdoba, 2015). Limestone size reduction for the WFGD process has been predominantly achieved through grinding using conventional ball mills (Hassibi et al., 1999).

Ball mills were invented in the 1870s as the first tumbling mills and have since then dominated fine grinding (Lynch, 2015). A ball mill typically consists of a rubber lined rotating drum loaded with steel balls. The cylindrical chamber rotates causing a tumbling action of the steel balls (lifted by the liners) which crushes the limestone. Figure 2-3 illustrates the breakage mechanism within the ball mill. Ball trajectory is a function of mill speed (rpm). Action proceeds from abrasion (low speed-limiting cataracting) to impact at higher speeds. Ball charge composition is aligned with the required product size grading: sufficient large balls for crushing and smaller balls to generate fine particle size.

Water is added to the mill to achieve the desired solids content of 30% to 35% (Gansley, 2008). A closed circuit includes a ball mill and classification step (refer to Figure 2-1). Overflow from the classifier hydrocyclone flows to the reagent feed tank, whereas the underflow is recycled to the ball mill.

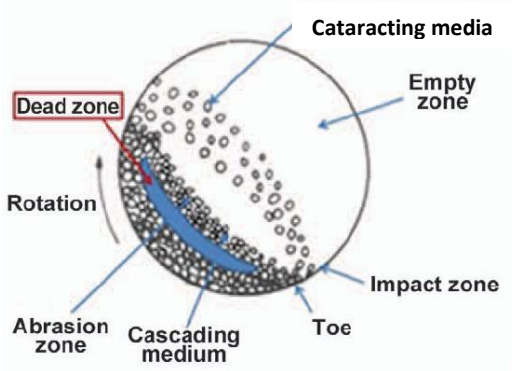

Figure 2-3: Breakage Mechanism Inside Ball Mill (Lynch, 2015)

According to Hassibi and others (1999), the ball mill is an attractive option for grinding because it has a large reduction ratio capability, resistance to abrasion and relatively low requirements for operating, control and maintenance.

The cost of the equipment in the ball mill circuit is dependent on the system capacity. In general, the investment cost (equipment, erection and civils) of the ball mill is less expensive (between 20 to 25%) than the VRM (Mutter, 2013). However, the ball mill operating costs are expected to be significantly higher since it is more energy intensive and has a high media and water consumption (Jorgensen, 2005).

2.2.2 Typical Ball Mill Circuit Process Design

2.2.2.1 Process Description Overview

Figure 2-4 shows a general ball mill circuit closed with a hydrocyclone. Ore is fed to the ball mill feed trunnion via a conveyor and chute system. Water is added to the mill to assist with the transfer of ore through the mill and allow finer particles to move toward the exist and limit further expenditure on the grinding energy. However, slurry density is maintained as high as possible, usually between 65% and 80% solids (Gupta and Yan, 2006), because a more dilute slurry will increase metal to metal contact of the steel balls, which will increase steel consumption and thus result in inefficient grinding. The steel balls facilitate grinding of the ore and the mill has lifters to promote the cataracting effect of the ore.

The mill product is discharged through the discharge trunnion and into the recycle tank. The ground ore is diluted and pumped to the classifier cyclone. The cyclone is located above the ball mill so that the cyclone underflow is recycled directly into the ball mill feed chute. The cyclone overflow is discharged into a mixing tank and pumped to downstream processes.

The circulating load is described by the mass of material returned to the ball mill feed divided by the fresh feed to the ball mill. The optimum circulating load for a ball mill is 250% (Bond, 1958).

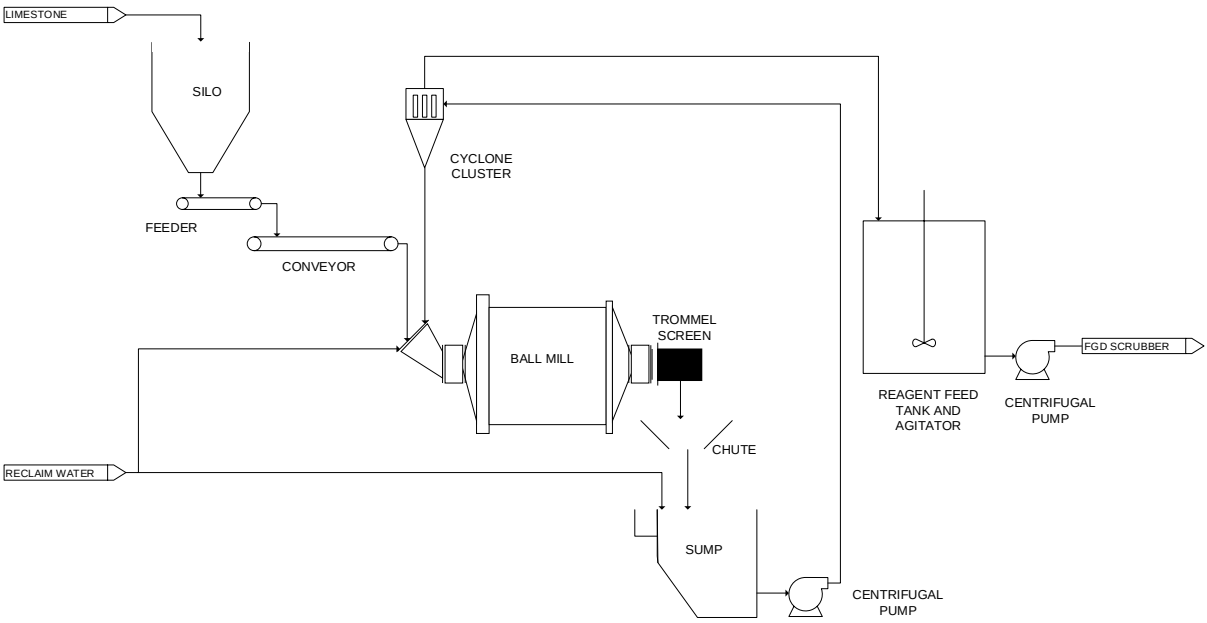

Figure 2-4: Flowsheet of a Closed Ball Mill Circuit

2.2.2.2 Types of Ball Mills

Ball mills have mainly two types of discharges; (1) grate discharge and (2) overflow discharge (Schlanz, 1987). Grate discharge refers to mills that are fitted with discharge grates between the mill shell and discharge trunnion. A lower pulp density is required, which allows for reduced

retention time within the mill. Consequently, there is a larger fraction of coarse particles and minimized overgrinding (required by closed circuit operation). Grate discharge mills are best suited for grinds down to 150 – 250 µm (Gupta and Yan, 2006). The overflow discharge is the most commonly used ball mill type and facilitates finer particle production. The overflow discharge mill is typically fitted with a trommel screen (1 mm aperture) at the discharge to collect worn grinding media. According to Schlanz (1987), the power consumption of the overflow discharge mill is up to 15% less than the grate discharge mill with similar grinding efficiencies.

2.2.2.3 Mill Drive

Ball mills are either supported at both ends by trunnions or ride on steel tires. The pinion shaft is driven through the prime mover drive, which consequently drives the girth gears bolted to the ball mill shell. An air clutch or gear system can be used to operate the prime movers. The location of the girth gear is usually specified by the manufacturer (Gupta and Yan, 2006).

2.2.2.4 Mill Size

Ore is fed to the tumbling ball mill via a feeder and conveyor system. The basic design parameters of the tubular ball mill include:

- Size rated as diameter x length.
- Feed system: feed hopper (between 40 cm and 100 cm) at an angle between 30° and 60°, and approximately 1.5 m above the center line of the mill.
- Feeder: spout feeder for a closed ball mill circuit with a hydrocyclone as the classifier.
- Discharge System: between 5 cm and 110 cm lower than the center line for overflow mills.

The feed trunnion has a slightly smaller diameter than the discharge trunnion opening to encourage slurry flow through the mill and to prevent push-back of the slurry through the feed trunnion. The common ball mill sizes, initial feed size and reduction ratio of feed to product under normal condition is shown in Table 2-2.

Table 2-2: **Tumbling Ball Mill Characteristics (Gupta and Yan, 2006)**

Parameter	Ball Mill
L/D Ratio	0.5 to 3.5
Feed Size	-19 mm -12.5 mm to 9 mm
Reduction Ratio	20:1 to 200:1

Lifters inside the ball mill promote the crushing operation by raising the particles to greater heights before cascading at the toe of the mill discharge. It also assists in saving wear of the

steel body of the mill. The number of lifters is determined using Equation 11 (Gupta and Yan, 2006).

$$Number\ of\ Lifters = 3.3 \times \pi \times D\ for\ double\ wave\ liners \\ = 6.6 \times D\ for\ single\ wave\ liners \quad (11)$$

where D is the mill diameter.

Double wave liners are generally suited for ball mills using media with top sizes less than 60 mm, while single wave liners are used for mills with media larger than 60 mm. The liners can be either grid or solid liners made of manganese steel, or Ni-hard or high carbon steel. Hard rubber or synthetic liners are typically used at a thickness of between 65 mm and 75 mm. The surface of the liners can be waved, ribbed or smooth. The waves are generally between 60 mm and 75 mm above liner thickness for single wave liners, and between 65 mm to 90 mm above liner thickness for double wave liners. The wave height is commonly 1.5 to 2 times the liner thickness. The rotational speed of the mill has a proportional impact on the liner wear.

2.2.2.5 Mill Energy

The specific energy (E_G) required for crushing rocks and liberating the mineral embedded in the rock can be determined using Bond's equation for size reduction of ore in a closed grinding circuit (Equation 12).

$$E_G = 10W_i\left[\frac{1}{\sqrt{P_{80}}} - \frac{1}{\sqrt{F_{80}}}\right] \quad (12)$$

where:

$W_i =$ Bond Work Index, which represents the energy required to reduce the ore from an infinite size to 100 µm

$P_{80} =$ 80% passing size of the product in µm

$F_{80} =$ 80% passing size of the feed in µm

2.2.2.6 Critical Speed

The critical speed of a mill is the rotational speed at which the charge centrifuges and no tumbling action occurs. Theoretically, at this speed, the media is carried around in a fixed position against the shell. The critical speed (N_C) can be calculated using Equation 13 (Gupta and Yan, 2006).

$$N_C = \frac{42.3}{\sqrt{D-d}} \quad (13)$$

where d is the charge diameter and D the mill diameter.

According to Gupta and Yan (2006), the position of the charge in a mill depends on the speed of rotation. If the ball mill speed is too low, sliding of material will occur, i.e. particles will not move up the wall of the mill as it rotates. Conversely, at a higher speed centrifuging of the mill charge can occur. Therefore, ball mills are usually operated at speeds of between 70% and 80% of critical, which allows for cataracting action of the charge (more impacting of particles).

2.2.2.7 Particle Filling

If the ball mill is overfilled, fines accumulate at the toe position of the mill, which results in a cushioning effect (absorbing impact and causing breakage). Conversely, when the mill is underfilled, contact of grinding balls results in excessive wear and retards the rate of breakage. Therefore, the optimum charge volume (V_R) could be determined using Equation 14 and maintained during operation.

$$V_R = \frac{Mass\ of\ Ore}{Density\ of\ Ore\ \times\ Mill\ Volume} \times 100\% \qquad 14$$

The mill is charged with media (generally steel balls) at a specific load (typically 40% to 50%) to ensure effective grinding of the ore. The specific gravity of the steel balls is approximately 7.85. However, ceramic balls (90% Al_2O_3) may be used for softer ores. The percentage mill volume occupied by the grinding media (V_B) is depicted by Equation 15.

$$V_B = \frac{Mass\ of\ Grinding\ Balls}{Density\ of\ Ball\ Material \times Mill\ Volume} \times 100\% \qquad 15$$

The fraction of the mill volume occupied by the bulk rock charge (J_R) and the bulk ball charge (J_B) is therefore represented by Equation 16 and Equation 17, respectively (Gupta and Yan, 2006).

$$J_R = \frac{M_R}{\rho_s \times V_M} \times \frac{1}{1-\varphi} \qquad 16$$

$$J_B = \frac{M_B}{\rho_B \times V_M} \times \frac{1}{1-\varphi} \qquad 17$$

where:

M_R = mass of the rocks

M_B = mass of the media balls

ρ_S = density of the ore solids

ρ_B = density of the media balls

V_M = internal volume of the mill

$\varphi =$ porosity of the bed

According to Gupta and Yan (2006), the preferred ratio $\frac{J_R}{J_B} \approx 0.4$ and the bulk rock occupies 20% to 25% of the mill inside volume.

2.2.2.8 Mill Power and Capacity

Some of the factors that influence the capacity of the ball mill includes:

- Dimensions of the mill
- Type of mill
- Rotational speed
- Mill loading
- Required product size
- Work index
- Mill shaft power
- SG of rock

Bond derived an equation to correlate the mill capacity (Q) with the shaft power (P_M) and specific energy (Equation 18).

$$Q = \frac{P_M}{E_G} \tag{18}$$

The mill shaft power can be calculated using Equation 19 (Gupta and Yan, 2006).

$$P_M = 7.33 J_B \Phi_C (1 - 0.937 J_B) \rho_B L D^{2.3} \left(1 - \frac{0.1}{2^{9-10\Phi_c}}\right) \tag{19}$$

where Φ_C is the percentage of critical speed.

The work index (W_i) used to calculate the specific energy in Equation 12 was described as a function of mineral and mill characteristics (moisture, particle size, reduction ratio, etc.) and must be corrected to obtain a reasonable value of mill capacity for design purposes. An expression for mill capacities with a diameter greater and less than 3.81 m was developed by Austin *et al.* (1984).

- For a mill diameter < 3.81 m (Equation 20):

$$Q = \frac{\left(6.13 D^{3.5} \left(\frac{L}{D}\right) \rho_b (J_B - 0.937 J_B^2) \left(\Phi_C - \frac{0.1\Phi_C}{2^{9-10\Phi_C}}\right)\right)}{C_F W_{i,TEST} 10 \left(\frac{1}{\sqrt{P}} - \frac{1}{\sqrt{F}}\right)} \tag{20}$$

- For a mill diameter > 3.81 m (Equation 21):

$$Q = \frac{\left(8.01 D^{3.3} \left(\frac{L}{D}\right) \rho_b (J_B - 0.937 J_B^2) \left(\Phi_C - \frac{0.1\Phi_C}{2^{9-10\Phi_C}}\right)\right)}{C_F W_{i,TEST} 10 \left(\frac{1}{\sqrt{P}} - \frac{1}{\sqrt{F}}\right)} \tag{21}$$

The correction factor (C_F) includes all corrections for calculating the work index. However, Rowland and Kjos (1980) recommends a factor of 6.3 for all ball mill capacities.

Circulating load and classification efficiency both have a critical impact on the mill capacity (Jankovic and Valery, 2012). Equation 22 can be used to calculate the circulating load based on the fines present in the feed (b), underflow (c) and overflow (d) of the classifier cyclone.

$$Recirculating\ Load = \frac{d-c}{c-b} \times 100\% \qquad 22$$

Figure 2-5 illustrates the relationship between the capacity factor and the circulating load. An increased circulating load indicates an increased capacity factor; however, it also results in a decreased classifier cyclone efficiency and thus a decreased capacity factor.

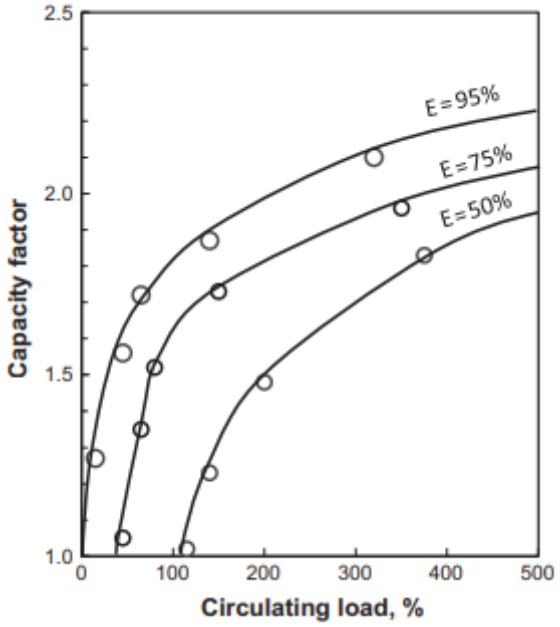

Figure 2-5: Impact of Circulating Load and Classification Efficiency (E) on Milling Circuit Capacity (Jankovic and Valery, 2012)

2.2.2.9 Grinding Media Initial Charge and Top-Up

Steel ball sizes are commercially available between 10 mm and 150 mm. The initial number, size and mass of each ball size depends on the load of the mill. Smaller steel balls allow for a larger surface area for grinding. The optimum ball charge consists of a wide range of ball sizes so that the space between the balls is filled with smaller balls, which promotes efficient grinding. The top size of the grinding media can be calculated using Equation 23 (Bond, 1958).

$$D_b = \sqrt{\frac{F_{80} \times W_i}{C \times \Phi_C} \times \sqrt{\frac{SG_s}{\sqrt{D}}}} \qquad 23$$

where:

D_b = the top size of the grinding media

C = 200 for ball mills and 300 for rod mills

SG_s = specific gravity of feed

The equilibrium charge refers to the state at which the number and mass of balls added to the mill equals the number of balls expelled from the mill plus the rate of loss in mass of balls due to abrasion and wear, i.e. the state at which the grinding conditions remain constant. Therefore, the initial charge should closely correlate to the equilibrium charge and is represented by Table 2-3. These values indicate the initial ball charge when grinding balls of specified sizes have to be charged.

Table 2-3: Equilibrium Ball Size for Initial Tumbling Ball Mill Charge (Gupta and Yan, 2006)

	Distribution Mass Percentage							
Ball Diameter (mm)	**114**	**101**	**89**	**76**	**63.5**	**51**	**38**	**25.4**
114	23							
101	31	23						
89	18	34	24					
76	15	21	38	31				
63.5	7	12	20.5	39	34			
51	3.8	6.5	11.5	19	43	40		
38	1.7	2.5	4.5	8	17	45	51	
25.4	0.5	1	1.5	3	6	15	49	100

The information in Table 2-3 can be used to compute the ball sizes for a specific charge. The following steps are required to calculate the charge (Gupta and Yan, 2006):

1. Calculate the geometric mean of the size intervals and the cumulative percentage size retained.
2. Calculate the factor F for each size class using 1.29^n, where n refers to the size class (n=1 is the largest size class, n=2 is the second largest, etc.).
3. To get the optimum ball charge, multiply the cumulative percentage retained by the factor F (calculated in Step 2) for each size class until the product is greater than 100. The size class greater than 100 is rejected.
4. Divide the percentage largest size ball in the optimum charge by the percentage of this charge found in the equilibrium charge (Table 2-3).
5. Calculate the cumulative percentage passing by multiplying the fraction calculated in Step 4 to each equilibrium mass percentage in Table 2-3.

6. Where the cumulative optimum ball charge is greater than 100, the remainder of the balls have a maximum size corresponding to the sizes in Table 2-3. The computation explained in Step 5 should be repeated to determine the size distribution.
7. Add the cumulative percentage passing of Step 5 and Step 6 to calculate the equilibrium ball charge.

During operation, the steel balls wear and the grinding characteristics change. Wear of the steel balls is dependent on the ore characteristics (hardness, composition, etc.) and influenced by the speed of the mill, mill diameter, specific gravity and the work index of the mineral. Steel ball consumption is in the range of 100 to 1000 g/t of new feed (Schlanz, 1987). According to Bond, the average mass loss of the grinding media in a wet application is described by Equation 24.

$$Average\ Grinding\ Media\ Mass\ Loss = 0.16(A_i - 0.015)^{0.33} \quad 24$$

where A_i is the abrasion index. The abrasion index for the Danielskuil limestone deposit is approximately 0.1, which is classified as slightly abrasive (Käsling and Thuro, 2010).

In order to maintain the grinding characteristics, the worn balls must be replaced. Usually, the largest size of ball (that was initially charged) is used to replace the worn balls.

2.2.2.10 Classifier Cyclone

The aim of the classifier cyclone is to classify particles based on the ratio of their centrifugal force to fluid resistance and therefore produce the fine product stream in the overflow at the desired size range. The feed enters the cyclone tangentially to form a vortex. While the larger particles move outward to the cyclone wall due to centrifugal forces, the finer particles are forced inward and are transported with most of the water up through the cyclone to the overflow (Arterburn, 2001).

Oversize material is channeled to the underflow, which is recirculated to the mill feed. The circulation load for a ball mill is usually between 250% and 400% (Bond, 1958).

2.2.3 Case Study: Medupi Power Plant WFGD

Reference Document: (Chang, 2018)

Medupi is one of Eskom's coal-fired power generating plants with a planned WFGD system for SO_2 removal. Limestone arrives via trucks and rail cars, after which it is reclaimed and conveyed to the limestone silos in the reagent preparation area. Limestone is fed from the silos to overflow ball mills via weigh belt feeders. Water is also added to the ball mills. Size reduction occurs in the grinding chamber of the ball mill, after which the slurry is collected in the mill sump and pumped to the hydrocyclone. The final limestone product gravitates from

the hydrocyclone overflow to the limestone slurry feed tank at a ratio of between 1.02 and 1.05 moles $CaCO_3$ per mole SO_2 to achieve a 98% SO_2 removal efficiency. The cyclone underflow is recycled back to the ball mill to achieve a circulating load of approximately 300%.

The limestone supplied to site is specified to have between 85% and 98% $CaCO_3$, a F_{100} of 19 mm and a bond index of between 11 and 13 kWh/ton.

The hourly limestone consumption for the WFGD process is approximately 126 t/h which amounts to 991,000 t/a based on an operating factor of 89.8%. The operating factor is the product of the 95% availability and 94.6% utilization. A summary of the reagent and water costs is tabulated below (Table 2-4). The reagent costs include the material and delivery of the reagent to the facility.

Table 2-4: Unit and Operating Costs of Eskom Medupi FGD Plant (Chang, 2018)

Costs	Units	Value
Limestone Unit Costs	R/t	475
Annual Operating Cost of Limestone	R/a	471,000,000
Water Costs	R/m³	20
*Annual Operating Cost of Water	R	197,000,000

* *Water costs include all technologies involved with the FGD process*

The WFGD feed preparation area at Medupi is water and energy intensive. Table 2-5 below summarizes the annual water and power consumption for the WFGD system.

Table 2-5: Power and Water Consumption of the WFGD Feed Preparation at Medupi (Chang, 2018)

Utility	Units	Reagent Preparation	Remaining WFGD	Absorber Pressure Drop	Total
Water	m³	3,613,669	2,884,733		**6,498,402**
Power	MWh	24,125	211,080	12,437	**247,642**

The limestone preparation area accounts for approximately 55.6% of the water consumption of the entire WFGD system. The power consumption of the feed preparation area is 9.7% of the total power consumption of the WFGD system. There is an opportunity for lowering operating cost by reducing the power consumption of the feed preparation area.

2.3 Alternative Limestone Milling Technologies

The limestone comminution design requires detailed evaluation to provide the most cost effective and energy efficient FGD system (Hassibi et al., 1999). According to Boehm et al. (2015), tumbling mills and roller mills still remain the most viable comminution route for a size

range between 10 mm and 10 µm. This section briefly covers alternative size reduction technologies to limestone ball milling in the WFGD process.

Stirred (or attrition) milling is generally used for applications of fine and ultra-fine grinding. Alternative wet grinding technologies for limestone size reduction include, but are not limited to, the following:

- Tower mill (Hassibi et al., 1999)
- Vertimill® (Metso)
- Vertical Stirred Mill (FLSmidth)
- HoroMill® (Oretec)
- HIGmill® (Outotec)
- Stirred Media Detritor (Metso)
- IsaMill®

Vertical ball mills could also be classified as being in the family of attrition mills (Hassibi *et al.*, 1999).

According to Hassibi and others, an attrition mill shows a power saving of up to 50% over a conventional ball mill. Moreover, it can also offer space, foundation and energy savings, as well as final grind size flexibility.

However, the capital cost of these mills and their ancillary equipment is substantially higher than that of a ball mill and should be investigated on a case by case basis (not part of this study). This research project aims to focus on dry milling as an alternative to conventional wet ball milling.

Wet grinding is typically used for FGD LSFO systems because the ground product is utilized in a wet process and the limestone, as supplied, could have a high moisture content. For dry milling, this would require a heated air source to dry the ore ultimately increasing the energy costs (Hassibi et al., 1999). However, dry grinding allows for less wear on mill linings and grinding media due to the absence of corrosion effects.

The vertical roller mill (VRM) has become a viable alternative for the ball mill arrangement because of its high grinding efficiency and the ability to dry, grind and classify within a single unit (Jorgensen, 2005).

2.4 Vertical Roller Mill

2.4.1 Background

The vertical roller mill is a dry grinding application that has been used since 1900 (Lynch, 2015). It applies breakage by compression to achieve size reduction of the ore and has a high internal circulating load. According to Lynch, the VRM is less energy intensive than the conventional ball mill.

A study conducted by Boehm et al. (2015) compared energy requirements of the vertical roller mill to that of tumbling mills on a laboratory scale basis. Three types of materials were tested; namely, marble, siderite ore and hematite ore (similar work index to limestone). It was concluded that even optimized grinding in ball mills could not produce better results than those obtained by the VRM. The VRM also consumed lower less energy than that of the laboratory scale ball mill.

2.4.2 Mechanism

In a VRM, the bed of material is exposed to a pressure high enough to cause fracture of the individual particles even though most of the individual particles are smaller than the thickness of the bed. The material bed is compacted between fixed grinding rollers and a rotating horizontal grinding table. Optimal grinding efficiency is influenced by the angle at which the tapered rollers are tilted.

Different configurations of rollers (two, three, four or six) are installed for different throughput rates. Large diameter rollers can also be arranged on a smaller grinding table surface, which is important since mill throughput increases relative to the square of the roller diameter (Loesche, 2016). Additional size reduction is achieved through shearing since the roller axis and grinding table axis do not intersect at the grinding table level.

Figure 2-6 depicts the forces utilized in a VRM.

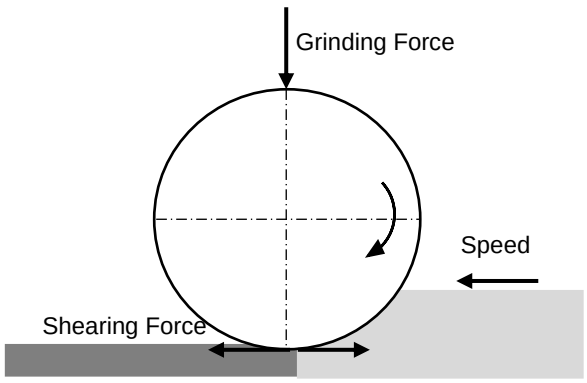

Figure 2-6: Forces Utilized in a VRM

For a given material, the mill capacity (Q) is represented by Equation 18, where the mill power in kW is divided by the energy (E) in kWh/t. According to Loesche, the power taken up by the mill can be expressed by Equation 25.

$$P = I \,.\, \mu \,.\, K_T \,.\, A \,.\, v \ \text{(kW)} \qquad 25$$

where:

A = roller surface area (one roller)

v = grinding track speed, m/s

$I =$ number of rollers

$\mu =$ friction factor (0.75 for limestone)

$K_T =$ specific roller pressure, kN/m² (100 for limestone)

Figure 2-7 depicts the different components of the Loesche VRM. Feed is introduced to the VRM either laterally (1) or centrally onto the rotating grinding table (2), after which a bed is formed between the rollers (3) and the table.

Material is pushed outward by centrifugal forces. The hot gas current (6) flows upward spontaneously evaporating any water contained in the grinding material and then captures material in the louvre ring (5), which transports the material to the classifier (7). The outlet (9) temperature ranges between 70°C and 130°C (typically 90°C).

The classifier rejects coarse material which falls back onto the grinding table (internal grit recirculation system (8)). The final product is carried by the hot gas and passes through the classifier.

A standard motor with a vertical gearbox (10) powers the mill. The force of the rollers stems from a hydraulic spring assembly and the roller weight.

A hot gas generator (HGG) is required if the moisture content of the ore is higher than 6%. However, if the material contains less than 6%, the heat generated by the fan is enough to evaporate most of the moisture. As a rule-of-thumb, the VRM exit gas stream (9) should contain less than 0.5% moisture.

Figure 2-7: Schematic of the Loesche Vertical Roller Mill

The grinding force (F_{Roller}) can be calculated by adding the roller weight (FR_{weight}) to the exerted pressure ($FR_{hydraulic}$) (Equation 26).

$$F_{Roller} = FR_{Weight} + FR_{Hydraulic} \quad (26)$$

The specific grinding force can then be calculated by dividing the grinding force by the surface area (A_{Roller}) as shown in Equation 27. The surface area is calculated by multiplying the roller width with the roller diameter (Equation 28).

$$P_{Roller} = F_{Roller}/A_{Roller} \quad (27)$$

$$A_{Roller} = W_{Roller} \times D_{Roller} \quad (28)$$

The VRM fan is responsible for pneumatically transporting the grinding product to the classifier and contributes between 45% to 60% of the overall mill power draw (Jankovic, et al., 2016). The fan motor power can be calculated using Equation 29.

$$P_{Shaft} = \frac{Flow \times Static\ Pressure \times F_{Dust} \times F_{Dyn}}{Efficiency \times 9.81 \times 3600} \quad 29$$

where:

F_{Dust} = flowrate of the dust particles (m³/h)

F_{Dyn} = dynamic flowrate of the gas stream (Nm³/h)

2.4.3 Loesche VRM Application

The Loesche VRM is predominantly employed to dry-grind coal, cement raw materials and industrial minerals, as well as mineral ores. Loesche patented the dry-grinding mill principle in 1928. In South Africa, Loesche mills are mostly utilized for coal grinding in the power industry and for grinding of cement raw materials.

2.4.4 Typical Loesche VRM Process Description

The Loesche grinding plant consists primarily of the following process stages and components:

1. Material feeding
2. Grinding and classifying
3. Rejects/circulation handling
4. Product separation
5. Mill fan
6. Hot gas generator (optional)
7. Process measuring and control technology

Loesche has two different processes for comminution; (1) overflow mode and (2) airflow mode. During overflow mode, the ground ore leaves the grinding chamber after the grinding process under its own gravitational force. The classification and grinding process are therefore separate. Conversely, in airflow mode, the material is discharged by means of an air flow via a classifier. In airflow mode, the grinding and classifying are combined in a single machine. The airflow mode will be investigated in this report.

A typical VRM airflow mode flowsheet is represented in Figure 2-8. The materials handling and VRM flowsheet will differ for each project depending on site requirements.

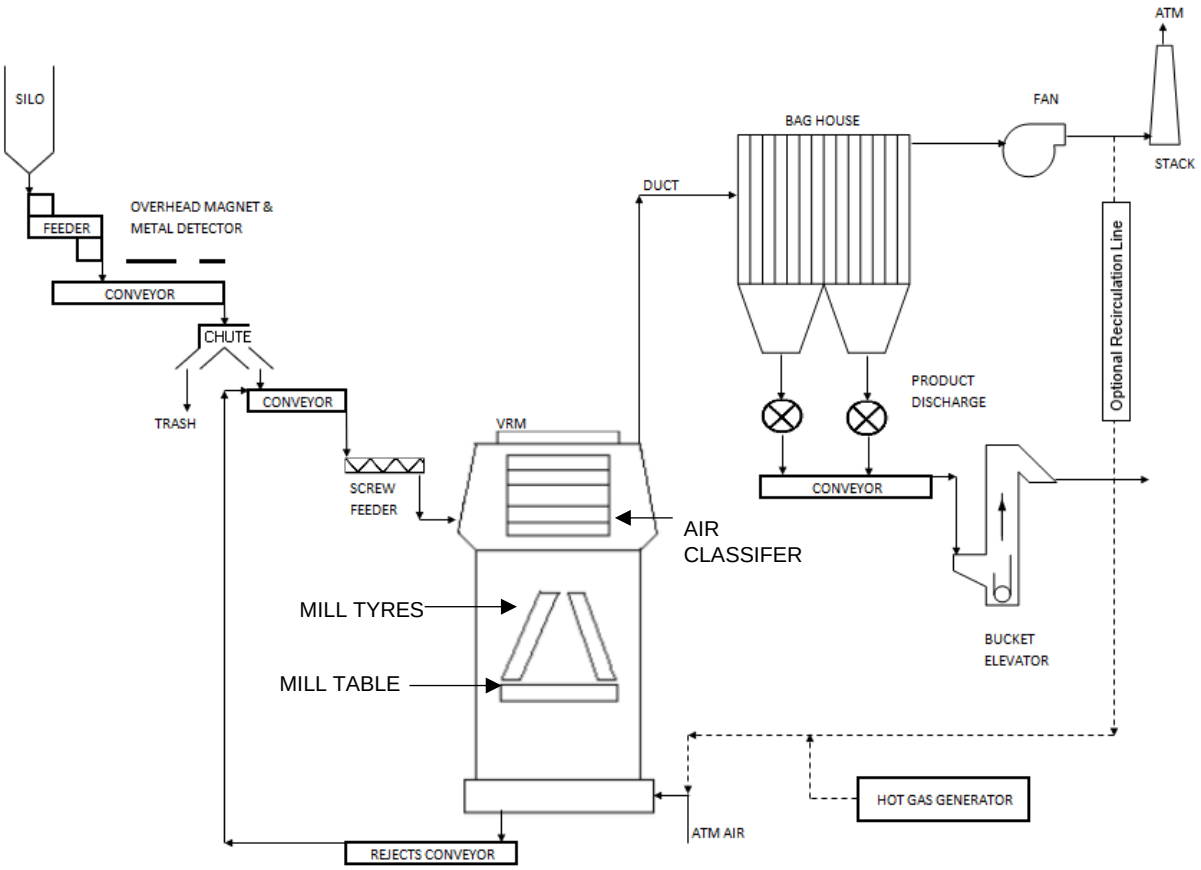

Figure 2-8: Typical VRM Flowsheet

The limestone ore is crushed and screened at Danielskuil with a cone crusher (Symons 5.5 ft short head cone crusher) to produce an 8 mm to 20 mm size range, which is delivered to Kusile for the FGD process. The limestone is initially stockpiled and subsequently reclaimed to process through the feed preparation area as illustrated in Figure 2-8.

An overhead magnet and metal detector are required ahead of the VRM to ensure no tramp metals enter the mill and damage the table or rollers. A rotary feeder is used to transfer the feed limestone (8 mm to 20 mm) into the grinding chamber and onto the center of the grinding table of the VRM. The grinding, drying and classifying of the limestone is performed inside the mill. A gearbox rotates the horizontal grinding table. Feed limestone is spread outwards due to centrifugal forces. The limestone passes under the hydro-pneumatically spring-loaded grinding rollers, which grind the material through compressive and shear force. The grinding rollers only turn because of the friction which exists between the rollers and the rotating bed of material, i.e. the rollers are not driven.

The depth of the limestone bed is determined by a dam ring around the grinding table. The limestone is ground by the rollers and flows over the dam ring entering the high velocity hot gas stream rising from the louvre ring surrounding the table.

The classifier is located directly above the grinding chamber and receives limestone from the rising hot gas stream, which travels upward through the mill body. Any moisture present in the limestone is evaporated as a result of the hot gas. The classifier, as with all milling circuits, controls the discharge size of the particles permitted to exit the circuit. Coarse particles are rejected and circulated back to the grinding table via a grit cone below the classifier rotor. The fines particles pass through the classifier and are transported through the duct to the pulse-jet-bag filter.

Ungrindable objects (such as plastic bottles, wood, or any other foreign material) are moved off the table with the louvre ring and scrapers are used to transfer the objects into a small rejects box, which can be separated via a slide gate valve from the mill and cleared. After an emergency stop, grinding material is also removed by scrapers into the rejects box.

The fine particles are transported in the gas stream generated by the mill fan and are then separated in the filter. The gas stream circulates through the mill and the complete ducting system. Mechanical flaps and/or a variable speed drive (VSD) fan are/is used to control and adjust the volumetric flow. Typically, a sampler is installed in the dust conveying route for the finished product between the bag filter and the product storage.

Distance buffers are included as a safety measure to prevent metallic contact of the grinding rollers and the grinding table.

A recirculating gas line with damper (as illustrated in Figure 2-8) is an option to retain heat (generated by the fan) within the circuit.

2.4.5 Loesche Hot Gas Generator (HGG)

As mentioned previously, if the moisture content of the ore entering the circuit is more than 6%, an HGG is required. The HGG consists of a combustion chamber with heat resistant steel with a burner muffle. Figure 2-9 illustrates the Loesche HGG, also commonly known as the LOMA Hot Gas Generator.

As a result of the flow pattern, the process gas stream cools both the protective jacket housing and the perforated jacket. The process gas enters the interior of the combustion chamber through the annular gap and holes in the perforated jacket. At this point, the gas mixes with the hot flue gases from combustion. However, the flame and hot flue gases are kept away from the perforated jacket. Typical heating media includes biogas, natural gas, blast furnace gas, and coke gas. Alternatively, fuels such as wood, lignite dust, and light and heavy oils can be used. According to Loesche, advantages of the LOMA HGG include:

- Low wear.

- Heat resistant steels are used for the combustion chamber – thus no refractory brickwork.
- Heat losses are minimized during start-up since it is not required to heat refractory brickwork.
- Good thermal shock resistance and rapid load changes with only a short delay.
- The combustion chamber has a high cooling rate which prevents overloading. An emergency chimney stack is not required in emergency-off cases and during start-up and shut-down.
- The HGG is available for inspection within a short time.
- Short installation times, small space requirement and light weight.

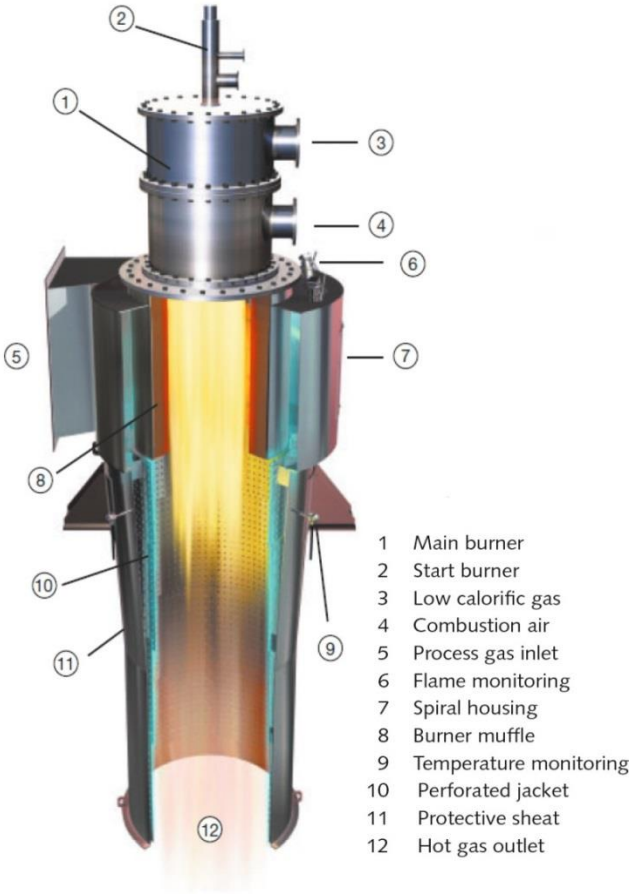

Figure 2-9: Loesche LOMA Hot Gas Generator

2.4.6 Advantages of the VRM

Advantages of the VRM include, but are not limited to, the following:

- The vertical roller mill is more energy efficient than tumbling mills based on the same size range and materials (Boehm et al., 2015). The energy consumption of the grinding plant can be reduced by between 30% and 50% for raw materials.

- There is an opportunity for off-site milling by a limestone supplier which will reduce the power plant CAPEX of an FGD system considerably. Figure 2-10 depicts the feed preparation process if limestone was milled off-site and added to the process. The saving in CAPEX will be offset to some extent by an increase in delivered limestone reagent cost.
- The VRM has a high grinding efficiency and is capable of drying, grinding, and classifying within a single unit (Jorgensen, 2005).
- The hydraulic roller relief system allows start-up of the full or empty mill with lower torque and improvement of the machine control response.
- The roller axis and the axis of the grinding table do not intersect at the grinding table level and thus create shearing forces which in turn create additional reduction.

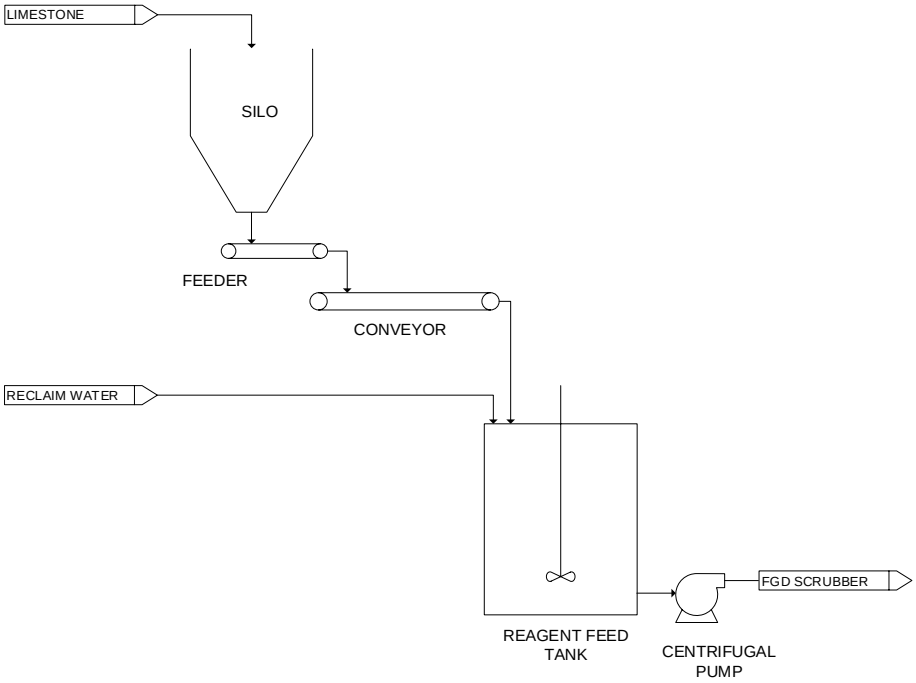

2-10: WFGD System with Reduced Feed Preparation Area because of Off-Site Milling

Wear components of the VRM include the rollers and grinding table liners. Wear resistant castings are used to reduce the grinding specific cost, maintain consistency of product fineness and increase operating cycles. Typical castings are fabricated from high chromium alloy or ductile iron base alloy with or without the inclusion of ceramic grains.

It is proposed to investigate and compare the costs and technical aspects of vertical roller milling to conventional ball milling of limestone for the WFGD process.

2.5 Ancillary Equipment Sizing

2.5.1 Classifier Hydrocyclones

A high-level calculation procedure to provide an initial estimate of the cyclone diameter and number of cyclones required has been proposed by Arterburn (2001). A multiplier (M) is selected based on the required product size (Table K-1 in Appendix K) and used to calculate the corrected cut-size (D_{50_C}) using Equation 30.

$$D_{50c}(application) = M \times \%P_{Overflow} \quad 30$$

Three correction factors (C_1, C_2, and C_3) are obtained from correlation graphs (Figure K-1, Figure K-2, and Figure K-3 in Appendix K) to account for the discrepancy in the feed density, pressure change and solid specific gravity, respectively. Equation 31 is used to calculate the base cut-size ($D_{50c}(base)$), which incorporates the correction factors.

$$D_{50c}(base) = \frac{D_{50c}(application)}{C_1 C_2 C_3} \quad 31$$

The cyclone diameter and flowrate are obtained from correlation graphs as illustrated in Figure K-4 and Figure K-5, respectively. The number of units is then calculated by dividing the total flowrate by the flow per unit.

2.5.2 Pumps

A centrifugal pump converts rotational energy of its impeller to energy in a moving fluid. Mechanical energy from the pump's engine is transformed to kinetic energy, which is subsequently transformed to hydrodynamic energy in a moving fluid. The basic principle of centrifugal pumping is to transport volumes of fluid or slurry from a low-pressure region to a high-pressure region (Wilson and Addie, 2006). The pump's impeller transfers a slurry from a lower reservoir (point A) to a higher reservoir (point E) as illustrated in Figure 2-11.

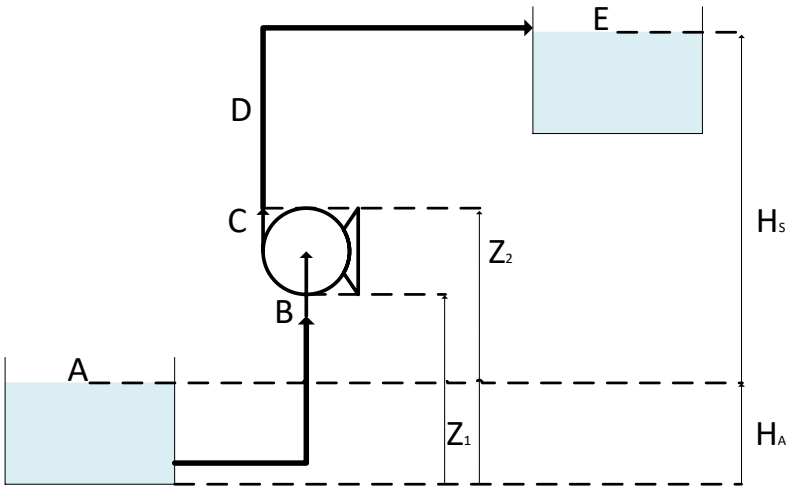

Figure 2-11: Schematic of Centrifugal Pumping Principle

The mechanics and impeller of the pump allows for the pressure inside the pump to be lower than the pressure inside the lower reservoir. This pressure difference allows for the slurry to flow from the lower reservoir to the pump, which causes entry loss (a pressure decrease of slurry while it enters into the suction pipe) and a pressure decrease of slurry while it flows through the pipe due to friction between the slurry and the inner surface of the pipe (Wilson and Addie, 2006). Pressure losses can also occur due to valves, fittings and bends in the pipelines. The same losses are observed when a slurry is pumped through the discharge line to the upper reservoir. The total head at point B (H_B) and C (H_C) is represented by the Bernoulli Principle shown in Equation 32 and Equation 33, respectively (Wilson and Addie, 2006).

$$H_B = \frac{P_B}{\rho g} + \frac{v_B^2}{2g} + z_1 \quad 32$$

$$H_C = \frac{P_C}{\rho g} + \frac{v_C^2}{2g} + z_2 \quad 33$$

where:

$P_B, P_C =$ pressure at point B and point C

$v_B, v_C =$ velocity at point B and point C

$z_1, z_2 =$ height of point B and point C

The total head (H) is therefore the difference between the head at point C and point B, which is shown in Equation 34.

$$H = \left(\frac{P_C}{\rho g} - \frac{P_B}{\rho g}\right) + \left(\frac{v_C^2}{2g} - \frac{v_B^2}{2g}\right) + (z_2 - z_1) \quad 34$$

The total head (H) can be related to the total suction head (H_S) by considering the additional losses, such as entry losses, losses due to friction and losses due to valves and fittings. The velocity and pressure at points A and E is equal to zero since it is stationary and open to the atmosphere. The height of point A and point E is H_A and ($H_A + H_S$), respectively. Therefore, the total head for the system illustrated in Figure 2-11 is shown in Equation 35 (Wilson and Addie, 2006).

$$H = H_S + \sum h_{losses} \quad 35$$

where $\sum h_{losses}$ is the sum of all the pressure losses in the pipe, including valves, fittings, bends, friction and entry losses.

Sizing of centrifugal pumps is conducted using Equations 59 through 89 listed in Table L-1 of Appendix L. It should be noted that a design factor of 15% is typically added to the volumetric flow rate used in the pump calculations.

2.5.3 Platework: Tanks, Hoppers, Chutes and Bins

Tanks are sized based on their residence time, volumetric flowrate and geometric shape. The residence time is selected based on the required buffer capacity. A higher residence time translates to increased buffer capacity but increased platework cost. Tanks can be cylindrical or rectangular with a flat, conical, or slanted bottom. The volume of the conical bottom (CB) or sloped bottom (SB) is shown by Equations 36 and 37, respectively.

$$V = \frac{1}{3}\pi r^2 h_b \quad (36)$$

$$V = \frac{\pi r^2 h_b}{2} \quad (37)$$

where h_b is the height of the sloped or conical bottom.

The total amount of steel required for each tank consists of the tank platework, tank legs, flanges and stiffeners, nozzles, cover plate and extras (such as brackets, etc.). Freeboard is the difference between the height of the slurry level in the tank and the total height of the tank, i.e. it is the clearance maintained between the maximum slurry level and the tank height to reduce spillage or overflow. The amount of steel required for fabrication of a tank is illustrated by Figure 2-12. The calculations for steel used for tanks and chutes are described in more detail in Appendix F.

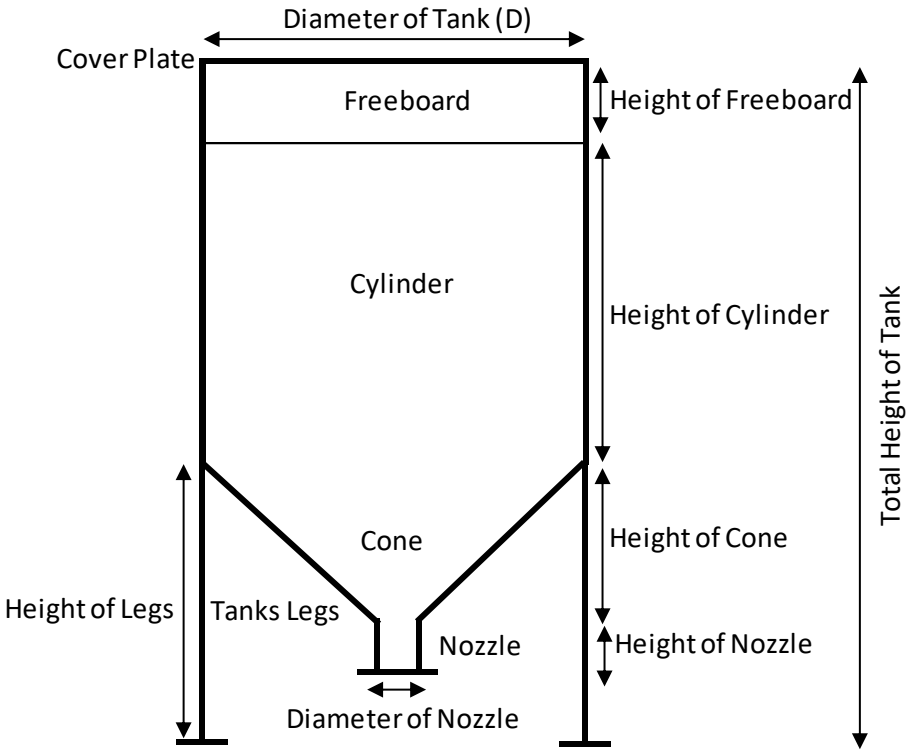

Figure 2-12: Steel Components of a Tank/Sump

2.5.4 Conveyors

Conveyors are sized based on the ore size, tonnage and lift requirements. The mass of the moving parts, $m_{moving\ parts}$ in kg/m, is calculated using Equation 38, where the rolling mass (in kg) and spacing (in m) of both the carry idlers and return idlers are known.

$$m_{Moving\ Parts} = 2m_{Belt} + \frac{m_{Rolling\ Mass,Carry\ Idlers}}{m_{Idler\ Spacing,Carry\ Idlers}} + \frac{m_{Rolling\ Mass,Return\ Idlers}}{m_{Idler\ Spacing,Return\ Idlers}} \quad 38$$

The belt mass, m_{Belt}, in kg/m is calculated using Equation 39.

$$m_{Belt} = W_{Belt}(1.13T_{Cover} + 2.8 \times PN_{Plies}) \quad 39$$

where:

W_{Belt} = width of the belt (m)

T_{Cover} = cover thickness (mm)

PN_{Plies} = polyester nylon number of plies

The friction power, $P_{friction}$ (kW), is calculated from Equation 40.

$$P_{Friction} = K_e(L_h + C_T) \times \frac{3.6m_{Moving\ Parts}v_{Belt}}{367} + K_L(L_{h,L} + C_T) \times \frac{m_{Design}}{367} \quad 40$$

where:

K_e = empty friction coefficient

h_L = horizontal length

C_T = terminal friction constant

v_{belt} = belt velocity

K_L = load friction coefficient

$L_{h,L}$ = horizontal loaded length

m_{Design} = design tonnage

The motor sizing power of the conveyor is the sum of the friction power, lift power and any additional tension. The motor power is selected based on the standard motor sizes as indicated in Table K-4 in Appendix K.

2.6 CAPEX Estimation

2.6.1 The Fixed Capital Investment (FCI)

The Fixed Capital Investment (FCI) or Capital Expense (CAPEX) of a project is the total cost of designing, constructing and installing a plant. It consists of the direct costs (D) and indirect costs (I) as indicated in Equation 41 (Peters and Timmerhaus, 1991).

$$FCI = Direct\ Costs + Indirect\ Costs \quad (41)$$

Components of the direct and indirect costs are listed in Table G-1 in Appendix G.

The total capital investment (TCI) consists of the FCI, contractor's fee (CF), contingency (C) and working capital (WC). The WC is the additional capital required after the FCI to start the plant and operate it until it starts earning revenue, i.e. a provision in the funds required to purchase equipment and complete installation. It is the sum of the inventories, trade receivables and cash, subtracted by the trade payables. The working capital is typically 15% of the TCI (Towler and Sinnott, 2008), and consists of the following:

- Two weeks' worth of raw material.
- Value of the product: two weeks' cost of production.
- Cash flow: one week's cost of production.
- Accounts receivable: one month's cost of production.
- Credit for accounts payable: one month's delivery cost.
- Spare parts estimate: 1% to 2% of the cost of the plant.

2.6.2 Types of Cost Estimates

The accuracy of a cost estimate depends on the phase of a project. Different phases of a project contain varying amounts of detailed engineering to predict the cost of the project as depicted in Table 2-6 (Towler and Sinnott, 2008).

Table 2-6: Type of Cost Estimates and the Corresponding Study Phase/Accuracy

Type of Cost Estimates			
Cost Estimate	**Description**	**Typical Study Phase**	**Accuracy**
Order of Magnitude Estimate	Extrapolate similar plant cost	Conceptual Study	±30%
Study Estimate	Knowledge of major pieces of equipment	Pre-Feasibility Study	±30%
Preliminary Estimate	Enough for budget authorization	Feasibility Study	±20%
Definitive Estimate	Basic on engineering and quotes from suppliers and contractors	Definitive Feasibility Study	±10%
Detailed Estimate	Based on detailed engineering	Front End Engineering Design (FEED)	±5%
Check Estimate	Based on complete design and concluded negotiations on procurement	As-bid	±5%

2.6.3 Method of Calculating Capital Investment

Table G-2 in Appendix G depicts the typical percentages of the FCI for direct and indirect cost segments (Peters et al., 2003). In this study, the percentage of the mechanical cost method is used to determine the components of the TCI of the two circuits.

An equation for computing the total direct and indirect costs has been proposed by Peters *et al.* (2003) and is provided below (Equation 42). This equation caters for the different components of the direct and indirect costs by multiplying the relevant factors with the equipment cost. The contractor's fee and contingency are then factored to the sum of the direct and indirect costs. The FCI is therefore the sum of the direct costs, indirect costs, contractor's fee and contingency. The working capital is 15% of the TCI.

$$C_n = \left[\sum E + \sum (f_1 E + f_2 E + f_3 E + \cdots)\right] f_I \qquad 42$$

where:

C_n = cost estimate

E = purchased equipment cost

$f_1, f_2, \ldots$ = multiplying factors for piping, electrical, instrumentation, etc.

f_I = indirect cost factor (always > 1)

Table G-3 in Appendix G shows the different percentages of the purchased equipment cost for a solids, slurry and fluid processing plant (Peters and Timmerhaus, 1991).

2.7 OPEX Estimation

The operational expenditure (OPEX) of a plant is the cost required to operate and maintain the plant to ensure production. It can be divided into manufacturing costs and general expenses. The manufacturing costs consist of direct production costs, fixed charges and plant overhead costs. The direct production costs include the following:

- Raw materials
- Operating labor
- Utilities (electricity, water, etc.)
- Maintenance and repairs
- Operating supplies
- Laboratory charges
- Patents and Royalties
- Reagents

The electricity charge applicable to a processing plant, such as an FGD feed preparation plant, includes the active power charge and the maximum demand charge. The latter refers to the maximum power value reached during an integrated period (usually 30 minutes) within the billing period. A penalty is payable on the electricity bill if the value is higher than the contracted power. Equation 43 presents the calculation for the maximum demand of a plant.

$$Maximum\ Demand = Connected\ Load \times \frac{Load\ Factor}{Power\ Factor} \quad (43)$$

where the load factor is the product of the utility factor and the diversity factor.

The distribution network capacity (R/kVA/month) is based on the voltage of supply and the annual utilized capacity measured at the point of distribution (POD) during all time periods. The distribution network demand charge (or maximum demand charge) is based on the voltage of supply and the chargeable demand measured at the POD applicable during peak and standard periods.

Table H-1 in Appendix H shows the distribution network charges as outlined in the Eskom 2019/2020 tariff book. The total monthly charge for a voltage between 500 V and 66,000 V is therefore R57.93 per kW per month.

2.8 Profitability Evaluation

2.8.1 Payback Time

An initial estimate for calculating the payback time of any plant is dividing the average annual cash flow by the total investment (refer to Equation 44), i.e. sum of the fixed capital investment and working capital (Towler and Sinnott, 2008).

$$Simple\ payback\ time = \frac{total\ investment}{average\ annual\ cash\ flow} \quad (44)$$

The assumption surrounding this equation is that all the capital is invested in year 0 and the revenue starts immediately, which is not generally the case. Realistically, the investment is spread over the first three years, and revenues only reach 100% after the second year of operation. No taxes or depreciation are considered in this equation.

2.8.2 Return on Investment

The return on investment (ROI) is where the net annual profit is divided by the total investment (Towler and Sinnott, 2008). Equation 45 is used to calculate the ROI as an average over the whole project.

$$ROI = \frac{cumulative\ net\ profit}{plant\ life\ \times initial\ investment} \times 100\% \quad (45)$$

The pre-tax ROI is often used (refer to Equation 46) if the depreciation term is less than the plant life and if an accelerated method of depreciation is used. The net present value (NPV) is then typically calculated. The pre-tax ROI does not include the depreciation charge.

$$pre\ tax\ ROI = \frac{pre\ tax\ cash\ flow}{total\ investment} \times 100\% \quad (46)$$

2.8.3 Net Present Value (NPV)

A more useful economic measure than the payback period or ROI is the net present value (NPV), because it allows for the time value of money and any annual variation in expenses and revenues. The NPV of a project is the sum of the present values (PV) of the future cash flows as indicated in Equation 47 (Towler and Sinnott, 2008). The initial investment is a negative cashflow.

$$NPV = \sum_{n=1}^{n=t} \frac{CF_n}{(1+i)^n} \quad (47)$$

where:

$CF_n =$ cash flow in year n

$i =$ interest rate

$t =$ life of plant in years

2.8.4 Interest Rate of Return (IRR)

The discounted cash flow rate of return (DCFROR) or interest rate of return (IRR) is the interest rate (i') at which the NPV is equal to zero as indicated in Equation 48 (Towler and Sinnott, 2008).

$$\sum_{n=1}^{n=t} \frac{CF_n}{(1+i')^n} = 0 \quad (48)$$

The IRR indicates the maximum interest rate that the project could pay and still break even by the end of the project life.

2.8.5 Depreciation and Salvage Value

For new and unused equipment in South Africa, PricewaterhouseCoopers (PWC) recommends a depreciable charge at a rate of 40% for the first year and 20% in the three following years. Therefore, if the life of the plant is longer than four years, there will be zero salvage value at the end of the plant life. This depreciable charge method is supported by Deloitte (Taxation and Investment in South Africa 2017).

2.9 Conclusion

It is seen from the reviewed factors that comparison of the two processing routes is a complex issue that requires meticulous evaluation of all the factors that can impact on the overall costs. There is also need for some contingency allowance for some unknown factors.

3. Methodology

3.1 Overview: Technical and Economic Evaluation

The technical and economic comparison is based on a limestone milling capacity of 100 t/h (dry basis) which is similar to the capacity specified for Eskom's Kusile wet limestone FGD installation. The limestone samples were obtained from Idwala Lime's Danielskuil mine and crushed/screened using the same ore body for both the ball mill and VRM testwork campaigns. This is the same site where Kusile sources their limestone for the FGD operation. The required data was sourced as described below.

1. <u>Wet limestone milling – ball mill operation:</u>
   - Operating data and flowsheet information from Eskom's Kusile FGD plant (including site walk).
   - Testwork at Mintek:
     - Limestone specific gravity with Gas Pycnometer.
     - Ball mill locked cycle test to determine specific energy consumption.
   - Published data on wet limestone milling plants including Medupi case study.

The battery limits of the wet limestone milling circuit cover the extraction point of the feed bin/silo and extend to the FGD reagent feed tank (Figure 3-1).

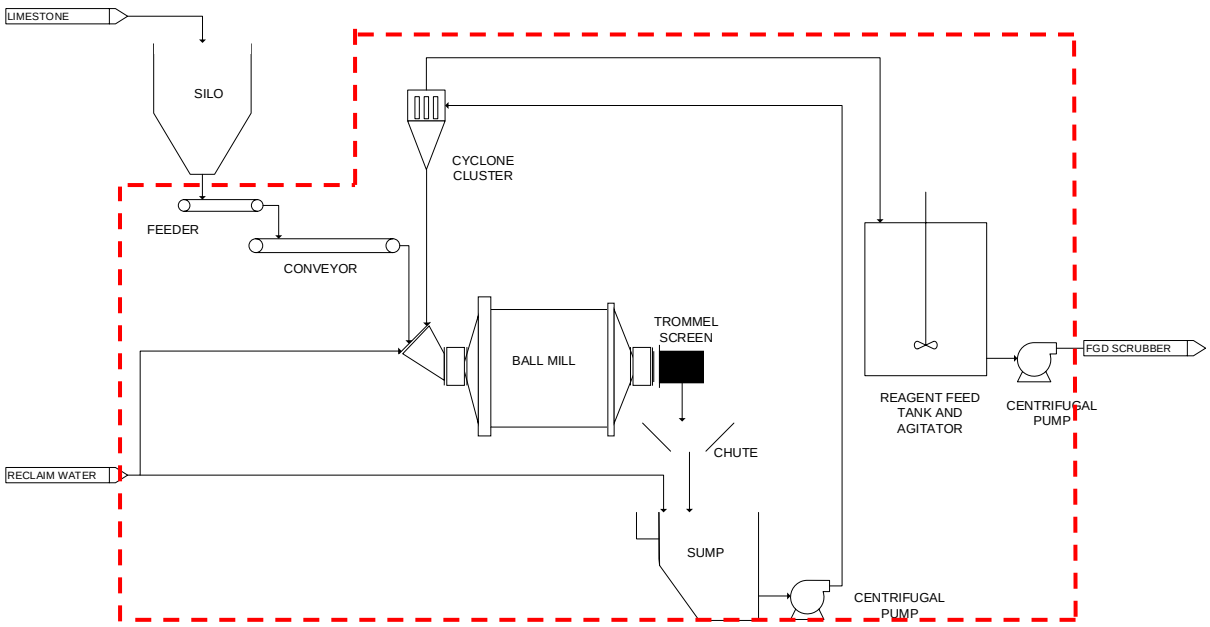

Figure 3-1: Battery Limits of Wet Limestone Ball Milling in FGD Feed Preparation Area

2. <u>Dry limestone milling: Vertical roller mill (VRM) operation:</u>

- Pilot-scale VRM testwork was conducted at the Loesche Test Centre in Germany using a limestone sample (96% $CaCO_3$) from the same source currently used by Kusile (Danielskuil, Idwala Lime).
- Technical and costing information from Loesche, South Africa.

Testwork allows for the comparison of power draw and grinding efficiency of the ball mill and VRM. Information obtained from test work was used to calculate and compare the capital expenditure and plant operating costs of dry milling versus wet milling.

The VRM circuit has the same battery limits as for the wet milling circuit on-site as depicted in Figure 3-2.

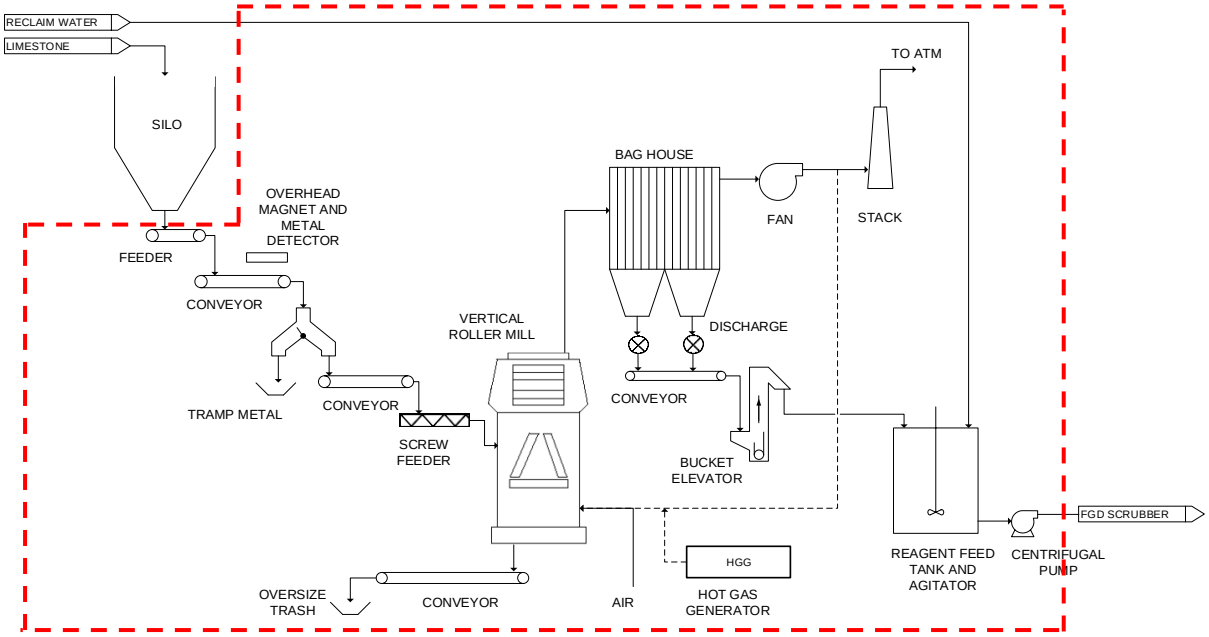

Figure 3-2: Battery Limits of Dry Limestone Milling by Vertical Roller Mill in FGD Reagent Preparation Area

3.2 Facilities

A summary of the facilities that were used throughout the duration of this study is presented in Table 3-1 below.

Table 3-1: Facilities used to Conduct Testwork or Analyze the Sample

Test	Equipment	Location	Date Completed
Chemical composition	XRF Analysis	Idwala, South Africa	12 Aug 2019
Size reduction (-19 mm)	Crushing and screening	Idwala, South Africa	12 Aug 2019
Specific gravity of sample	Gas Pycnometer	Mintek, South Africa	9 Dec 2019
Particle size distribution	Screen analysis	Mintek, South Africa	9 Dec 2019
Wet Locked Cycle Test (LCT)	Laboratory-scale ball mill	Mintek, South Africa	13 Dec 2019

Dry VRM pilot-scale test	Vertical Roller Mill	Loesche, Germany	3 Dec 2019
Site walk (existing plant)	N/A	Kusile, South Africa	27 Jan 2020

3.3 Sample Preparation

Idwala Industrial Holdings Ltd (Idwala Lime) supplied 2 tons of limestone sample for the VRM testwork and 60 kg for the ball mill testwork required for this study.

Idwala Lime operates a high-grade calcitic limestone (approximately 96% $CaCO_3$) mining and lime production facility near Danielskuil in the Northern Cape, South Africa. Limestone obtained from the open cast mine is crushed and screened to produce the required stone size ranges for the lime kiln plant and for stone product sales. The required P_{100} of 19 mm (specified by Loesche GmbH) was drawn from a product stockpile that matched this sizing. The chemical composition of the samples was determined through XRF analysis. The 60 kg sample was shipped to Mintek, South Africa, for laboratory scale ball mill testwork. The 2 tons sample was shipped to Loesche, Germany, for the pilot-scale VRM testwork.

3.4 Wet Milling Testwork

3.4.1 Eskom's Kusile Operation

A site visit was completed on the 27th of January 2020 at the current FGD limestone milling operation at Eskom's Kusile plant. During the site visit, information regarding the operating conditions, equipment (major and ancillary), materials handling, wear rates and utilities surrounding the wet milling operation was shared. This information was used as the basis for calculating the costs involved with wet limestone milling (refer to Section 4.1.1 for relevant information).

3.4.2 Mintek

Wet laboratory-scale ball mill testwork was conducted at Mintek during the week of the 9th of December 2019. The chemical composition of the 60 kg limestone sample was analyzed at Danielskuil prior to delivery at Mintek and was found to contain 96.3% $CaCO_3$ (refer to Figure J-1 and Figure J-2 in Appendix J). Particle size analysis was conducted on a sub-sample of the 60 kg limestone using sieves and a laboratory scale (refer to Figure J-5 and Figure J-6 in Appendix J, respectively). The specific gravity (SG) of the limestone was determined using a Gas Pycnometer. The locked cycle test was conducted using a laboratory-scale ball mill and interconnected software, which determines the specific energy exerted per ton of limestone.

3.4.2.1 Procedure: Gas Pycnometer (Solids Specific Gravity)

The procedure that was followed to determine the specific gravity of the limestone sample is described in Appendix O.

A Gas Pycnometer determines the specific gravity of a solid by detecting the pressure change as a result of gas displacement by the solid object. A baseline is established by inserting a gas at a known pressure into an empty chamber and then measuring the pressure. A solid is then added to the chamber and the gas (at the same pressure) is expanded into the sample chamber again. The difference between the original pressure reading and the newly measured pressure with the known volume of the empty chamber allows the volume of the sample to be determined (gas law).

3.4.2.2 Procedure: Locked Cycle Test

3.4.2.2.1 Operating Conditions

The grinding mill conditions were calculated prior to starting the locked cycle test (refer to Table A-1 and Table A-2 for the grinding conditions and ball charge, respectively). The laboratory-scale ball mill at Mintek used for this testwork has an inside diameter (D_i) of 0.265 m and an inside length (L_i) of 0.305 m. Assumptions were made during testwork because the operating conditions of the Eskom Kusile operation were not available at the time of conducting this testwork. The following assumptions were made:

- Percentage grinding media in the mill: 35%
- Slurry solids volume percentage: 45%
- Circulating load: 250%
- The target mill speed: 64 rpm (as advised by Mintek).

3.4.2.2.2 Locked Cycle Test

Figure 3-3 illustrates the locked cycle test flowsheet that was used during testwork. Figure J-11 in Appendix J presents the ball mill set-up at Mintek (open position). The procedure is described below:

1. The grinding conditions were determined as discussed in Section 3.4.2.2.1.
2. The mill was loaded with the calculated mass of limestone, water and grinding media composition (refer to Figure J-12 in Appendix J).
3. The mill was closed (refer to Figure J-13 in Appendix J), the software used to track the mill energy consumption was calibrated (refer to Figure J-14 in Appendix J), after which the mill was started.
4. The mill ran until the first arbitrary specific energy set point was reached and then stopped. The time the mill took to reach the set-point was also recorded.
5. The mill was opened, and the slurry was discharged into a bucket (slurry on the steel balls and inside the mill was washed off with raw water).
6. The slurry was then fed to a Roligan vibrating screen (refer to Figure J-15 in Appendix J) with a screen aperture of 53 µm. Water was added during screening until the

underflow was clear of solids. The oversize and undersize were collected separately in buckets.

7. The undersize was filtered with a pressure filter and placed in an industrial scale oven at 80°C.
8. The oversize was weighed, filtered and dried. The dried oversize was weighed again and the percentage solids in the wet oversize was subsequently calculated using Equation 49.

$$\%Solids = \left(1 - \frac{wet\ mass - dry\ mass}{wet\ mass}\right) \times 100 \qquad 49$$

9. The new specific energy target was calculated using the Specific Energy Target Calculation (refer to Section 3.4.2.2.3)
10. The oversize solids concentration was assumed to be constant, i.e. it was assumed that the moisture in the oversize remained relatively constant for all runs.
11. The make-up solids were combined with the dried oversize solids to ensure the total mass of solids in the mill for the second run was equal to the mass initially added (as illustrated in Figure 3-3).
12. Step 2 and step 3 were repeated. The mill ran until the new specific energy set point was reached and timed, after which the slurry was cleaned from the mill and processed over the Roligan screen. Water was added to the screen until the underflow was clear of solids.
13. Step 7 was repeated for the undersize.
14. The wet oversize was weighed. The mass of water and solids were calculated using the assumed constant solids concentration calculated in Step 8. The make-up solids and water were then weighed and combined with the wet oversize and fed to the mill together with the grinding media.
15. Steps 9, 12, 13 and 14 were repeated 8 times until the specific energy stabilized, i.e. three runs in a row reached a similar specific energy.

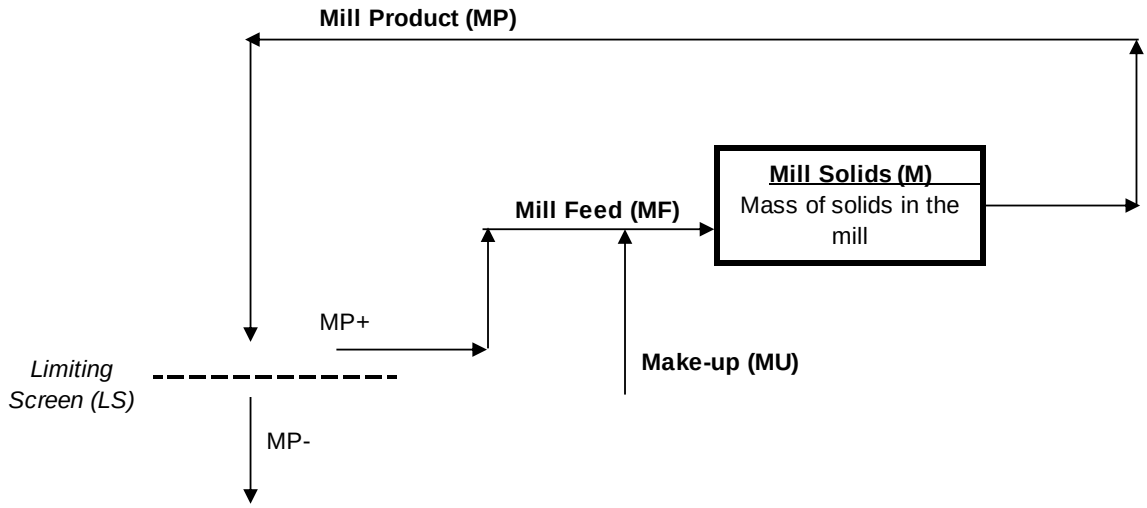

Figure 3-3: Flowsheet of Locked Cycle Test Procedure

3.4.2.2.3 Locked Cycle Test Specific Energy Target Calculation

The energy input (E_{Input}) of the previous run was calculated from Equation 50 by multiplying the mass of solids (m_S) by the actual specific energy input (E_{actual}) that was achieved for that run.

$$E_{input} = m_s \times E_{actual} \quad (50)$$

The assumed oversize dry mass was calculated by multiplying the assumed oversize solids concentration fraction with the wet oversize mass. The assumed undersize dry mass is therefore the mass of the solids added to the mill minus the assumed dry oversize mass. The undersize production rate is the dry undersize mass divided by the energy input from Equation 50. The energy required to produce the target undersize (E_{Target}) is represented by Equation 51.

$$E_{Target} = \frac{m_s}{\left(1 + \frac{Recirculation\ Load}{100}\right)} \frac{1}{Undersize\ Production\ Rate} \quad (51)$$

The energy input for the next cycle ($E_{input,new}$) is represented by Equation 52. The circuit specific energy was calculated as the energy input divided by the dry solids in the undersize as represented in Equation 53.

$$E_{input,new} = \frac{E_{target}}{m_s} \quad (52)$$

$$E = \frac{E_{input}}{dry\ solids\ mass\ in\ underflow} \quad (53)$$

3.5 Dry Milling Testwork

Loesche conducted dry milling test work at their VRM pilot plant facility in Düsseldorf, Germany. Three laboratory LM3.6 grinding mills are available at the Loesche test plant for performing grinding tests.

The laboratory-scale VRM was fed with minus 19 mm limestone ore. The power draw was measured at a product fines generation of 85% and 95% minus 45 µm. A particle size analysis was conducted on the feed and product. Figure 3-4 illustrates the pilot-scale VRM with a view of the grinding table, feed tube and rollers.

Figure 3-4: Picture of a Laboratory Scale Vertical Roller Mill (Boehm et al., 2015)

After completion of the testwork, the following information was provided by Loesche:

1. Mill, classifier and fan power consumption for operation at 85% and 95% minus 45 µm.
2. Mill size (100 t/h at 95% minus 45 µm), including table diameter and roller diameter, for CAPEX costing and maintenance spare parts costs.
3. Expected working life of wear components (hours: grinding table liners and mill rollers) from which the wear rate per ton of feed material can be calculated.

Figure 3-5 depicts the sample and test flow diagram for the dry milling conducted by Loesche.

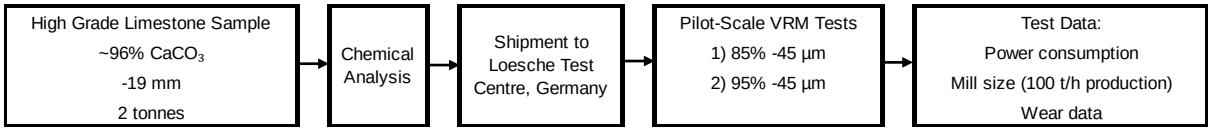

Figure 3-5: Sample and Test Flow Diagram for Dry Milling Test Work

3.6 Deliverables

The deliverables that were identified to complete this project include:

- Testwork results analysis and discussion.

- Block Flow Diagram's (BFD's): a simplified high-level overview of the process used to understand the basic structure of the circuit.
- Process Design Criteria (PDC's): the set of criteria for each circuit and unit operation that the process must abide by (this is the basis of the design).
- Process Flow Diagrams (PFD's): a diagram to present the general flow of plant processes and equipment, and how the major equipment of a plant is integrated.
- Typical Piping and Instrumentation Diagrams (P&ID's): a detailed diagram that displays each piece of equipment, piping, instrumentation and control.
- Mechanical Equipment Lists (MEL's): a list of all the equipment to be bought and delivered to site. The list includes a description of each item and sizing detail (including installed power).
- CAPEX comparison
- OPEX comparison
- A list of all excluded items that were not considered in this project.

During the Kusile site visit, it was identified that two ball mills (with a third ball mill on standby) are used to process 100 t/h, i.e. 50 t/h per mill. However, the testwork programs were based on a single mill processing 100 t/h. For comparability, both the dry and wet milling applications are investigated on a 100 t/h basis.

As mentioned previously, if the moisture content of the feed to the Loesche VRM is higher than 6%, an HGG is required to generate heat for the circuit (which will increase the CAPEX and OPEX). Since the reported limestone moisture content is 0.3%, the HGG is excluded from the main cost comparison; however, a second cost estimate is provided for the scenario where an HGG is required.

The stockpile and conveying areas are large enough so that the maximum rainfall in Delmas (where Kusile is situated) will not increase the moisture content of the limestone feed to more than 6%. The silo is also covered to avoid dilution with rainfall.

The three scenarios that are investigated therefore include:

1. Single 100 t/h wet ball mill circuit (1100): includes all deliverables listed above.
2. Single 100 t/h VRM circuit without HGG (2100): includes all deliverables listed above.
3. Single 100 t/h VRM circuit with HGG (2200): only a cost estimation is provided.

3.6.1 Document Numbers

Table 3-2 presents the drawings or documents included in this report. The first three letters of the document number indicate the document type. The first number after the three letters is either a 1 (wet system) or 2 (dry system). The second number after the three letters indicates

the major option (1) or the alternative/additional consideration (2) – HGG as discussed in Section 3.6. The last number refers to the page number. A list of drawing equipment symbols and abbreviations is set out in Appendix M.

Table 3-2: Drawing and Document Number Index

Drawing Number	Drawing Name	Page Number
BFD1101	Ball Mill Circuit Block Flow Diagram	1
BFD2101	VRM Circuit Block Flow Diagram	1
PFD1101	Ball Mill Circuit Process Flow Diagram	1
PFD2101	VRM Circuit Process Flow Diagram	1
PFD2201	VRM Circuit with HGG Process Flow Diagram	1
PID1101	Ball Mill Circuit Piping and Instrumentation Diagram	1
PID1102	Ball Mill Circuit Piping and Instrumentation Diagram	2
PID1103	Ball Mill Circuit Piping and Instrumentation Diagram	3
PID1104	Ball Mill Circuit Piping and Instrumentation Diagram	4
PID1105	Ball Mill Circuit Piping and Instrumentation Diagram	5
PID2101	VRM Piping and Instrumentation Diagram	1
PID2102	VRM Piping and Instrumentation Diagram	2
PID2103	VRM Piping and Instrumentation Diagram	3
PID2104	VRM Piping and Instrumentation Diagram	4
PID2105	VRM Piping and Instrumentation Diagram	5
Document Number	**Drawing Name**	**Page Number**
PDC1101	Ball Mill Circuit Process Design Criteria	1
PDC2101	VRM Circuit Process Design Criteria	1
MEL1101	Ball Mill Circuit Mechanical Equipment List	1
MEL2101	VRM Circuit Mechanical Equipment List	1
CAP1101	Ball Mill Circuit Capital Expenditure	1
CAP2101	VRM Circuit Capital Expenditure	1
CAP2201	VRM Circuit with HGG Capital Expenditure	1
OPE1101	Ball Mill Circuit Operational Expenditure	1
OPE2101	VRM Circuit Operational Expenditure	1

3.7 Costing

Costing analysis plays an important role in an organization's decision-making process and allows investigation into the development of any new process or process modification, for example, using the VRM as opposed to a conventional wet ball mill. Following testwork, quotations were obtained for the mechanical equipment in all three options; the two main options and one alternative option (as discussed in 3.6).

Except for Loesche, no vendor information is supplied in this document due to confidentiality agreements. However, for most of the equipment, budget quotations were obtained from multiple vendors (for the same piece of equipment, such as the ball mill) to ensure a more accurate estimate of the project cost. Furthermore, the same cost was selected for a piece of equipment that occurs in both circuits (such as a feeder, conveyor, etc.), to ensure the options are comparable.

The components of the FCI are based on a percentage of the mechanical cost as described in Table G-3 in Appendix G. The operational costs were estimated separately (based on testwork) and are discussed further in Section 4.8.

4. Results and Discussion

4.1 Testwork

4.1.1 Kusile Wet Milling Information

A site visit to Kusile Power Station was completed on the 27th of January 2020. The Kusile feed preparation area consists of three 59 t/h closed ball mill circuit trains (two duty and one standby) as illustrated in the block flow diagram below (Figure 4-1).

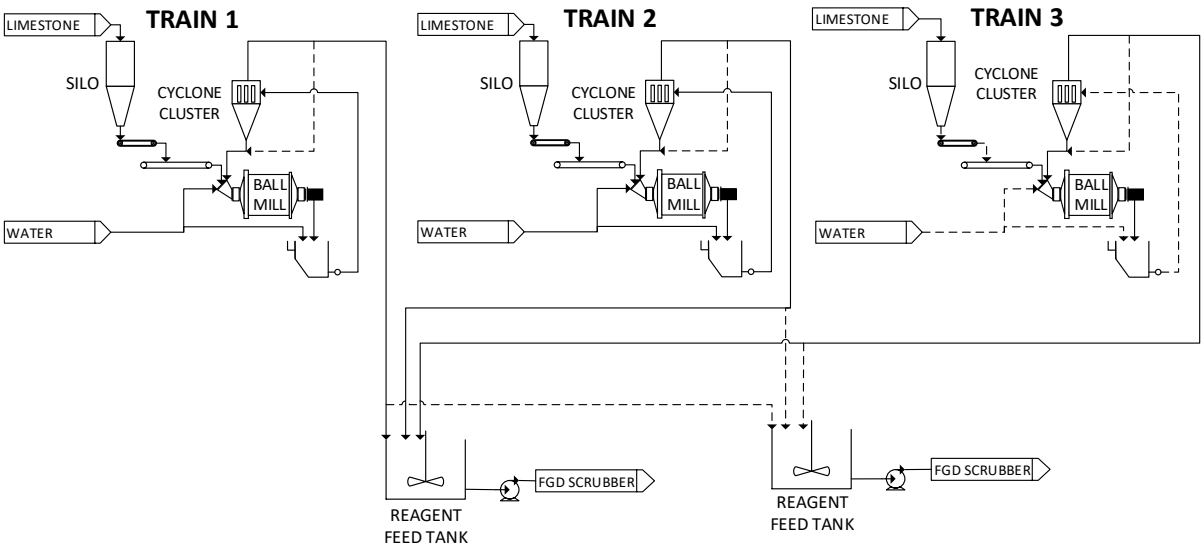

Figure 4-1: Kusile Power Station Feed Preparation Block Flow Diagram

Limestone is transported from Idwala Lime's Danielskuil mine site to the truck discharge facility at Kusile. The trucks discharge into an underground hopper feeder and conveyor system, after which it is stockpiled via a stacker machine.

The limestone is reclaimed as required and conveyed into the daily storage silos prior to being fed to the ball mills. The limestone is extracted from the daily storage silo via a variable speed belt feeder and discharged onto a horizontal conveyor, which transports the limestone to the ball mill feed chute. The three ball mill trains have identical circuits (mill and cyclone cluster) and capacities (59 t/h each). Water is also added to the ball mill to decrease the solids concentration from 99.7% fresh limestone feed to 71.0% solids inside the ball mill. The process water used for milling is recycled water recovered from the downstream water reclamation process.

Each mill has a ball loading system used to top-up the grinding media. The grinding media composition is depicted in Table 4-1. The grinding media load makes up 28.5% of the total mill load (442 tons). As the grinding media wears, the power draw (as seen in the control room) decreases and additional grinding media is added until the original power draw of 1,563 kW is

obtained. This corresponds to a specific energy consumption of 26.5 kWh/t. The grinding media wear rate was found to be 550 g/t.

Table 4-1: Grinding Media Steel Ball Charge (Kusile)

Ball Diameter (mm)	Ball Mass (t)
60	35
50	38
40	31
30	13
25	9
Total	**126**

The mill is fitted with a trommel screen at its discharge, which removes any oversize (plus 1 mm) material or worn grinding media. The trommel screen undersize flows into the ball mill underflow sump. Water is added to this sump to reduce the solids content to 55%. The slurry is then pumped to the cyclone cluster located directly above the ball mill. The cyclone cluster consists of 14 cyclones (12 duty and 2 standby). The overflow from the cyclone cluster (approximately 40% of solids fed to the cyclone cluster end in overflow) flows by gravity to the reagent feed tank, while the underflow is recycled back to the mill feed. The overflow is also initially recycled to the ball mill to build up the circulation load of 400%.

There are two reagent feed tanks, and any of the three trains can discharge into either of these two tanks.

The total installed power of each mill is 1,900 kW, i.e. 3,800 kW for two mills in operation. An installed power of 3,700 kW for a 100 t/h mill with the same conditions was recommended by a ball mill supplier.

Information provided by Kusile is summarized in Table 4-2.

Table 4-2: Limestone Feed Preparation Parameters at Kusile Power Station (27 January 2020)

Parameter	Units	Value
Size	mm	<19
$CaCO_3$ Content	wt%	93.2-94.4
$MgCO_3$ Content	wt%	1.3-2.8
SiO_2 Content	wt%	0.3-3.1
Other inert components	wt%	<2
Moisture Content	wt%	0.04-0.13
Bond Work Index	kWh/t	12
Limestone Utilization	mole/mole	0.99-1.01
Reagent Preparation System Capacity	D_{95}	43.2
Capacity	t/h	55.5

4.1.2 Locked Cycle Test Results

The wet ball mill locked cycle test was conducted at Mintek during the week of the 9th of December 2019. The procedure as described in Section 3.4.2.2 was followed. X-ray fluorescence (XRF) analysis was used to determine the chemical composition of the sample. The sample contained 96.3% $CaCO_3$, 1.4% $MgCO_3$ and 1.1% SiO_2. The solids specific gravity was analyzed using a Gas Pycnometer as discussed in Section 3.4.2.1, and was found to be 2.79.

Due to the unavailability of Kusile's resources at the time of conducting the testwork, certain assumptions were made regarding the wet ball milling application. These assumptions include:

- Grinding media load of 35% (compared to 28.5% provided by Kusile).
- Slurry solids volume percentage of 45% (compared to 46.9% later provided by Kusile).
- Target mill speed of 64 rpm (recommended by Mintek).
- Standard circulating load of 250% for wet ball milling application (compared to 400% later provided by Kusile).
- Target grind size of 85% passing 45 µm (compared to 95% passing 45 µm later provided by Eskom).

The locked cycle test was completed as discussed in Section 3.4.2.2. The oversize moisture content was determined to be 25%. The ball mill inside length and diameter were measured as 265 mm and 305 mm, respectively. It was assumed that 100% of the voids between the ball mills were filled with slurry. The mass of solids required for each test was calculated to be 2,954 g as indicated in Table A-1 in Appendix A. The ball mill distribution was calculated as presented in Table A-2 in Appendix A.

The initial specific energy estimate was calculated using Bond's equation for specific energy requirement for size reduction in a closed circuit (Equation 12).

$$E_G = 10 \times 12 \times \left[\frac{1}{\sqrt{40}} - \frac{1}{\sqrt{12{,}500}}\right] = 17.9\ kWh/t$$

It should be noted that the specific energy required to reduce the feed particle to 80% passing 35 µm (as is the case at Kusile) is 19.2 kWh/t.

Ten iterations were completed, with the final three iterations converging to a specific energy input of 15.4 kWh/t for the circuit (refer to Table A-3 in Appendix A). This corresponds to an absorbed power of 1,542 kW for a 100 t/h ball milling application. The screen undersize product contained 15% passing 45 µm.

As mentioned in the previous section, the specific energy requirement provided by Kusile was 26.3 kWh/t, which corresponds to an absorbed power 2,649 kW for a 100 t/h circuit. It is therefore clear that the increased circulation load (400%) and finer grinding (P_{95} of 45 µm) plays a significant role on the total absorbed power of the circuit. The high recirculating load indicates that the ball mill is not achieving the target grind, which results in more particles reporting to the cyclone underflow and thus recirculated back to the mill. It can therefore be concluded that there is an opportunity for Eskom's Kusile Power Station to reduce their specific energy requirement by operating their circuit more efficiently, i.e. optimizing their feed rate, ball load, etc.

4.1.3 Loesche Testwork Results

Idwala Lime prepared and shipped 2 tons of limestone sample to the Loesche testing facility in Düsseldorf, Germany. Two tests were conducted at different mill adjustments;

- Test 1: lower dam ring height (7 mm) and lower working pressure (90 bar)
- Test 2: higher dam ring height (20 mm) and higher working pressure (150 bar)

The standard mill operation is based on a mill outlet temperature of approximately 90°C. The fineness of the sieve aperture was adjusted according to the requirement (P_{95} of 45 µm and P_{85} of 45 µm). The total power consumption is the sum of the mill power, classifier power and fan power. The results are summarized in Table 4-3 (refer to Table A-4 in Appendix A for raw data). For Test 1, a specific energy of 6.7 kWh/t and 5.6 kWh/t was achieved for a P_{95} and a P_{85} of 45 µm, respectively. A higher dam ring and working pressure (Test 2), indicated a higher specific energy of 16.1 kWh/t and 13.7 kWh/t for a P_{95} and a P_{85} of 45 µm, respectively. It should be noted that the theoretical ball mill circuit specific energy for a product of 85% passing

45 µm was determined to be 15.4 kWh/t during the locked cycle test (compared to 13.7 kWh/t for the Loesche VRM).

Table 4-3: Loesche VRM Laboratory-Scale Testwork Results

Parameter	Units	Test 1		Test 2	
Dam Ring	**mm**	**7**		**20**	
Working Pressure	**bar**	**91**		**150**	
Percentage passing 45 µm	%	94.5	85.1	96.0	86.7
Specific Energy	kWh/t	6.7	5.6	16.1	13.7
Total Absorbed Power	kW	6.0	6.5	8.0	9.1
Tonnage	t/h	0.9	1.2	0.5	0.7

The resulting surface area for Test 1 and Test 2 also increased from approximately 3,000 cm^2/g to 5,000 cm^2/g.

Once the testwork data was generated, the information was sent to the Loesche South Africa office in Johannesburg, South Africa. A proposal was generated using the information obtained from testwork. A Loesche mill type LM31.3 was suggested ("31" referring to the size of the grinding table and "3" referring to the number of rollers). The installed power required for this application is a 1,200 kW motor for the mill, 500 kW motor for the mill fan and a 100 kW motor for the classifier. This amounts to a combined installed power of 1,800 kW (compared to a combined 3,800 kW installed power for the ball mills at Kusile or 3,700 kW installed power that was recommended for a 100 t/h ball mill).

The typical Loesche flowsheet is presented by Figure 2-8 in Section 2.4. Limestone is fed via a feeder and conveyor system underneath an overhead magnet (rejects tramp metals) and a metal detector, which identifies any undetected metal and rejects it with a diverter chute. The limestone is then fed to the Loesche VRM via a set of screw feeders onto the grinding table (to provide a seal against air leakage). The mill product is carried by the hot gas through the duct into the bag house. A fan is used to generate gas flow and allow the "cleaned" gas to be discharge into the atmosphere via a stack. The product is discharged onto a conveyor belt and into a bucket elevator that feeds the reagent feed tank.

As mentioned previously, if the moisture of the feed limestone is higher than 6%, an HGG is required to generate additional heat for evaporation. The HGG has a 6.02 MW heating capacity and requires a 4 m^3 intermediate tank. Figure 4-2 presents the basic flowsheet of the VRM with a capacity of 100 t/h, including the HGG based on the relevant testwork information.

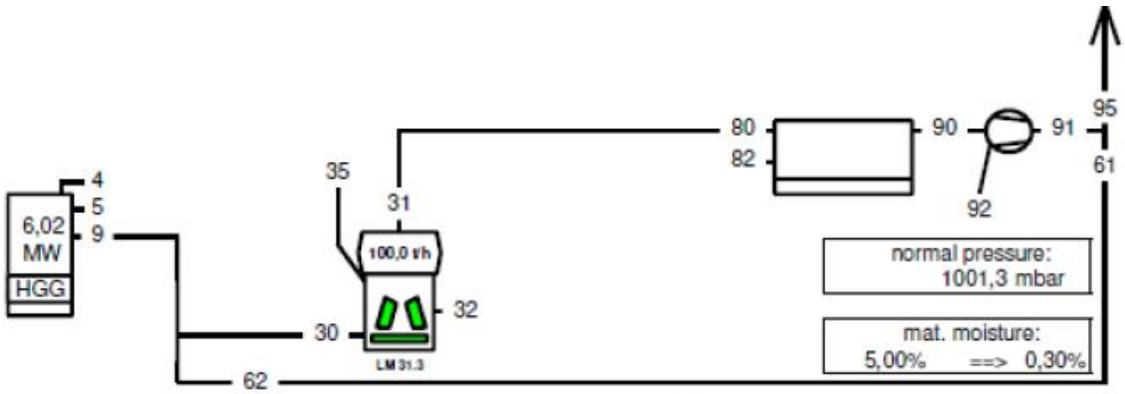

Pos.		nm³/h	m³/h	°C	°C(d.p.t.)	mbar	O2,w[%]	GJ/h
5	secondary air	29.761	31.929	15,0	7,5	996,3	20,71	0,581
4	burning gas	6.661	55.233	1954,0	54,0	996,3	1,72	21,669
9	firing gas	36.421	98.065	450,0	27,0	996,3	17,23	22,250
62	recirculating gas	92.209	126.183	94,4	50,8	996,3	16,55	11,588
30	gas mill inlet	128.630	225.105	196,9	46,2	996,3	16,75	33,838
35	evaporation water	6.155	7.110	15,0		925,3		-12,059
31	mill outlet gas	144.930	211.000	90,0	50,4	925,3	16,31	25,304
90	gas filter fan inlet	152.558	224.178	87,4	49,1	910,3	16,53	17,758
91	gas filter fan outlet	153.324	210.473	97,4	50,9	1001,3	16,55	19,884
61	rec. gas beh. filter fan	92.209	126.578	97,4	50,9	1001,3	16,55	11,958
95	gas to stack	61.116	83.896	97,4	50,9	1001,3	16,55	7,926
32	false air mill	10.145	10.830	15,0	7,5	1001,3	20,71	0,198
82	false air filter	7.628	8.143	15,0	7,5	1001,3	20,71	0,149
92	false air filter fan	767	818	15,0	7,5	1001,3	20,71	0,015

Figure 4-2: Hot Gas Generator Flow Sheet and Testwork Information

Stream 31 in Figure 4-2 represents the outlet temperature of the VRM at 90°C. The HGG generates a gas stream of 450°C, which is combined with the recycle stream (stream 62) of 94.4°C to deliver a hot gas stream at 196.9°C to the VRM. It should be noted that the results presented in Figure 4-2 imply conditions at sea level. The site altitude under consideration (i.e. Kusile) is approximately 1,500 m above sea level. **Table *4-4*** presents the dust load present in the VRM gas stream at sea level compared to the higher altitude at Kusile. The typical dust load for a vertical roller mill is between 400 g/m³ and 800 g/m³ (Pfeiffer, 2012). It is evident that the dust load is decreased with an increased altitude of 1,500 m.

Table 4-4: Dust Load in Exit Gas Stream of VRM at Sea Level versus 1,500 m Above Sea Level

Parameter	Units	At Sea Level	Kusile Site
Site Altitude	m	0	1500
Atm Pressure	kPa	101.3	84.6
Production Rate	t/h	100	100
Mill Exit Gas Flow	m³/h	211,000	252,114
Dust Load	g/m³	474	397

The mill operating conditions can be adjusted to accommodate the change in gas flowrate to maintain product fineness. There will be an impact on the gas handling equipment, specifically the dust collector and fan. In the dust collector, the air/cloth ratio will increase, which will increase wear on the filter bags. However, an adequately sized filter will still operate

satisfactorily. In summary, there will be an increase in the gas volume but the mill operation will not be affected. If the gas handling equipment is adequately sized, no change will be required, however, operating margins will be reduced. Wet ball milling will not be affected by the increased altitude.

The VRM circuit without the HGG contains dust laden air in the mill exhaust gas, whereas if the HGG is included, the exhaust gas includes the fuel combustion products, which may require appropriate permitting.

Since the limestone provided to Kusile contains less than 1% moisture, the VRM is not considered in the main cost comparison. However, it is considered as an alternative option.

4.2 Process Design Criteria and Block Flow Diagrams

The PDC for each option were generated and are attached in Appendix B of this report. The reference codes in column “REF./CONF.” represent the following:

- A Assumed/Indicative
- C Kusile Data
- D Design Basis
- E Engineering Calculation
- H Recommendation
- I Industry Standard
- M Mass Balance
- O Information by Others
- P Published Data
- T Testwork
- V Vendor Generated Data

4.2.1 PDC: Ball Mill Circuit

Table B-1 in Appendix B presents the PDC of the 100 t/h wet ball mill limestone process corresponding to the block flow diagram illustrated in Figure 4-3 (BFD1101).

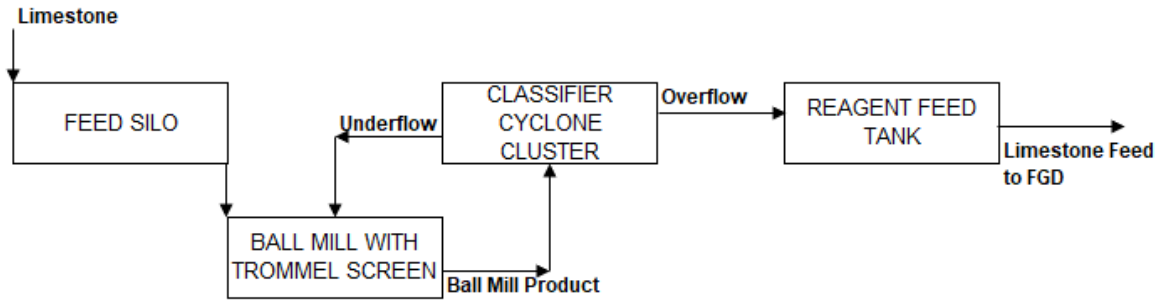

Figure 4-3: BFD1101 – Ball Mill Circuit Block Flow Diagram

The operating factor of 89.8% is based on the information provided by Kusile during the site visit. The annual throughput therefore amounts to 786,648 t/a. The wear components of the ball mill circuit include the mill liners, grinding media, cyclone liners, etc.

The ball mill is an overflow discharge type ball mill with an internal diameter of 4.8 m and an effective grinding length of 9.75 m (vendor recommended). The installed and absorbed power of the mill is 3,800 kW and 2,649 kW, respectively.

The sizing is based on the Kusile site conditions because of the required product grind size of 95% passing 45 µm. It should however be noted that, as indicated from the locked cycle test, there is an opportunity to increase the operating efficiency at Kusile and thus decrease the absorbed energy of the mill.

The classifier cyclone cluster consists of 20 on-line cyclones and 4 standby cyclones. The operating pressure is 65 kW with a cut of 51 µm (cyclone simulations). The split to overflow is 20.3% to achieve the circulating load of 400%. All assumptions in the PDC are marked with the letter “A”.

4.2.2 PDC: Loesche VRM Circuit

Table B-2 in Appendix B contains the PDC of the 100 t/h dry Loesche VRM limestone process corresponding to Figure 4-4.

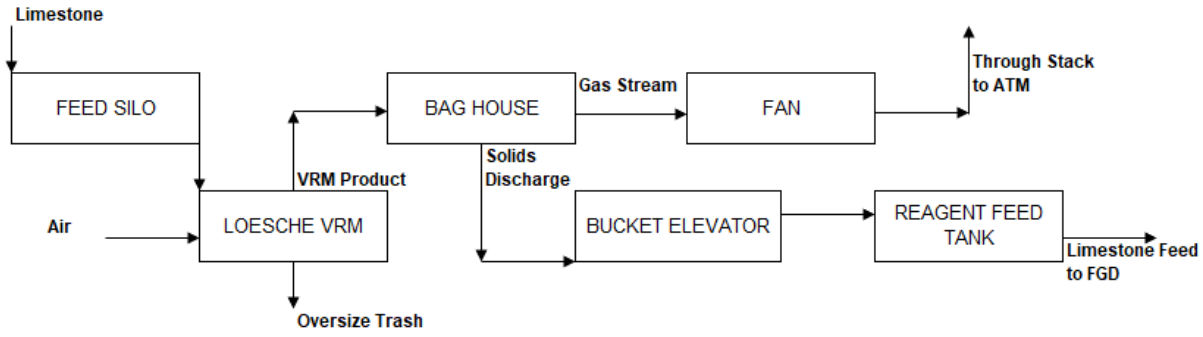

Figure 4-4: BFD2101 – VRM Circuit Block Flow Diagram

According to Loesche, the lifetime of the grinding parts (one grinding table and 3 grinding tires) will exceed 7,500 hours running time at the 100 t/h product rate. The mean time to repair is 3 days and a visual maintenance inspection is required twice a year for a duration of 24 hours. This corresponds to an operating factor of 94.5%; however, since the limestone consumption is driven by the gas flow and SO_2 concentration in the flue gas, the same limestone production as for the ball mill (786,648 t/a) is specified, corresponding to an 89.8% operating factor. The additional hours are used for maintenance of the ancillary equipment, such as the bag house and fan.

4.3 Process Flow Diagrams and Stream Tables

Figure C-1 represents the PFD of the wet ball milling circuit, which includes its corresponding stream table. The total reclaim water consumption is 253.9 m³/h, of which 40.5 m³/h is added to the ball mill feed trunnion. The reclaim water consists of 3.0% solids. 100 t/h of fresh limestone is added to the ball mill feed chute together with 400 t/h of classifier cyclone underflow (circulation load of 400%). The ball mill discharge solids concentration is 71.1 wt% and 213.4 m³/h of reclaim water is fed to the ball mill underflow sump to reduce the solids concentration to 55.0 wt%.

The cyclone overflow consists of 30 wt% solids and the split of solids to the overflow is 21.2%. The limestone returned to the mill consists of 71.0% solids.

Figure C-2 in Appendix C represents the PFD of the dry Loesche VRM circuit, which includes its corresponding stream table. Since the FGD system requires a wet limestone reagent, water is added to the limestone reagent feed tank. Therefore, no water saving is observed when comparing the VRM with the ball mill in this study because 253.9 m³/h of reclaim water is required to dilute the limestone product to the required solids concentration of 30 wt%.

Approximately 211 m³/h of hot gas is discharged through the stack.

4.4 Piping and Instrumentation Diagrams

Typical P&ID's of the two different circuits are included in Appendix D of this report. Figure D-1, Figure D-2, Figure D-3 and Figure D-4 present typical P&ID's of the wet ball milling circuit, whereas Figure D-5, Figure D-6, Figure D-7 and Figure D-8 present typical P&ID's of the dry VRM circuit. It should be noted that no pipe sizing is included in the P&ID's since the piping was calculated as a percentage of the mechanical costs as discussed in Section 2.6.3. A list of symbols (including valves and instrumentation) is provided in Appendix M. The equipment numbering is also shown on the P&ID's.

4.4.1 Control Philosophy: Wet Ball Mill Circuit

All bins, tanks, hoppers and sumps are fitted with level indicators. The feed conveyor (1100-CV-001) and belt feeder (1100-FE-001) are interlocked with the level of the feed silo (1100-SI-001) and fitted with a speed element. The conveyor is fitted with a weightometer to measure the fresh limestone feed rate to the ball mill (1100-ML-001). The feeder has a variable speed drive (VSD) motor, which is controlled by the weightometer to ensure a constant limestone feed of 100 t/h to the mill. A dust extraction system is included for the limestone feeder and conveyor system.

The reclaim water to the wet ball milling circuit is controlled with a modulating valve (fails closed) to ensure the required solids concentration of 71.1% is achieved in the mill. The mill

is fitted with a level indicator, temperature transmitter and speed element. The hydraulic power pack (1100-HD-001) of the mill is fitted with a level, pressure and temperature transmitter. Spray water is added to the trommel screen (1100-SC-001) and controlled with an actuated valve, which fails closed.

The mill discharge sump (1100-SU-001) contains a drain line with an actuated valve that fails open so that the content of the sump is drained and discharged onto the spillage floor to be pumped back into the circuit. No spillage sumps and sump pumps are included in the P&ID's.

The slurry pump (1100-PP-001) suction line is fitted with a pressure transmitter, isolation valve, actuated valve, drain line and reducer. The pump discharge line is fitted with a pressure indicator, actuated drain line, magnetic flowmeter and densitometer. When there is a shut down or failure, flush water fails open and is added to the suction and discharge lines. The actuated valve on the suction line fails closed, while the drain line actuated valve fails open. Similarly, the drain line on the discharge line fails open and any remaining slurry is washed with flush water to the spillage sump. Both flush water lines are fitted with check valves to ensure no slurry flows back up through the flush water line.

Feedback control is implemented to ensure the correct density is pumped to the classifier cyclone cluster (1100-CY-001). The density is measured on the pump discharge line. If the density is higher than the set point, the reclaim water modulating valve opens and more water is added to the ball mill discharge sump to decrease the density. Conversely, if the density is too low, the reclaim water is reduced so that the density is increased.

The pump is fitted with a VSD, which controls the pump speed and is interlocked with the level of the ball mill discharge sump. The flowmeter fitted on the discharge line indicates the volumetric flow of the slurry corresponding to the VSD setting.

Carbon steel rubber lined (CSRL) piping was selected for slurry pumping since limestone is abrasive. The tanks are coated with epoxy resin.

The cyclone cluster feed is fitted with a pressure indicator, which controls the number of operating cyclones. Each cyclone in the cluster is fitted with an actuated valve. The cyclone overflow and underflow discharge into different launders, which are sloped. In PID1103 (Figure D-3 in Appendix D), the cyclone cluster contains 10 on-line cyclones with 2 standby cyclones to indicate a typical P&ID for a cyclone cluster. However, based on the design, there are 20 on-line cyclones with 4 standby cyclones.

The reagent feed tank (1100-TK-001) has an agitator (1100-AG-001) and thus the drain valve fails closed since the solids remain suspended. The agitator motor will be on emergency

power. The instrumentation on the reagent tank discharge line is identical to the mill sump discharge line with the same control philosophy.

4.4.2 Control Philosophy: Dry VRM Circuit

All bins, tanks, hoppers and sumps are fitted with level indicators. The feed conveyor (2100-CV-001) and belt feeder (2100-FE-001) are interlocked with the level of the feed silo (2100-SE-001) and fitted with a speed element. An overhead belt magnet (2100-BM-001) is located above the feed conveyor and removes any tramp metals. A metal detector (2100-MD-001) is used to detect any metals that the belt magnet could not remove. The metal detector sprays the ore with paint at the detected area, which is then removed with a diverter chute (2100-CH-004). The ball mill feed conveyor (2100-CV-002) is fitted with a weightometer which controls the belt feeder speed (fitted with a VSD) to ensure a constant feed to the VRM of 100 t/h. A dust extraction system is included for the entire dry VRM circuit.

The VRM (2100-ML-001) is fed via the limestone screw feeder (2100-FE-002), which is fitted with a VSD, and the VRM screw feeder (2100-FE-003), which is direct-on-line (DOL). The limestone screw feeder VSD is controlled by the pressure in the VRM product duct. The position of the rollers is monitored, as well as the pressure in the discharge product stream. A small spray water stream (19 mm stainless steel pipe) is fed to the mill grinding table to stabilize the grinding bed and reduce vibration of the mill. However, the heat generated by the VRM fan rapidly evaporates this water.

Any oversize or tramp material (such as plastics, wood, etc.) is rejected and transported with the rejects' conveyor (2100-CV-003) to a trash bin. The rejects conveyor is also fitted with a weightometer (2100-WT-002).

The mill hydraulic system (2100-ZM-001) is fitted with a level, pressure and temperature transmitter. The lubrication oil system (2100-ZM-002) is fitted with a flow, pressure and temperature transmitter. A chiller (2100-CL-001) is required to cool down potable water for cooling of the lubrication oil system.

A pressure indicator is fitted on the feed and product gas ducts. The mill product is carried to the bag house (2100-DC-001) where solids are separated from the gas stream. The level of the bed formed in the bag house is measured and the sliding gates subsequently open to discharge the limestone product onto the reagent tank feed conveyor (2100-CV-004) via the screw feeders (2100-FE-004 and 2100-FE-005), and into the bucket elevator (2100-BE-001). The bucket elevator discharges the limestone product into the reagent feed tank (2100-TK-001), which is then pumped (2100-PP-001) to the FGD scrubber. The reagent tank feed

conveyor has a weightometer. The bucket elevator is fitted with a speed element and temperature transmitter.

The VRM fan (2100-FA-001) allows for flow of the gas through the VRM to the stack (2100-SX-001). Dampers are fitted into the gas duct and air is recycled back to the VRM to ensure a constant hot gas stream.

Reclaim water is added to the feed reagent tank and is fitted with a modulating valve to control the density of the discharge line. The density of the discharge line is measured with a densitometer. The reagent feed tank contains an agitator (2100-AG-001). The drain valve of the reagent feed tank fails closed since the solids remain suspended because of the agitator (2100-AG-001).

The slurry pump suction line is fitted with a pressure transmitter, isolation valve, actuated valve, drain line and reducer. The pump discharge line is fitted with a pressure indicator, actuated drain line, magnetic flowmeter and densitometer. When there is a shut down or failure, flush water fails open and is added to the suction and discharge lines. The actuated valve on the suction line fails closed, while the drain line actuated valve fails open. Similarly, the drain line on the discharge line fails open and any remaining slurry is washed with flush water to the spillage sump. Both flush water lines are fitted with check valves to ensure no slurry flows back up through the flush water line.

4.5 Mechanical Equipment List (MEL) and Costs

The MEL for the wet ball milling circuit (MEL1101) and the dry Loesche VRM (MEL2101) is presented in Table E-1 and Table E-2 in Appendix E, respectively. The tank and chute schedule is presented in Table F-1 and Table F-2 of Appendix F, respectively.

Table F-3 and Table F-4 in Appendix F represent the tank and chute schedules for the dry VRM circuit. At the time of compiling this report, the cost of steel to mill and fabricate is R28,900/t. The “all-in” rate for steel is R64,500/t, which includes the supply, fabrication, installation, P&G, freight and galvanizing. The pump calculations are presented in Table L-2 in Appendix L, with the corresponding pump curves shown in Figure L-1 and Figure L-2.

A ball mill with an inside diameter of 4.8 m and effective grinding length of 9.75 m was selected for the wet milling application. The ball mill has an installed power of 3,700 kW. The Loesche LM31.3 was selected for the dry circuit, which has a combined installed power of 1,800 kW (mill motor, fan motor and classifier motor).

A summary of the installed power and mechanical cost for each circuit is presented in Table 4-5. Certain minor equipment costs or costs similar for both circuits were excluded from this study and are outlined in Section 4.6 below.

The exchange rate at the time of conducting this study is R15.3/US$ and R16.7/€.

Table 4-5: Summary of the Mechanical Power and Cost

Circuit	Wet Ball Mill Circuit	Dry VRM Circuit
Total Installed Power	3,752 kW	1,893 kW
Total Absorbed Power	2,695 kW	1,593 kW
Equipment Cost	R 44,808,800	R 58,329,700
Platework (chutes, sumps and hoppers)	R 879,650	R 855,000
Total Mechanical Cost	**R 48,327,500**	**R 59,184,700**

The total installed power for the dry VRM circuit is 1,893 kW compared to 3,752 kW for the wet ball mill circuit. There is also a significant reduction in power consumption as indicated by the reduced absorbed power in the dry VRM circuit (1,593 kW) compared to the conventional wet ball milling circuit (2,695 kW).

Budgetary quotations were obtained for equipment (including mills, pumps, feeders, conveyors, agitators, etc.), while the required mass of steel required for platework (chutes, tanks and sumps) was calculated as outlined in Section 2.5.3 and the price of steel (R64,500/t of steel) was used to estimate the total cost. The total steel mass (platework and support structures) required for both circuits was found to be similar, i.e. 13,638 kg for the wet circuit and 13,255 kg for the dry circuit. Even though there are less tanks or sumps in the dry milling circuit, there are more chutes.

The total mechanical cost of the dry VRM circuit was found to be 23.9% more expensive than the wet ball mill circuit: this lies within the estimated 20% to 25% predicted by Mutter (2013). The VRM makes up 72.1% of the total mechanical cost of the dry circuit, while the ball mill constitutes 83.2% of the total mechanical cost of the wet milling circuit.

4.6 Exclusions

Certain equipment/systems were excluded from this study because they were either a minor cost or similar for both circuits. The following items were excluded in the cost estimation for both circuits:

- Cranes and hoists
- Samplers
- Spillage sumps
- Fire water
- Wash and spray points
- Dust extraction
- Emergency power
- Eye wash stations

- Daily storage silo
- Safety showers

Any items not explicitly outlined in either the mechanical equipment list or CAPEX/OPEX were also not included in this study.

4.7 CAPEX Comparison

4.7.1 Wet Ball Mill Circuit and Dry Loesche VRM Circuit Comparison

The TCI estimates for both circuits are summarized in Table 4-6 below. The different components of the TCI were calculated as a percentage of the purchased equipment for a slurry plant and solids plant as outlined in Table G-3 (Appendix G).

Table 4-6: Fixed Capital Investment (FCI) Comparison of Conventional Wet Ball Mill Plant versus the Dry Loesche VRM Plant

Component	Wet Ball Mill Plant	Dry VRM Plant
Purchased Equipment	R 48,327,500	R 59,184,700
Purchased Equipment Installation	R 18,847,700	R 23,673,900
Control and Instrumentation (installed)	R 6,282,600	R 5,326,600
Piping (installed)	R 14,981,500	R 9,469,500
Electrical (installed)	R 4,832,800	R 5,918,500
Buildings (including services)	R 14,015,000	R 14,796,200
Yard improvements	R 4,832,800	R 7,694,000
Service facilities (installed)	R 26,580,100	R 23,673,900
Land	R 2,899,700	R 3,551,100
Total Direct Costs	R **141,599,700**	R **153,288,300**
Engineering and Supervision	R 15,948,100	R 19,530,900
Construction Expense	R 19,814,300	R 23,082,000
Total Direct and Indirect	R **177,362,000**	R **195,901,300**
Contractor's Fee (CF)	R 8,868,100	R 9,795,100
Contingency (C)	R 17,736,200	R 19,590,100
Fixed Capital Investment (FCI)	R 203,966,300	R 225,286,500
Working Capital (WC)	**R 35,994,100**	**R 39,756,400**
TOTAL CAPITAL INVESTMENT (TCI)	**R 239,960,400**	**R 265,042,950**

The TCI for the dry Loesche VRM circuit is 10.5% higher than for the wet ball mill circuit (difference of R25,082,550). As mentioned in the literature study of this report, the higher TCI was expected for the dry Loesche VRM circuit. The working capital for both circuits is 15% of the TCI.

The different cost components, calculated as a percentage of the TCI, are provided in Table G-4 and Table G-5 in Appendix G, respectively. Cost components for both the circuits lie within the guidelines as indicated in Table G-2 in Appendix G.

Figure 4-5 presents the different components of the direct costs for the wet ball mill circuit compared to the dry Loesche VRM circuit.

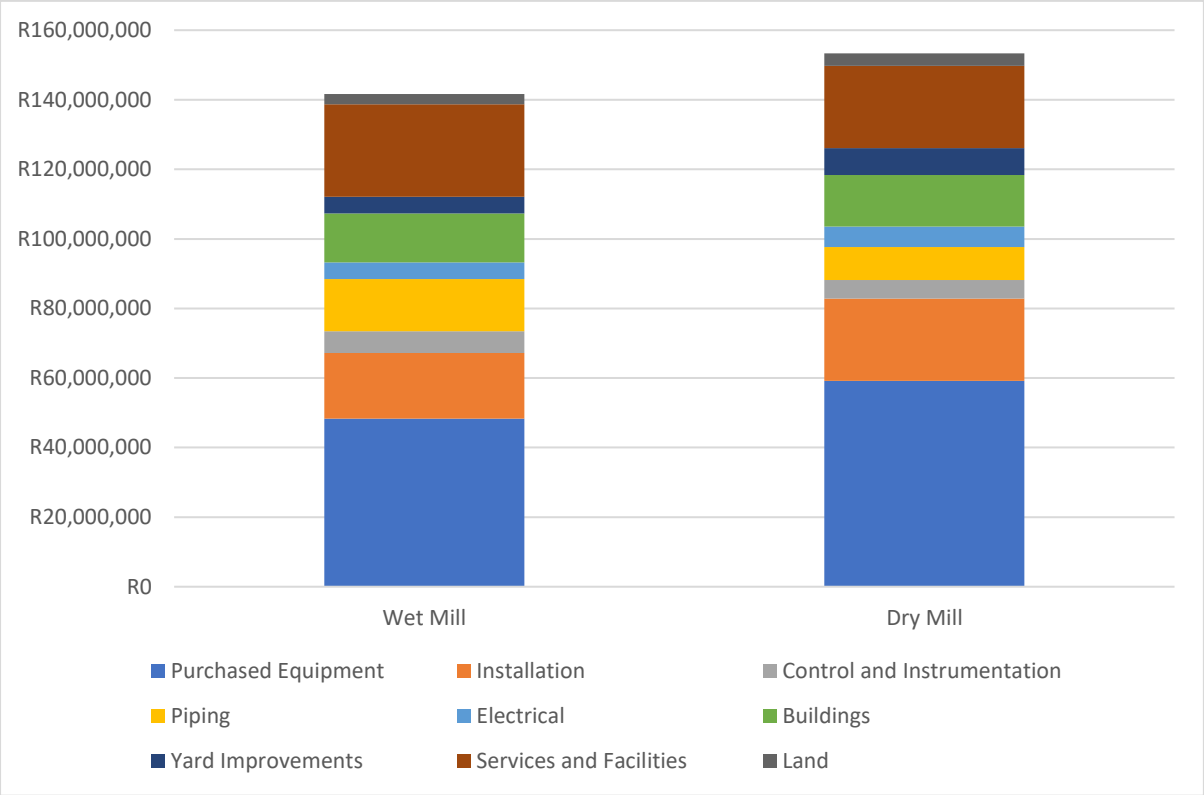

Figure 4-5: Direct Cost Comparison of the Wet Ball Mill Circuit compared to the Dry Loesche VRM Circuit

The direct cost of the dry Loesche VRM circuit makes up 68.0% of the FCI, compared to 69.4% for the wet ball milling circuit. The purchased equipment is 23.7% and 26.3% of the FCI for the wet milling circuit and dry Loesche VRM circuit, respectively. The indirect cost of the wet milling circuit is 17.5% of the FCI, compared to 18.9% for the dry Loesche VRM circuit.

4.7.2 CAPEX: Hot Gas Generator

A quotation was obtained for the Loesche HGG to compare the project cost in the case where the limestone feed contains more than 6% moisture. Table 4-7 compares the FCI for the dry Loesche VRM plant with and without the HGG.

Table 4-7: FCI Comparison for Dry VRM Circuit with and without the HGG

Component	Dry VRM Plant	Dry VRM Plant with HGG
Purchased Equipment	R 59,184,700	R 63,927,700
Purchased Equipment Installation	R 23,673,900	R 25,571,100
Control and Instrumentation (installed)	R 5,326,600	R 5,753,500
Piping (installed)	R 9,469,500	R 10,228,400
Electrical (installed)	R 5,918,500	R 6,392,800
Buildings (including services)	R 14,796,200	R 15,981,900
Yard improvements	R 7,694,000	R 8,310,600
Service facilities (installed)	R 23,673,900	R 25,571,100
Land	R 3,551,100	R 3,835,700
Total Direct Costs	R **153,288,300**	R **165,572,700**
Engineering and Supervision	R 19,530,900	R 21,096,100
Construction Expense	R 23,082,000	R 24,931,800
Total Direct and Indirect	R **195,901,300**	R **211,600,600**
Contractor's Fee (CF)	R 9,795,100	R 10,580,00
Contingency (C)	R 19,590,100	R 21,160,100
Fixed Capital Investment (FCI)	R 225,286,500	R 243,340,700
Working Capital (WC)	R **39,756,400**	R **42,942,500**
TOTAL CAPITAL INVESTMENT (TCI)	**R 265,042,950**	**R 286,283,200**

The TCI for the dry circuit including the HGG is 8.0% higher than for the scenario where the HGG is not included. Figure 4-6 presents the difference in the components of the TCI of the three different circuits; (1) wet ball milling circuit, (2) dry Loesche VRM circuit without the HGG, and (3) dry Loesche VRM circuit with the HGG.

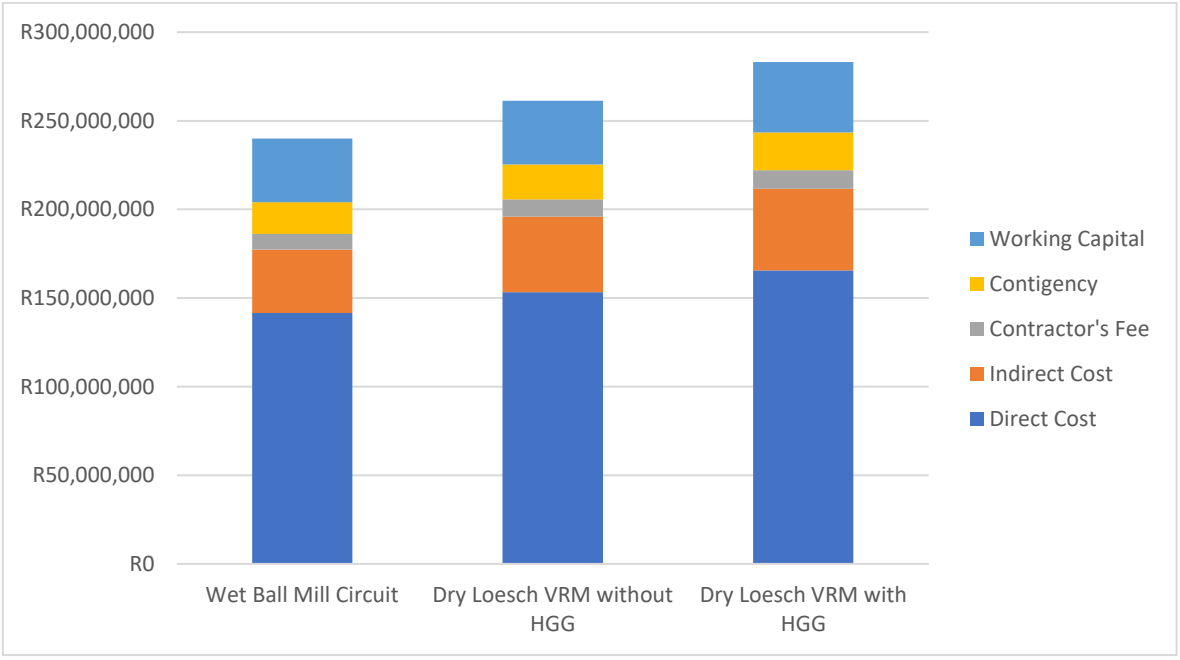

Figure 4-6: Comparison of the FCI of the Wet Milling Circuit and Dry Loesche VRM with and without HGG

The mechanical cost for the dry milling plant including the HGG is 32.3% higher than for the wet ball mill circuit and corresponds to a 19.3% increase in the TCI from the wet ball milling circuit.

4.8 Operating Cost Comparison

4.8.1 Wet Ball Mill Circuit and Dry Loesche VRM Circuit Comparison

A comparison of the power consumption (active and maximum demand charge) for the conventional wet ball mill circuit and dry circuit is provided in Table 4-8 below.

Table 4-8: Power Cost Comparison for the Wet Ball Mill Circuit Compared to the Dry Loesche VRM Circuit

POWER	UNITS	Wet Ball Mill Circuit	Dry Loesche VRM Circuit
Feed Rate	t/h	100	100
Operating Factor	%	89.8	89.8
Absorbed Electrical Active Power	kW	2,734	1,703
Circuit Specific Power Consumption	kWh/t	27.3	17.0
Annual Production	t/a	786,650	786,650
Active Power Rate	R/kWh	1.06	1.06
Active Power Cost	**R/a**	**22,800,500**	**14,199,200**
Maximum Demand Rate	R/kW/month	50.37	50.37
Monthly Maximum Demand Charge	R/month	133,400	81,100
Annual Maximum Demand Charge	**R/a**	**1,601,250**	**973,150**
Total Power Cost	**R/a**	**24,401,700**	**15,172,300**

The annual power cost is 37.8% less for the dry Loesche VRM circuit compared to the wet ball mill circuit. The absorbed power (as determined in Section 4.5) was multiplied by the operating hours in a year to determine the annual power consumption. The price of electricity at the time of this study is 106 c/kWh, which was used to calculate the annual cost of power per milling circuit. The maximum demand power charge was calculated based on Eskom's 2019/2020 tariff as presented in Table H-1 in Appendix H.

A comparison of the annual OPEX for the dry VRM circuit and the wet dry mill circuit is provided in Table 4-9.

Table 4-9: Operational Expense (OPEX) of the Wet Ball Mill Circuit compared to the Dry Loesche VRM Circuit

	Ball Mill Circuit		Dry VRM Circuit	
OPEX Components	**R/a**	**% of OPEX**	**R/a**	**% of OPEX**
Limestone Cost (@ R219/tonne)	172,275,900	67.6	172,275,900	72.1
Labour	1,300,000	0.5	1,300,000	0.5
Water @ R20/kL	39,514,900	15.5	39,514,900	16.5
Power@ 106c/kWh	24,401,700	9.6	15,172,300	6.4
Consumables	7,172,600	2.8	1,103,800	0.5
Strategic/Critical Spares	8,553,500	3.4	8,211,200	3.4
Operational Spares	1,600,500	0.6	1,312,600	0.5
TOTAL	**254,819,200**	**100.0**	**238,890,700**	**100.0**

The overall operating cost is 6.3% less for the dry Loesche VRM circuit compared to the wet ball milling circuit (difference of R15,928,500) because of the lower power consumption and reduced consumables (grinding media).

The cost of limestone from the Danielskuil mine site is R219/t (Kalkor, 2020). The annual cost of limestone for both circuits will therefore be R 172,275,900 (refer to Table H-2 in Appendix H for the limestone cost calculation).

The cost of water is added in this comparison for a plant that will use raw water as opposed to recycled water. Refer to Table H-3 in Appendix H for the water consumption calculation. The labor requirements (number of skilled/unskilled personnel) for both circuits are similar, which translates to the same cost to company (CTC) for both circuits. No reagents or fuel consumption is required for either of the comminution circuits.

The consumables include media consumption (steel balls) and liner replacement for the wet ball milling circuit. The roller and grinding table replacement are included in the consumables for the dry Loesche VRM circuit.

There are three types of spare parts; (1) critical, (2) strategic and (3) operational. Critical spares refer to spare parts required for critical equipment that will negatively impact or stop production. Strategic spares are stored on site to avoid delays due to long lead times. Operational spare parts are stored on site to ensure operation of the plant even if the spare parts are easily accessible. The critical, strategic and operational spare parts were provided by the relevant vendors. Table H-4 and Table H-5 in Appendix H presents the spares costs for the wet milling circuit and dry Loesche VRM circuit.

4.9 Profitability Analysis

The price of gypsum (bulk) at the time of conducting this study was found to be R267/t (Kalkor, 2020). The revenue for both the wet and dry circuits was therefore calculated to be approximately R361,304,200. For the purpose of this study, it was assumed that there is a demand for gypsum to be 100% saleable, however, a market evaluation is required to determine the actual amount of gypsum to be sold on an annual basis.

The following assumptions were made for calculating the profitability analysis:

- The plant life is 20 years.
- Annual interest rate is 12%.
- Corporate income tax is 35%.
- Depreciable charge at a rate of 40% for the first year and 20% for the three subsequent years (as recommended by PWC and Deloitte for machinery in South Africa).
- Expenses were incurred throughout the year and thus the discount factor was applied on a mid-year basis.
- Constant (flat) OPEX.

Certain components of the OPEX are expected to change at a rate different to inflation (higher or lower) such as utilities costs, labour costs, etc. However, for the purpose of this study, a constant (flat) OPEX has been assumed.

The annual profit for the dry Loesche VRM circuit is 15.0% higher than for the wet ball mill circuit because of the reduced OPEX.

Table 4-10: Profitability Analysis for the Wet Ball Mill Circuit compared to the Dry Loesche VRM Circuit

Parameter	Units	Wet Ball Mill Circuit	Dry VRM Circuit
Total Capital Investment	R	239,961,000	265,043,000
Total Direct Costs (PPE)	R	141,600,000	153,289,000
OPEX	R/a	254,820,000	238,891,000
Revenue	R/a	361,305,000	361,305,000
Profit	R/a	106,485,000	122,414,000
LOM	years	20	20
ROI	%	39.9	48.5
Interest Rate	%	12	12
Corporate Income Tax	%	35	35
NPV	R	**348,407,000**	**408,573,000**
IRR	%	20.2%	21.3%
Discounted Payback Period	years	4.1	3.8

The payback period for the break-even point is 4.1 years for the wet ball mill circuit and 3.8 years for the dry Loesche VRM circuit. The higher profit for the dry Loesche VRM circuit results

in a slightly faster payback period even though the CAPEX is more. The return on investment (ROI) over the 20 years is calculated as 39.9% and 48.5% (8.6% higher) for the wet and dry circuit, respectively.

The NPV calculation spreadsheet for the wet and dry circuit is presented in Table I-1 and Table I-2 in Appendix I, respectively. The NPV for the dry Loesche VRM circuit is approximately R60,166,000 more (17.3% increase) than for the wet ball mill circuit. The corresponding IRR for the dry Loesche VRM circuits were found to be 1.1% higher than for the wet ball mill circuit at 21.3% and 20.2%, respectively.

4.10 Off-Site Milling of Limestone

Off-site milling of limestone has the potential to significantly reduce the CAPEX for any coal-fired power plant which plans on building an FGD plant. The savings from the CAPEX will be offset to some extent by the increased cost of limestone delivery. The limestone grinding will occur at the limestone mine site using a dry VRM circuit (similar to the circuit described in the previous sections) and the dry, milled limestone will be transported to the relevant FGD plant. The mechanical equipment cost could be reduced by up to 91.0% from the wet ball milling circuit and 92.7% compared to the dry Loesche VRM circuit. The power consumption could be reduced by up to 97.9% and 96.7% compared to the wet ball mill circuit and on-site dry Loesche VRM circuit, respectively.

Challenges regarding stockpiles, cost of special tankers for transportation of fine material and other special considerations should be investigated when considering this option.

4.11 Summary and Discussion

The results of this study are summarized as follows:

- The high-grade limestone sample has a work index of 12 kWh/t. According to Bond's equation, the theoretical specific energy required to reduce a particle size from F_{80} of 12.5 mm to P_{80} of 35 µm (Kusile product size specification) in a closed circuit, is 19.2 kWh/t. The actual circuit specific energy of the wet ball milling application at Kusile is 26.5 kWh/t. The locked cycle test was used to determine the specific energy required to reduce the limestone particle size to a slightly coarser product of 85% passing 45 µm. The circuit specific energy was found to be 15.4 kWh/t from the locked cycle test. The corresponding theoretical specific energy from the Bond equation is 17.9 kWh/t.
- The dry Loesche VRM testwork was conducted at two dam ring settings (7 mm and 20 mm) and two product grind sizes (P_{85} and P_{95} of 45 µm) at each of the dam ring settings. The circuit specific energy includes the energy from the mill, classifier and fan. The lower dam ring indicated significantly lower specific energy requirements of

6.7 kWh/t and 5.6 kWh/t for 95% passing and 85% passing 45 μm, respectively. The 20 mm dam ring setting resulted in a specific energy of 16.1 kWh/t and 13.7 kWh/t for 95% passing and 85% passing 45 μm, respectively. The dam ring setting is a function of the grinding requirements. For this project, the results from the higher dam ring size (20 mm) were used as advised by Loesche. The specific energy of 13.7 kWh/t for grinding to 85% passing 45 μm is less than the 15.4 kWh/t obtained from the wet ball milling locked cycle test. These values correspond to an absorbed power of 1,370 kW and 1,540 kW for the dry Loesche VRM mill and the wet ball mill, respectively. Furthermore, the dry Loesche VRM required a specific energy of 16.1 kWh/t for a grind size of 95% passing 45 μm, which translates to 1,610 kW absorbed power. In comparison, the absorbed power for the wet ball mill at the Kusile plant is 2,650 kW. The power consumption for the dry Loesche VRM is significantly less than for the wet ball mill circuit.

- No water saving is realized for the Loesche VRM circuit even though it operates on a dry basis, because the FGD process requires a limestone slurry to be sprayed into the scrubber for contact with the flue gas. Water is therefore added to the milled limestone to reduce the solids concentration to 30%.
- The total installed power of the wet and dry circuits including all major equipment is 3,752 kW and 1,893 kW, respectively. The mechanical cost of the wet ball milling circuit (including ancillary equipment) is R48,327,500 (the ball mill makes up 78.7%). The dry Loesche VRM circuit has a mechanical cost of R59,184,700. The cost of the Loesche VRM is 69.0% of the mechanical cost. The mechanical cost of the dry Loesche VRM circuit is therefore 22.4% more expensive than for the wet ball milling circuit. The TCI of the wet ball milling circuit was calculated to be R239,960,300 compared to R265,042,900 for the dry Loesche VRM circuit. Therefore, a 10.5% increase in the total capital investment is expected for the dry Loesche VRM circuit.
- If the limestone feed to the mill contains more than 6.0% moisture, the dry Loesche VRM circuit requires an HGG. Since the limestone moisture content provided to Kusile is 0.3%, the HGG was not included in the main cost comparison. The TCI is R286,283,200 for the dry Loesche VRM circuit including the HGG, which is 19.3% more expensive compared to the wet ball mill circuit, and 8.0% more expensive compared to the dry Loesche VRM circuit without an HGG.
- The price of limestone at the time of conducting this study is R219/t, which amounts to an annual raw material cost of R172,275,900 for both circuits. The cost of water (R39,514,900 for both circuits) was included for an overall view of the operating cost.

- The overall absorbed power is 2,734 kW for the wet ball mill circuit and 1,703 kW for the dry Loesche VRM circuit. The annual power cost for the ball mill circuit is R24,401,700 for the wet ball mill circuit and R15,172,300 for the dry Loesche VRM circuit. Therefore, a power saving of 37.8% is realized for the dry Loesche VRM circuit compared to the wet ball mill circuit.
- The overall OPEX was therefore calculated to be 6.3% less for the dry Loesche VRM circuit at R238,890,700 compared to R254,819,200 for the wet ball mill circuit.
- The profitability of the two circuits was investigated by conducting an NPV calculation in Excel. The annual profit is R106,485,000 for the wet ball mill circuit and R122,413,513 for dry Loesche VRM circuit. The life of each plant is assumed to be 20 years, with an interest rate of 12% and corporate tax of 35%. The depreciable charge was applied at a rate of 40% for the first year and 20% for the three subsequent years. The NPV of the dry Loesche VRM circuit is R408,573,000, which is R60,166,000 (or 17.3%) more than for the wet ball mill circuit. The IRR for the wet and the dry circuits was found to be 20.2% and 21.3%, respectively. The discounted payback period is approximately 4.1 years for the wet circuit and 3.8 years for the dry circuit. The ROI for the wet ball mill circuit is 39.9%, compared to 48.5% for the dry Loesche VRM circuit.

The results summarized above indicate that there is a benefit to selecting the dry Loesche VRM circuit compared to the wet ball mill circuit for the grinding of limestone during the FGD process. The total capital investment of the dry Loesche VRM circuit is 10.5% higher, however, the NPV, IRR and DPBP are advantageous compared to the wet ball mill circuit because of the reduced power consumption and consumables. The power consumption is reduced by 37.8% for the dry Loesche VRM circuit.

5. Conclusion

In this study the technical and economic aspects of the conventional wet ball mill circuit were compared to the dry Loesche VRM circuit for the grinding of limestone in the FGD feed preparation area. Both milling technologies were found to be a viable option for grinding limestone with a top size of 19 mm to a P_{95} of 45 µm.

It was found that even though the capital investment of the dry Loesche VRM circuit is 10.5% higher, overall it is more economical. The power consumption of the dry circuit is 37.8% less than for the wet milling circuit. This reduced power consumption, combined with the decreased grinding media consumption, results in a 6.3% reduction in the operational expense of the dry Loesche VRM circuit. Consequently, an increase of 17.3% in the NPV is realized for the dry circuit compared to the wet ball mill circuit. The IRR for the wet and dry circuits is 20.2% and 21.3%, respectively. It can therefore be concluded that there is an overall financial benefit to installing the dry Loesche VRM circuit (as opposed to the conventional wet ball milling circuit) for the grinding of limestone in the feed preparation area of the FGD plant.

There is an opportunity for further power plant cost reduction (CAPEX) by milling of the limestone off-site. In this option, the dry Loesche VRM circuit is located at the limestone mine and the dry, milled limestone is transported to the FGD site. Investigation regarding special trucking and stockpiling requirements should be studied prior to selecting this option.

It should be noted that the results obtained from this study are specific to this project and characteristics of the limestone ore as tested. The study excluded certain components and was only used to compare the different circuits, and not to provide an accurate overall project cost estimate. A detailed engineering study is required to increase the accuracy of the cost estimate. Recommendations for further investigation are discussed in Section 6 of this report.

6. Recommendations

The recommendations following this study include:

- Idwala Lime operates a high-grade calcitic limestone (approximately 96% $CaCO_3$) mining and lime production facility near Danielskuil in the Northern Cape. Limestone transportation costs to Eskom's coal-fired power stations (located in Mpumalanga and Limpopo) are therefore substantial. Limestone with a lower grade (85 – 88% $CaCO_3$) is available from a source in North-West or Limpopo province. Although the lower grade limestone will result in increased reagent consumption, it has the advantage of reduced transportation costs. An investigation into the impact of low-grade limestone on the FGD process should be investigated. The investigation should include the increased capacity, impact on the gypsum quality, etc.
- Off-site milling would save on both capital costs and space of the limestone receiving area and rail siding, with milled limestone delivered in road tankers to a limestone storage bin/silo near the reagent feed tank. The potential CAPEX savings for Eskom would be offset to some extent by an increase in OPEX due to higher delivered reagent cost. The off-site milling plant would require a 100 t/h dry Loesche VRM circuit. This provision as well as storage capacity of milled limestone for seven days' consumption, will guarantee security of supply to the power plant.
- From the information obtained on the Kusile limestone milling plant, it is suggested that the current power consumption could be reduced by increasing the efficiency of the process, i.e. operating the plant at the design capacity and mill load, feeding the cyclone with the designed density, adding the correct amount of steel balls, etc. The power consumption could possibly be reduced by up to 26.7% based on the theoretical specific energy consumption of 19.2 kWh/t. However, further investigation is required to support this potential reduction.
- For a detailed cost estimate with a higher degree of accuracy, it is recommended that a detailed engineering study be conducted for each of these plants.

7. Ethics statement

This research project did not involve animal experimentation or human participation as per the definition in A.4 of the Senate Standing Orders on Higher Degrees.

8. References

Abulnaga, B. (2002). Slurry Systems Handbook. McGraw-Hill Handbooks

Altermann, W., & Wotherspoon, J. M. D. (1995). The carbonates of the Transvaal and Griqualand West sequences of the Kaapvaal craton, with special reference to the Lime Acres limestone deposit. *Mineralium Deposita*, *30*(2), 124–134. https://doi.org/10.1007/BF00189341

Agnello, V. N. (2005). Dolomite and Limestone in South Africa : Supply and Demand, Directorate: Mineral Economics, Pretoria, 1–67.

Arterburn, R.A. (2001). The Sizing and Selection of Hydrocyclones, 1-19. https://www.911metallurgist.com/blog/wp-content/uploads/2015/10/SIZING-AND-SELECTION-OF-HYDROCYCLONES.pdf

Austin, L.G. Klimpel, R.R. & Luckie, P.T. (1984). Process Engineering of Size Reduction: Ball Milling, SME/AIME, New York. 1-5

Bekker, D. (2017). The Manufacture of Cement, Lime and Related Materials. Who Owns Whom African Business Information.

Boehm, A., Meissner, P., & Plochberger, T. (2015). An energy based comparison of vertical roller mills and tumbling mills. *International Journal of Mineral Processing*, *136*, 37–41. https://doi.org/10.1016/j.minpro.2014.09.014

Bond, F.C. (1958). Grinding Ball Size Selection. *Mining Engineering,* 592.

Burnett, T.A., Stephenson, C.D., Sudhoff, F.A., Veitch, J.D. (1984). Economic Evaluation of Limestone and Lime Flue Gas Desulfurization Processes. United States Environmental Protection Agency, EPA-600/S7-83-029

Cai, R., Huang, Y., Li, Y., Wu, Y., Zhang, H., Zhang, M., Yang, H. & Lyu, J. (2019). Effects of the Limestone Particle Size on the Sulfation Reactivity at Low SO_2 Concentrations Using a LC-TGA. Materials Journal. Beijing, China.

Carpenter, A. M. (2012). *Low water FGD technologies*. *IEA Clean Coal Center* (Vol. December 2).

Chang, D. (2018). *Medupi Flue Gas Desulphurisation: Technology Selection Study Report*. Johannesburg.

Córdoba, P. (2015). Status of Flue Gas Desulphurisation (FGD) systems from coal-fired power plants: Overview of the physic-chemical control processes of wet limestone

FGDs. *Fuel*, *144*, 274–286. https://doi.org/10.1016/j.fuel.2014.12.065

DemcoTech Engineering (2017). Idwala Carbonates Project Sheet, Idwala Loesche Mill Materials Handling, Port Shepstone, http://demcotech.com/wp-content/uploads/2018/02/Idwala-Loesche-Mill-Materials-Handling-System.pdf

Evans, C. S., & Newell, K. D. (2013). The Mississippian Limestone Play in Kansas : Oil and Gas in a Complex Geologic Setting. *Kansas Geological Survey Public Information Circular*, *33*(March), 1–6.

Gaigward, R., & Boward, W. L. (2003). Wet Flue Gas Desulfurization Technology Evaluation. *Sargent and Lundy Report Project No. 11311-000*, (January), 1–50.

Gansley, R. (2008). Wet FGD System Overview and Operation. *WPCA Wet FGD Seminar, Power Gen International*, *Orlando, Florida December*.

Głomba, M. (2010). Technical description of parameters influencing the pH value of suspension absorbent used in flue gas desulfurization systems. *Journal of the Air and Waste Management Association*, *60*(8), 1009–1016. https://doi.org/10.3155/1047-3289.60.8.1009

Gupta, A. & Yan, D.S. (2006). Chapter 7. Tubular Ball Mills. *Mineral Processing Design and Operations*, 172-211, Perth, Australia

Haripersad, N. & Swart, P. (2015) RSA Sorbent Status and Application to Electricity generation. FFF Independent Power Generation in Southern Africa, Johannesburg

Harrison, D.J.. (1993). Industrial Minerals Laboratory Manual: Limestone. Retrieved from http://mapapps2.bgs.ac.uk/geoindex/home.html?layer=BGSHydroMap

Hassibi, H., Rogers, K. J., & Yang, M. (1999). Advances in Fine Grinding and Mill System Application in the FGD Industry. *Distribution*, *Symposium presentation* 1–6.

Jankovic, A., Ozer, C., Valery, W., & Duffy, K. (2016). Evaluation of HPGR and VRM for dry comminution of mineral ores. *Journal of Mining and Metallurgy A: Mining*, *52*(1), 11–25. https://doi.org/10.5937/jmma1601011j

Jankovic, A. & Valery, W. (2012). Closed Circuit Ball Mill - Basics Revisited. Minerals Engineering. Elsevier 148-153

Jorgensen, S. W. (2005). Vertical Roller Mills versus Ball Bills. *FLSmidth*. Copenhagen, Denmark

Kalkor (2020). http://www.kalkor.co.za/site/content/id/price-list

Käsling, H. & Thuro, K. (2010). Determining abrasivity of rock and soil in the laboratory. 11th IAEG Congress, Auckland, New Zealand, p235 1973-1980

KC Cottrell (2016). Flue Gas Desulfurization. https://www.eecpowerindia.com/codelibrary/ckeditor/ckfinder/userfiles/files/KC%20Cottrell.pdf

King, R.P. (2002). Introduction to Practical Fluid Flow.

Kohl, A.L. and Nielsen, R.B. 1997. Gas Purification (Fifth Edition). Chapter 7 - Sulfur Dioxide Removal. 466-669

Loesche (2016). Loesche-Mills for Solid Fuels. https://www.loesche.com/sites/default/files/list-content/brochure/2017-08/132-Loesche-Mills-for-Solid-Fuels-Coal-Mill-E-2016.pdf

Lynch, A. L. (2015). *Comminution Handbook*. The Australian Institute of Mining and Metallurgy.

Mutter, M. (2013). Cement grinding: VRM or ball mill? *World Cement*. https://www.worldcement.com/europe-cis/26022013/cement_grinding_ball_mills_vertical_roller_mill_032/

Ozkahraman, H. T. (2010). Breakage mechanisms and an encouraging correlation between the Bond parameters and the friability value. *Journal of the Southern African Institute of Mining and Metallurgy*, *110*(3), 153–159.

Paterson & Cooke (2006). Slurry Pumping Design, Section 3

Peters, M.S., Timmerhaus, K.D. & West, R. (2003). *Plant Design and Economics for Chemical Engineers*, Fifth Edition, McGraw-Hill

Pretorius, I., Piketh, S. J., Burger, R. P., & Neomagus, H. (2015). A Perspective of South African Coal-Fired Power Station Emissions. *The Clean Air Journal*, *26*(3), 27-40.

Ramsaroop, B. R. (2012). Flue Gas Desulphurization using Natural Calcium Based Sorbents MSc dissertation, University of Kwazulu-Natal

Rowland, C.A. & Kjos, D.M. (1980). Mineral Processing Plant Design. New York: SME/AIME; 239-278

Schlanz, J.W. (1987). Grinding: An Overview of Operation and Design. North Carolina State University

Srivastava, R. K., & Jozewicz, W. (2001). Flue gas desulfurization: The state of the art.

Journal of the Air and Waste Management Association, *51*(12), 1676–1688.

Towler, G & Sinnott, R. (2008). Chemical Engineering Design. Principles, Practice and Economics of Plant and Process Design. 297-392

Warman Slurry Pump Handbook and Technical Bulletins (2000). Belmont, WA, Warman International Ltd, pp 71-73

Wilson, K. & Addie, G. (2006). Slurry Transport Using Centrifugal Pumps, 3rd Edition.

Appendix A: Testwork Results

Table A-1: Locked Cycle Test Ball Mill Conditions

INPUT DATA	
% grinding media in mill	**35.0**
Specific gravity of balls	**7.85**
mill diameter (inside liners (m))	**0.265**
mill length (inside liners (m))	**0.305**
specific gravity of ore	**2.7869**
% filling of voids with pulp	**100**
mill discharge trunnion diameter (m)	**0**
CALCULATED DATA	
% solids by mass of pulp	**69.51**
fractional vol. of ball charge	**0.3500**
1/2 angle subtending trunnion (rad)	**1.5708**
$J_{trunnion...}$(fraction)	**0.3500**
ball charge mass (g)	**27 731**
total charge volume (m^3)	**0.00589**
volume of slurry (m^3)	**0.00236**
mass of solids in mill (kg)	**2.954**
volume of water (litres)	**1.295**
slurry density(sg)	**1.804**
% solids by volume	**45.00**

Table A-2: Locked Cycle Test Ball Mill Charge

minimum ball size (mm) =	**10**			
ball size (mm)	cum %	size %	size mass (kg)	Actual ball sizes (mm)
70	100.00	46.04	12.768	-45+40
60	53.96	27.96	7.753	-35+30
50	26.00	15.38	4.264	-25+20
40	10.63	7.29	2.022	
30	3.33	3.33	0.924	
total		100.00	**27.731**	
torque (Nm) = 14		net power draw [based on torque) (kW)] =		0.09
mill speed as fraction of critical =		**0.75**		

Table A-3: Raw Testwork Data for Locked Cycle Test Conducted at Mintek

Locked cycle milling test results

Operator input

Feed conditions for cycle

Energy input for next cycle

Circuit Specific Energy

Mill speed 63rpm

M 2954 gram 0.002954 tonne

Target circulating load 250 % Target re-circulating load

Mass of undersize required 844 Target undersize mass at steady state

Filter cake moisture calculation

wet mass 449.5 39 min 25 sec

dry mass 336.3

% solids 74.8

Target % solids in mill feed 69.51%

Total water required per cycle 1295

Factor for calculation *3.5*

% solids in +2mm filter cake 75%

Cycle no	MU (g)	Water to add (g)	Actual energy input (basis of mill contents M) (kWh/t)	Energy input (kWh)	Filter cake mass MP+ (g)	Assumed dry mass MP+ (g)	Assumed MP- (g)	Undersize production rate (g/kWh)	Energy required to produce target Undersize (kWh)	Energy input for next cycle on basis of mill contents (kWh/t)	Recirculating load (%)	Target recirculating load (%)	Water in O/s recycle (g)	Circuit Specific energy based on circuit product kWh/t	Milling Time	Actual dry mass (g) MP -	Variation from estimate %	Recirculating load based on dry mass %
1	2954	1295	15.83	0.04676	1322	988.97	1965.03	42022.14	0.0201	6.80	50.33	250	332.8	23.80	31min 25sec	1945.6	-0.99	51.8
2	1965	962	6.81	0.02012	1553	1162.29	1791.71	89065.71	0.0095	3.21	64.87	250	391	11.23	13min 36sec	777.9	-56.59	279.8
3	1792	904	3.21	0.00948	2710	2027.96	926.04	97659.34	0.0086	2.93	218.99	250	682	10.24	6 min 29 sec	758.2	-18.12	289.6
4	926	613	2.95	0.00871	2929	2191.12	762.88	87543.40	0.0096	3.26	287.22	250	737	11.42	5min 52 sec	755.3	-1.00	291.1
5	763	558	3.27	0.00966	2958	2213.12	740.88	76699.24	0.0110	3.73	298.71	250	745	13.04	6 min 31 sec	758.0	2.31	289.7
6	741	550	3.73	0.01102	2919	2184.05	769.95	69878.44	0.0121	4.09	283.66	250	735	14.31	7 min 18 sec	769.7	-0.03	283.8
7	770	560	4.28	0.01264	2886	2159.47	794.53	62842.74	0.0134	4.55	271.79	250	727	15.91	8 min 28 sec	826.8	4.06	257.3
8	795	568	4.63	0.01368	2759	2064.15	889.85	65061.59	0.0130	4.39	231.97	250	695	15.37	9 min 14 sec	789.8	-11.24	274.0
9	890	600	4.39	0.01297	2830	2117.40	836.60	64512.30	0.0131	4.43	253.10	250	713	15.50	8 min 45 sec	836.6	0.00	253.1
10	837	582	4.43	0.01309	2814	2105.43	848.57	64844.59	0.0130	4.41	248.11	250	709	15.42		814.6	-4.00	262.6

Table A-4: Loesche Pilot Scale Testwork Results (Düsseldorf, Germany)

Dam Ring Height		**7 mm**		**20 mm**	
Measurement no	**#**	**1**	**2**	**1**	**2**
Grinding Table Speed	1/min	97.8	97.8	97.8	97.8
Working Pressure	bar	91.0	90.8	150.3	150.4
Classifier Speed	1/min	439.5	359.6	439.5	319.6
Gas Flow After Filter	m³/h	1526	1523	1399	1397
Mill Differential Pressure	mbar	18.4	18.2	16.4	16.1
Exit Temperature	°C	90.4	90.0	89.7	90.6
Mill Power	kW	3.4	3.8	5.8	6.7
Classifier Power	W	110.7	69.8	88.2	44.8
Fan Power	kW	2.5	2.7	2.1	2.3
Air Temperature	°C	20.0	19.3	20.1	19.9
Mill Inlet Temperature	°C	187.8	198.0	173.1	185.0
Specific Power Consumption	**kWh/t**	**6.7**	**5.6**	**16.1**	**13.7**
Product Size Grading					
200 µm	m-%				
125 µm	m-%		0.1		0.1
90 µm	m-%	0.0	0.5	0.0	1.1
63 µm	m-%	0.7	5.1	0.5	6.1
45 µm	**m-%**	**5.5**	**14.9**	**4.1**	**13.3**
40 µm	m-%				
32 µm	m-%	17.1	27.2	10.5	23.0
25 µm	m-%				
20 µm	m-%	37.7	45.8	27.0	38.0
Surface Area	cm²/g	3328	2890	5953	5340
Load Factor	-	0.7	1.0	0.5	0.7

Appendix B: Process Design Criteria

Table B-1: PDC1101 – Conventional Wet Ball Mill Circuit Process Design Criteria

PROCESS DESIGN CRITERIA		
PROJECT:	FGD Feed Preparation Trade-Off	Revision: A
PROCESS AREA:	Feed Preparation Milling Circuit	
DESCRIPTION:	Ball Mill	By: C Swart
DOCUMENT NUMBER:	PDC1101	Date: 2020.01.28

	UNITS	VALUE	REF. / CONF.	SOURCE / COMMENT	REV
Plant Design Basis					
Temperature (Ave)	°C	25.0	D		A
Temperature (Min)	°C	-5.0	D		A
Temperature (Max)	°C	40.0	D		A
Atmospheric Humidity (Min)	%	40.0	D		A
Atmospheric Humidity (Max)	%	60.0	D		A
Height Above Sealevel	m	2,100.0	D		A
Plant Capacity					
Operating Factor	%	89.8	E		A
Operating Hours	h/a	7,866	E		A
Feed Solids (Design)	t/h	100.0	D		A
Annual Throughput	t/a	786,648	E		A
Materials Properties					
Solids S.G.	ratio	2.79	T	Measured with a Gas Pycnometer at Mintek	A
Liquid Density	t/m^3	1.0	D		A
Feed Solids Content	%	99.7	C	Power Point Presentation by Kusile Engineers (Eskom)	A
Abrasion Index	Ai	0.1	A	Typical	A
Bond Work Index	kWh/t	12.0	C	Power Point Presentation by Kusile Engineers (Eskom)	A
Particle Feed Size Distribution					
F_{100}	mm	19.0	O	Provided by Idwala and measured at Mintek	A
$F_{77.6}$	mm	12.5	O	Provided by Idwala and measured at Mintek	A
$F_{1.4}$	mm	8.0	O	Provided by Idwala and measured at Mintek	A
Sample Composition					
$CaCO_3$	wt%	96.3	O	Provided by Idwala Lime	A
$MgCO_3$	wt%	1.38	O	Provided by Idwala Lime	A
SiO_2	wt%	1.08	O	Provided by Idwala Lime	A
Fe_2O_3	wt%	0.28	O	Provided by Idwala Lime	A
Al_2O_3	wt%	0.23	O	Provided by Idwala Lime	A
Mn_2O_3	wt%	0.46	O	Provided by Idwala Lime	A
TiO_2	wt%	0.01	O	Provided by Idwala Lime	A
Cl	wt%	0.01	O	Provided by Idwala Lime	A
SO_3	wt%	0.13	O	Provided by Idwala Lime	A
K_2O	wt%	0.06	O	Provided by Idwala Lime	A
Na_2O	wt%	0.01	O	Provided by Idwala Lime	A

P_2O_5	wt%	0.01	O	Provided by Idwala Lime	A
Other	wt%	0.00	O	Provided by Idwala Lime	A

Comminution

Feed Silo

Capacity per Silo	days	2.0	A		A
Number of Silos	number	2.0	A		A

Ball Mill

Mill Type	text	Ball Mill	D		A
Model	text	Overflow Discharge	D		A
Inner Diameter	m	4.8	V	Vendor Budgetary Quote	A
Effective Grinding Length	m	9.75	V	Vendor Budgetary Quote	A
Installed Power	kW	3,700.00	V	Vendor Budgetary Quote	A
Absorbed Power	kW	2,649.0	C	Based on Kusile Specific Energy	A
Drive Type	text	Inching Drive	C	With speed reducer and break	A
Feed Size F80	mm	12.8	O		A
Mill Circulating Load (Nominal)	wt%	300	A	Typical	A
Mill Circulating Load (Design)	wt%	400	C	Power Point Presentation by Kusile Engineers (Eskom)	A
Specific Energy	kWh/t	26.5	E		A
% of Critical Speed	%	75.0	A	Typical	A
Grinding Media Size (mm)					
60	tons	35.0	C	Power Point Presentation by Kusile Engineers (Eskom)	A
50	tons	38.0	C	Power Point Presentation by Kusile Engineers (Eskom)	A
40	tons	31.0	C	Power Point Presentation by Kusile Engineers (Eskom)	A
30	tons	13.0	C	Power Point Presentation by Kusile Engineers (Eskom)	A
25	tons	9.0	C	Power Point Presentation by Kusile Engineers (Eskom)	A
Grinding Media Type	text	Steel balls	A		A
Grinding Media Consumption	g/Mt	550	C	Power Point Presentation by Kusile Engineers (Eskom)	A
Total Charge	wt%	28.5	C	Power Point Presentation by Kusile Engineers (Eskom)	A
Electricity Requirement	A	154.0	C	Power Point Presentation by Kusile Engineers (Eskom)	A
Mill Discharge Solids Content	wt%	71.1	C	Power Point Presentation by Kusile Engineers (Eskom)	A

Trommel Screen

Aperture	mm	1.0	A	Typical	A

Ball Mill Discharge Sump

Residence Time	min	1.0	E	Typical	A
Discharge Solids Concentration	wt%	55.0	C	Power Point Presentation by Kusile Engineers (Eskom)	A

Ball Mill Classifier Cyclone

Cyclone On-Line	number	20	V	Vendor Budgetary Quote	A
Cyclones Standby	number	4	V	Vendor Budgetary Quote	A
Operating Pressure	kPa	65.0	V	Vendor Budgetary Quote	A
Feed Solids Concentration	wt%	55.6	C	Kusile Information and Cyclone Simulation	A

Overlfow P_{85}	wt%	45.0	C	Power Point Presentation by Kusile Engineers (Eskom)	A
Overflow Density	t/m³	1.23 - 1.25	C	Power Point Presentation by Kusile Engineers (Eskom)	A
Solids Split to Overflow	wt%	20.3	C	Vendor Budgetary Quote	A
$D_{50}c$	µm	51.0	C	Vendor Budgetary Quote	A
FGD Reagent Feed Tank					
Residence Time	min	10	A		A
Solids Concentration in Discharge	wt%	30	O	Power Point Presentation by Kusile Engineers (Eskom)	A

Table B-2: PDC2101 – Dry VRM Circuit Process Design Criteria

PROCESS DESIGN CRITERIA

PROJECT:	**FGD Feed Preparation Trade-Off**	**Revision: A**
PROCESS AREA:	**Feed Preparation Milling Circuit**	
DESCRIPTION:	**Vertical Roller Mill**	By: C Swart
DOCUMENT NUMBER:	**PDC2101**	Date: 2020.01.28

	UNITS	VALUE	REF. / CONF.	SOURCE / COMMENT	REV
Plant Design Basis					
Temperature (Ave)	°C	25.0	D		A
Temperature (Min)	°C	-5.0	D		A
Temperature (Max)	°C	40.0	D		A
Atmospheric Humidity (Min)	%	40.0	D		A
Atmospheric Humidity (Max)	%	60.0	D		A
Height Above Sealevel	m	2,100.0	D		A
Plant Capacity					
Operating Factor	%	89.8	D	Design Basis	A
Operating Hours	h/a	7,866	E		A
Feed Solids (Design)	t/h	100.0	D		A
Annual Throughput	t/a	786,648	E		A
Materials Properties					
Solids S.G.	ratio	2.8	T	Measured with a Gas Pycnometer at Mintek	A
Liquid Density	t/m³	1.0	D		A
Feed Solids Content	%	99.7	C	Power Point Presentation by Kusile Engineers (Eskom)	A
Abrasion Index	Ai	0.1	A	Typical	A
Bond Work Index	kWh/t	12.0	C	Power Point Presentation by Kusile Engineers (Eskom)	A
Particle Feed Size Distribution					
F_{100}	mm	19.0	O	Provided by Idwala and measured at Mintek	A
$F_{77.6}$	mm	12.5	O	Provided by Idwala and measured at Mintek	A
$F_{1.4}$	mm	8.0	O	Provided by Idwala and measured at Mintek	A
Sample Composition					
$CaCO_3$	wt%	96.3	O	Provided by Idwala	A
$MgCO_3$	wt%	1.38	O	Provided by Idwala	A
SiO_2	wt%	1.08	O	Provided by Idwala	A

Fe_2O_3	wt%	0.28	O	Provided by Idwala	A
Al_2O_3	wt%	0.23	O	Provided by Idwala	A
Mn_2O_3	wt%	0.46	O	Provided by Idwala	A
TiO_2	wt%	0.01	O	Provided by Idwala	A
Cl	wt%	0.01	O	Provided by Idwala	A
SO_3	wt%	0.13	O	Provided by Idwala	A
K_2O	wt%	0.06	O	Provided by Idwala	A
Na_2O	wt%	0.01	O	Provided by Idwala	A
P_2O_5	wt%	0.01	O	Provided by Idwala	A
Other	wt%	0.00	O	Provided by Idwala	A

Comminution

Feed Silo

Capacity per Silo	days	2.0	A		A
Number of Silos	number	2.0	A		A

Vertical Roller Mill (VRM)

Mill Type	text	VRM	V		A
Model	text	LM 31.3	V	Loesche Proposal	A
Number of Grinding Tyres	number	3	V	Loesche Proposal	A
Lifetime of Wear Parts	hours	7,500	V	Loesche Proposal	A
Diameter of Table	m	3.1	V	Loesche Proposal	A
Installed Power	kW	1,200	V	Loesche Proposal	A
Absorbed Power	kW	1,160	V	Loesche Proposal	A
Drive Type	text	LM	V	Loesche Proposal	A
Drive Shaft Speed	rpm	990.0	V	Loesche Proposal	A
Rated Voltage	V	380.0	V	Loesche Proposal	A
Rated Frequency	Hz	50.0	V	Loesche Proposal	A
Feed Size F80	mm	12.5	D		A
Gas Feed Temperature	°C	196.9	D		A
Gas Consumption	Nm^3/h	128.6	V	Loesche Proposal (HHG)	A
Classifier Type	text	LKS D	V	Loesche Proposal	A
Classifier Drive Type	text	VSD	V	Consisting of multi-V-pulleys and power belts	A
Classifier Rated Output	kW	100.0	V	Loesche Proposal	A
Classifier Rated Speed	rpm	1,500.0	V	Loesche Proposal	A
Classifier Rated Voltage	V	380.0	V	Loesche Proposal	A
Classifier Rated Frequency	Hz	50.0	V	Loesche Proposal	A
Mill Product Size P85	µm	45	D	Loesche Testwork in Germany (Test 1)	A
Specific Power Consumption	kWh/t	13.5	T	Loesche Testwork in Germany	A
Mill Product Size P95	µm	45	D	Loesche Testwork in Germany (Test 2)	A
Specific Power Consumption	kWh/t	16.1	T	Loesche Testwork in Germany	A
VRM Outlet Temperature	°C	90	V	Loesche Proposal (HHG)	A

Mill Dedusting System

Type of Dust	text	Milled Limestone	V	Loesche Proposal	A
Raw Gas Flowrate at Filter Inlet	Am^3/h	222,092.0	V	Loesche Proposal	A
Dust Content in Cleaned Gas	mg/Nm^3	< 20	V	Loesche Proposal	A
Compressed Air Consumption	Nm^3/h	110.0	V	Loesche Proposal	A
Compressed Air Pressure	bar	6-7	V	Loesche Proposal	A

High Pressure Mill Fan

Air Flow	Am^3/h	261,468	V	Loesche Proposal	A

Inlet Temperature	°C	87.4	V	Loesche Proposal (HHG)	A
Pressure Drop	mbar	65.0	V	Loesche Proposal	A
Outlet Temperature	°C	97.4	V	Loesche Proposal (HHG)	A
Rated Output	kW	500.0	V	Loesche Proposal	A
Rated Speed	rpm	3,000.0	V	Loesche Proposal	A
Rated Voltage	V	380.0	V	Loesche Proposal	A
Rated Frequency	Hz	50.0	V	Loesche Proposal	A

Hot Gas Generator (Optional)

Type of Hot Gas Generator (HGG)	text	LP	V	Loesche Proposal (HHG)	A
Type of Heater	text	LOMA Type LF	V		A
Secondary Air Flowrate	Nm³/h	29.8	V	Loesche Proposal (HHG)	A
Secondary Air Temperature	°C	15	V	Loesche Proposal (HHG)	A
Burning Gas Flowrate	Nm³/h	6.7	V	Loesche Proposal (HHG)	A
Burning Gas Temperature	°C	1,954	V	Loesche Proposal (HHG)	A
Power of HGG	kW	6,020	V	Loesche Proposal (HHG)	A
Firing Gas Temperature	°C	450	V	Loesche Proposal (HHG)	A

FGD Reagent Feed Tank

Residence Time	min	10	A		A
Solids Concentration in Discharge	wt%	30	O	Power Point Presentation by Kusile Engineers (Eskom)	A

Appendix C: Process Flow Diagrams

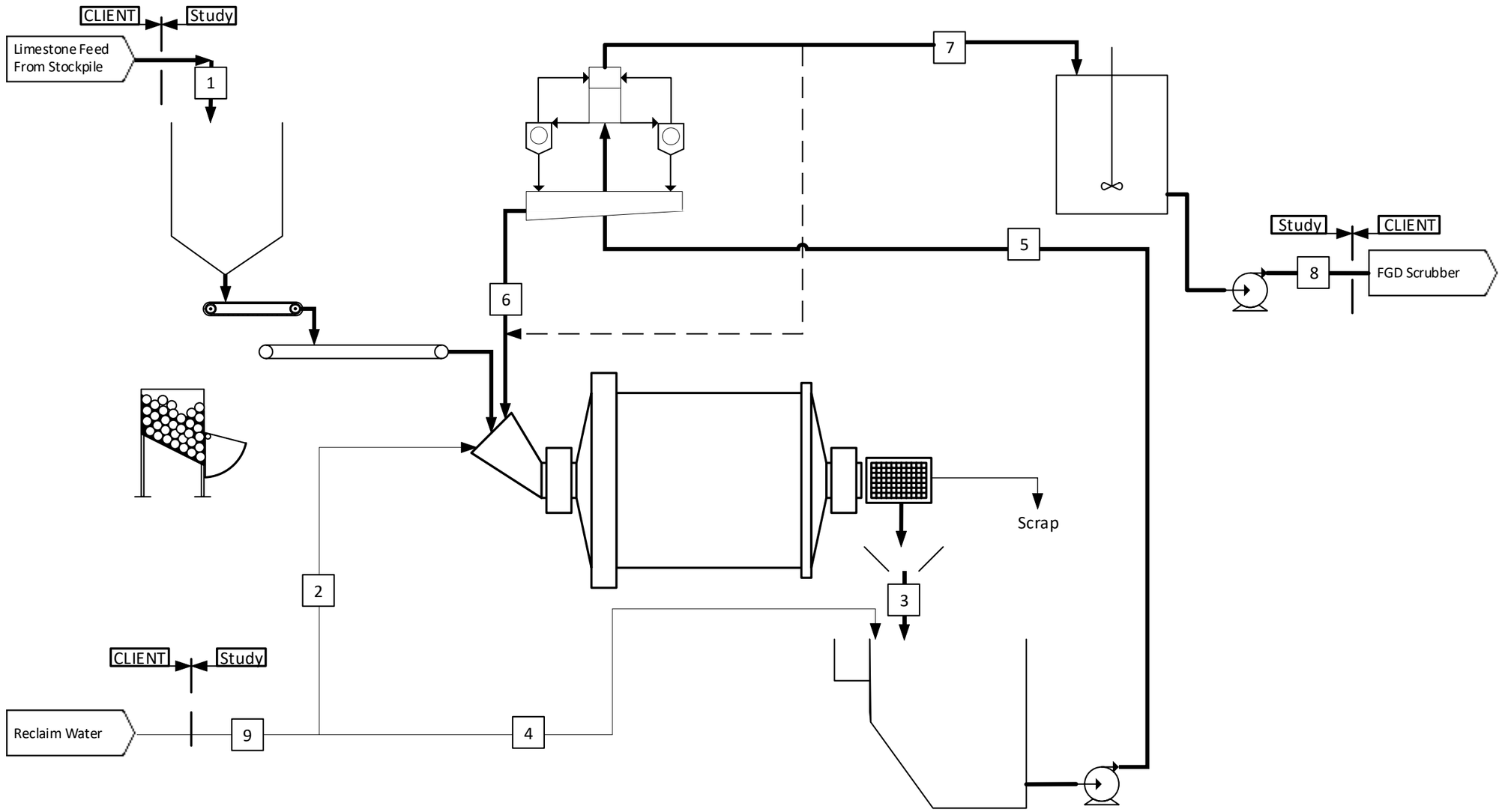

Stream Number	Units	1	2	3	4	5	6	7	8	9
Solids Tonnage	tonnes/h	100.0	1.2	501.2	6.5	507.8	400.0	107.8	107.8	7.8
Water Flowrate	m^3/h	0.3	40.1	203.7	211.1	414.8	163.4	251.5	251.5	251.2
Solids Concentration	wt%	99.7	3.0	71.1	3.0	55.0	71.0	30.0	30.0	3.0
Pulp Density	t/m^3	2.77	1.02	1.84	1.02	1.55	1.84	1.24	1.24	1.02
Solids SG	-	2.79	2.79	2.79	2.79	2.79	2.79	2.79	2.79	2.79

LEGEND

- MATERIAL FLOW
- PRIMARY FLOW
- SECONDARY FLOW
- INTERMITTENT FLOW

Figure C-1: PFD1101 – Process Flow Diagram Conventional Wet Ball Mill Circuit

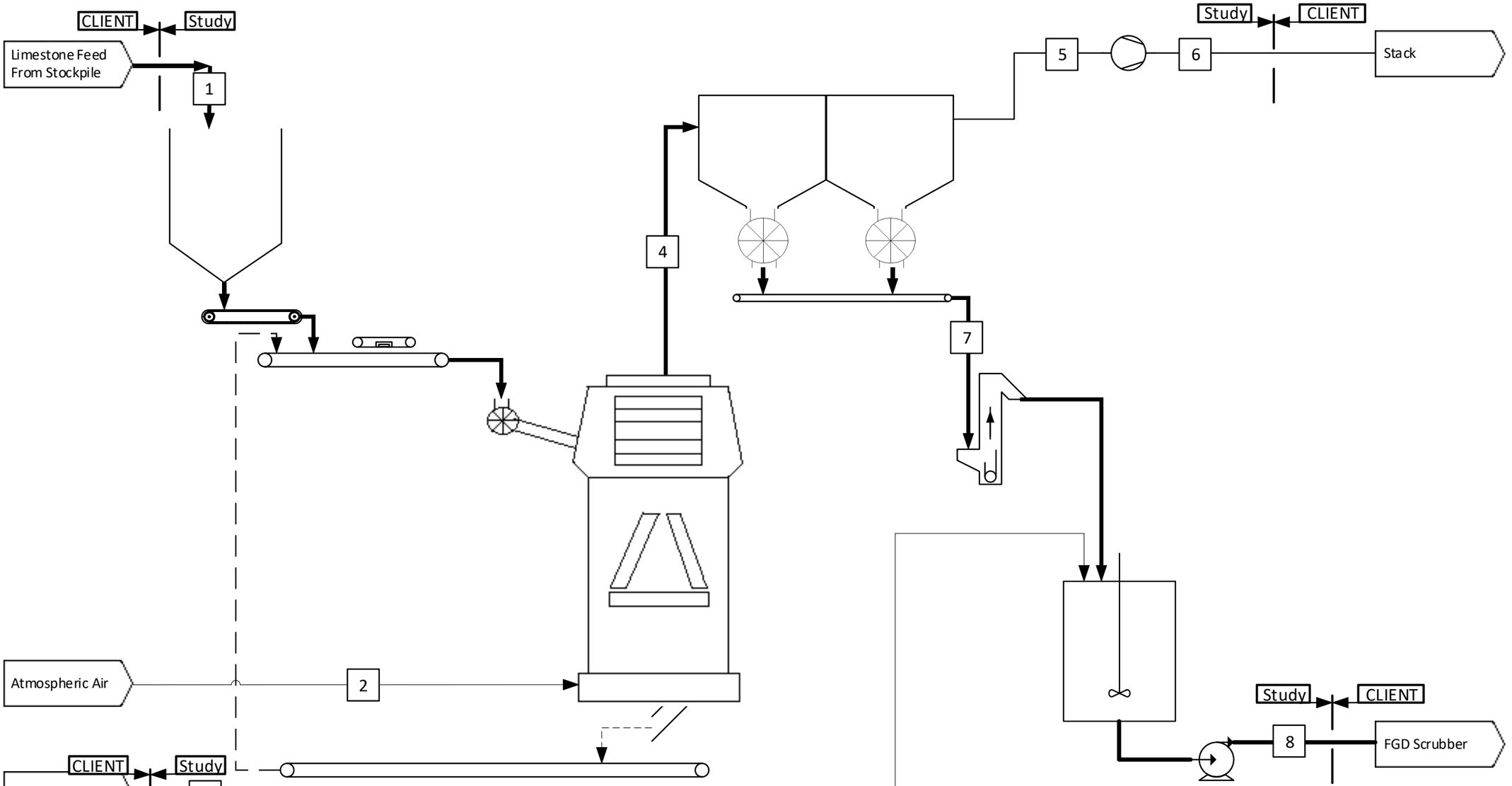

Stream Number	Units	1	2	3	4	5	6	7	8
Solids Tonnage	tonnes/h	100.0	-	7.8	100.0	0.0	0.0	100.0	107.8
Water Flowrate	m^3/h	0.3	-	251.2	-	-	-	0.3	251.5
Gas	Nm^3/h	-	128.6	-	144.9	152.6	153.3	-	-
Solids Concentration	wt%	99.7	-	3.0	100.0	-	-	100.0	30.0
Pulp Density	t/m^3	2.77	-	1.02	-	-	-	2.77	1.24
Solids SG	-	2.79	-	2.79	2.79	2.79	2.79	2.79	2.79
Temperature	°C	25.0	25.0	25.0	90.0	87.4	97.4	90.0	40.0
Pressure	mbar	1001.3	1001.3	1001.3	925.3	910.3	1001.3	1001.3	1001.3

Figure C-2: PFD2101 – Process Flow Diagram Dry Milling Loesche VRM

Appendix D: Typical Piping and Instrumentation Diagrams

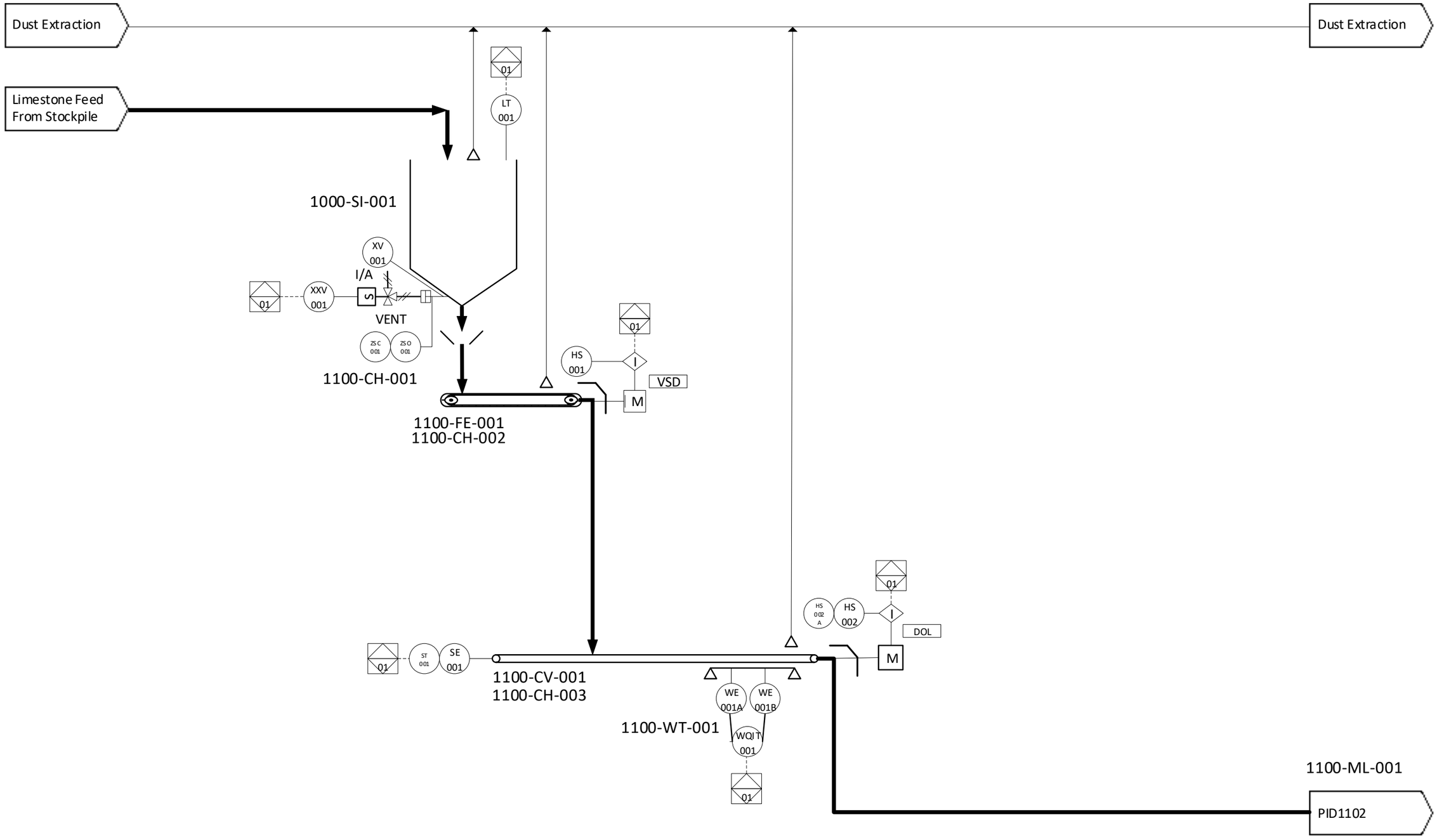

Figure D-1: PID1101 – Ball Mill Circuit Piping and Instrumentation Diagram Page 1

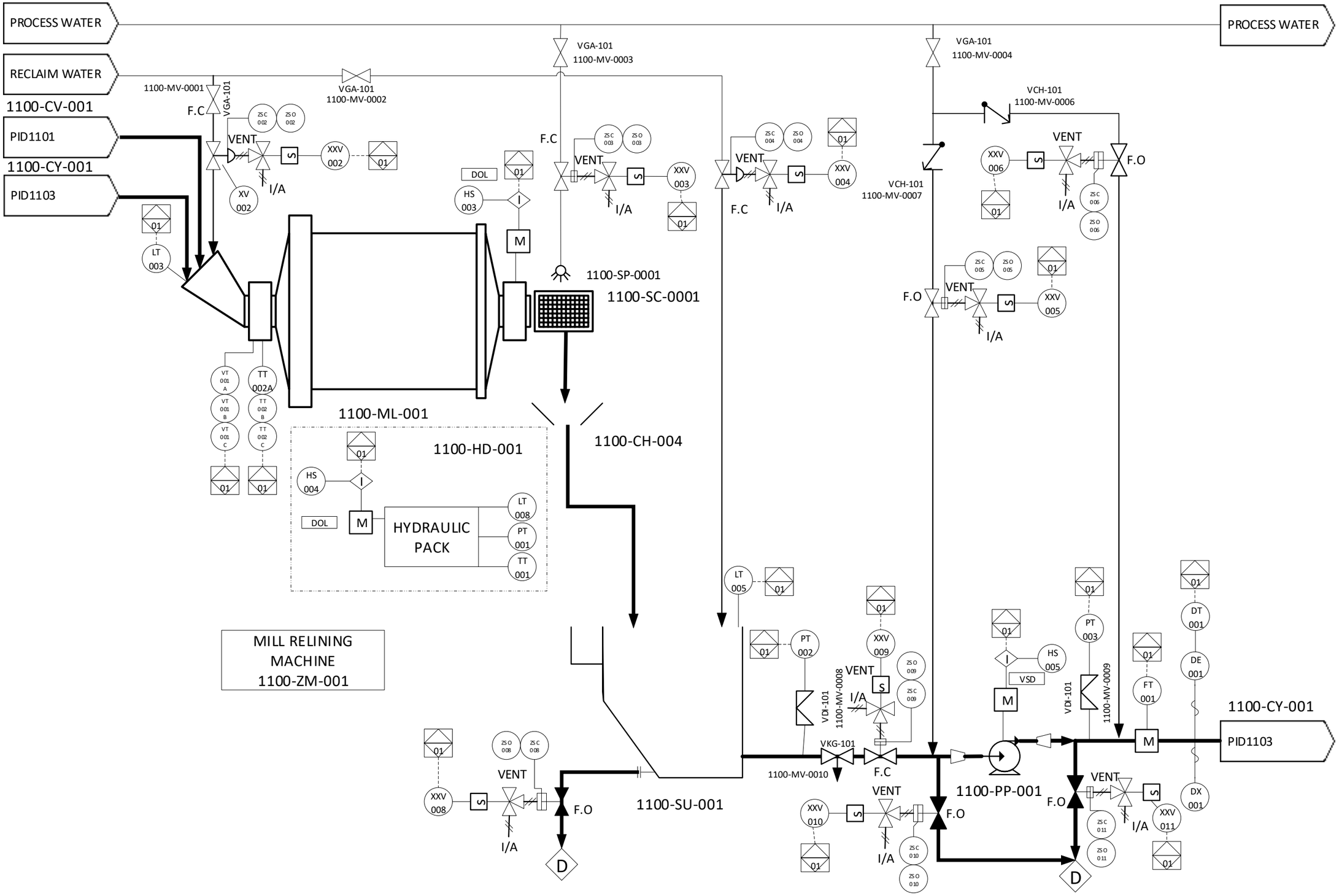

Figure D-2: PID1102 – Ball Mill Circuit Piping and Instrumentation Diagram Page 2

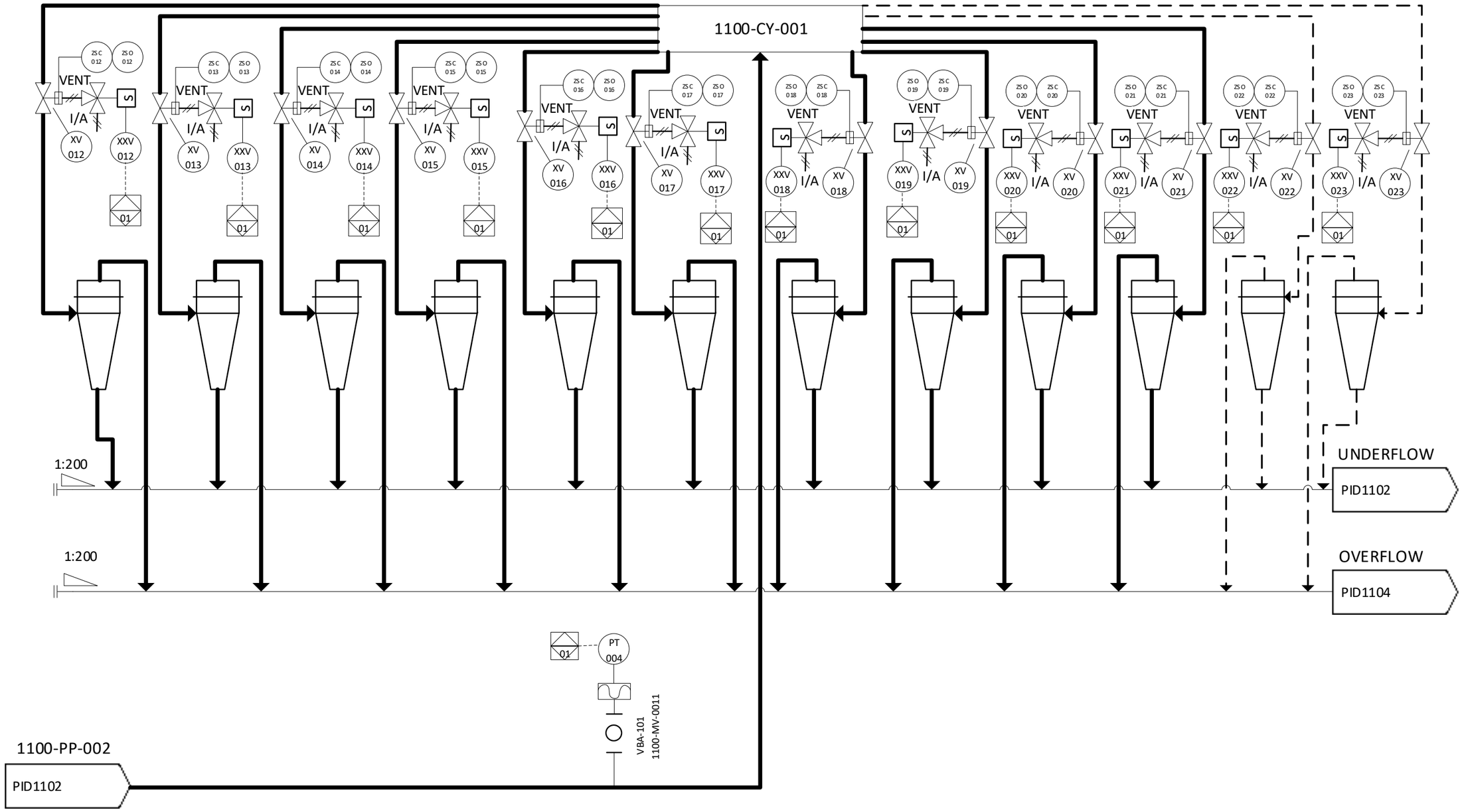

Figure D-3: PID1103 – Ball Mill Circuit Piping and Instrumentation Diagram Page 3

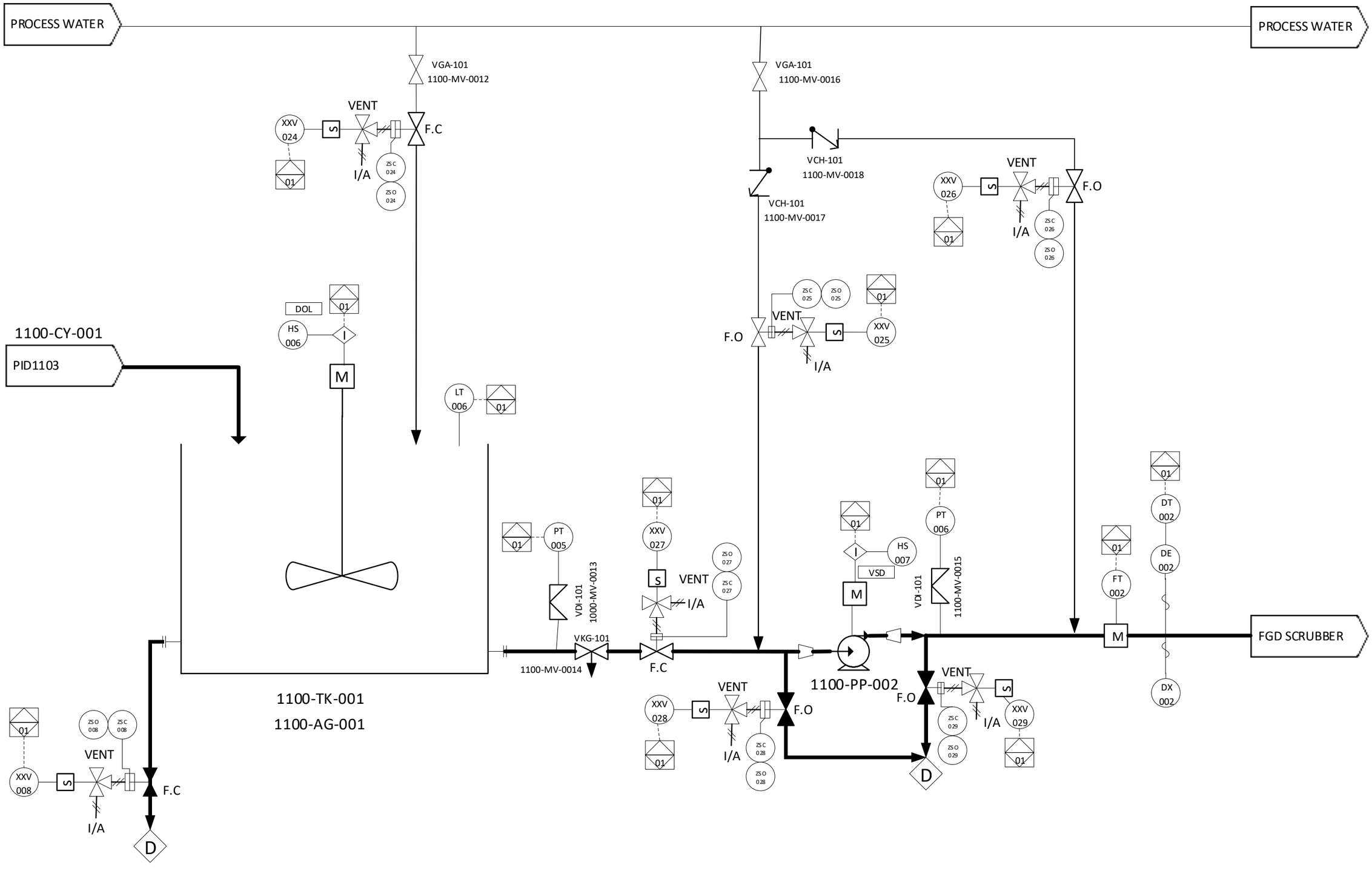

Figure D-4: PID1104 – Ball Mill Circuit Piping and Instrumentation Diagram Page 4

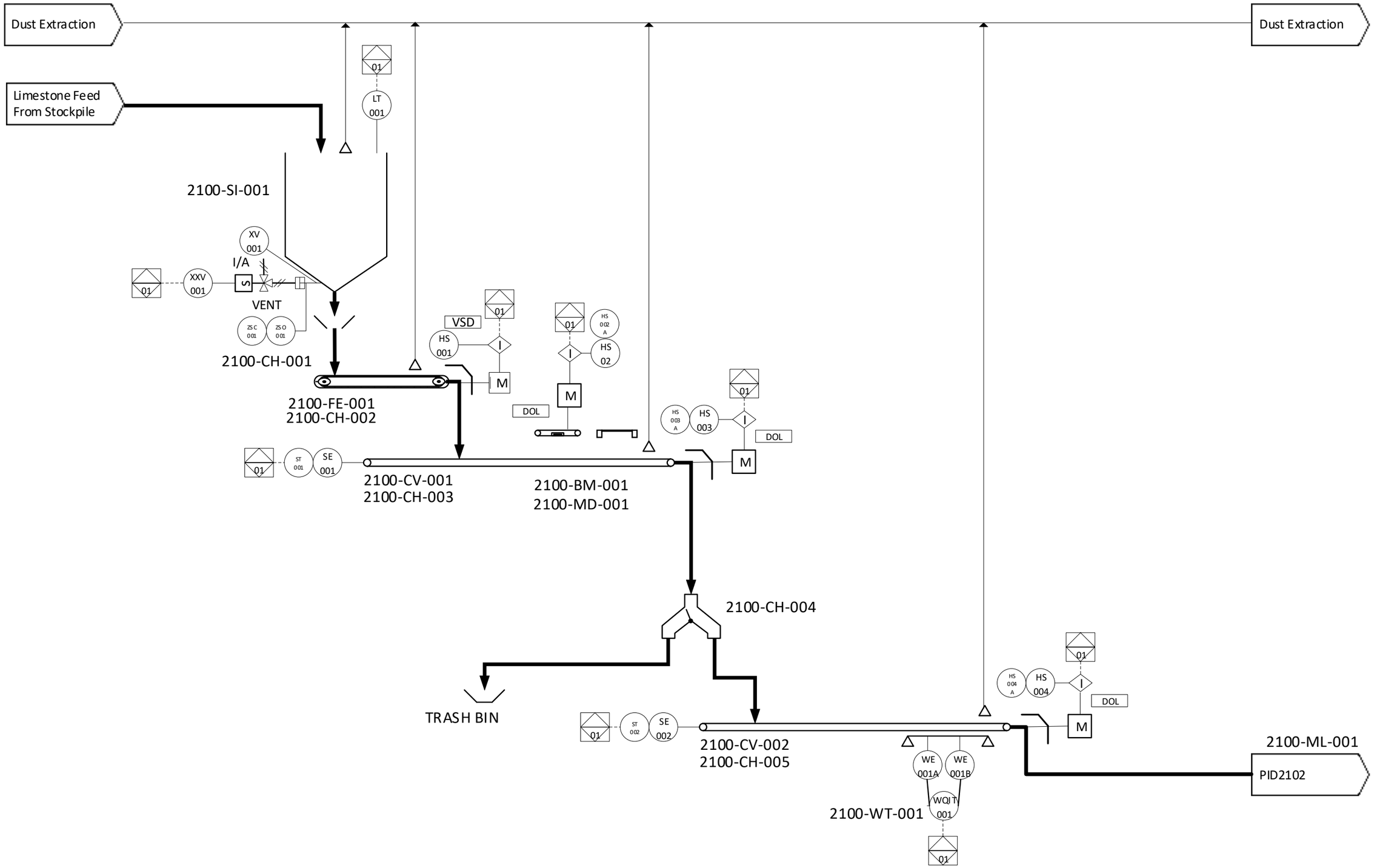

Figure D-5: PID2101 – Dry Milling Loesche VRM Piping and Instrumentation Diagram Page 1

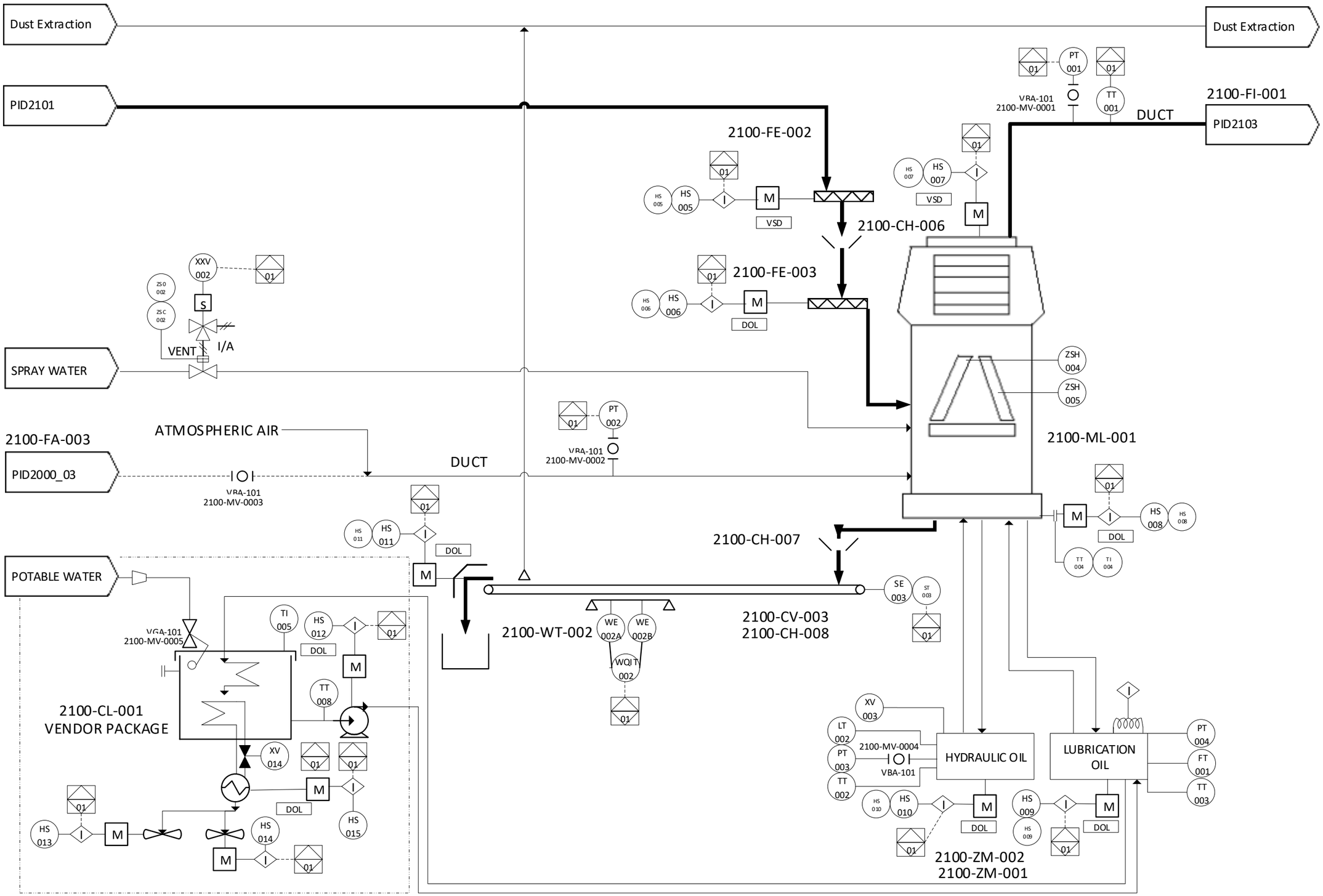

Figure D-6: PID2202 – Dry Milling Loesche VRM Piping and Instrumentation Diagram Page 2

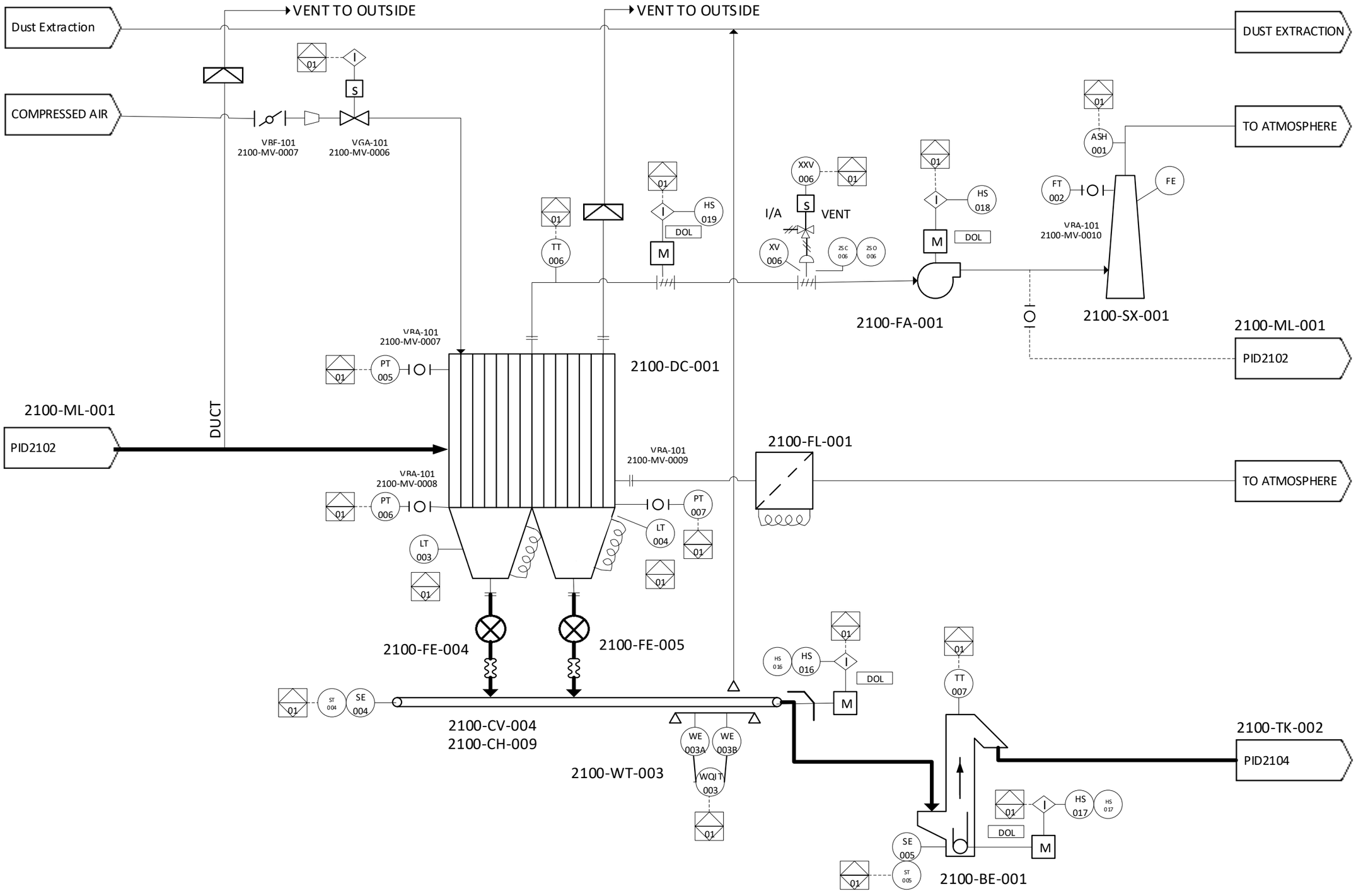

Figure D-7: PID2203 – Dry Milling Loesche VRM Piping and Instrumentation Diagram Page 3

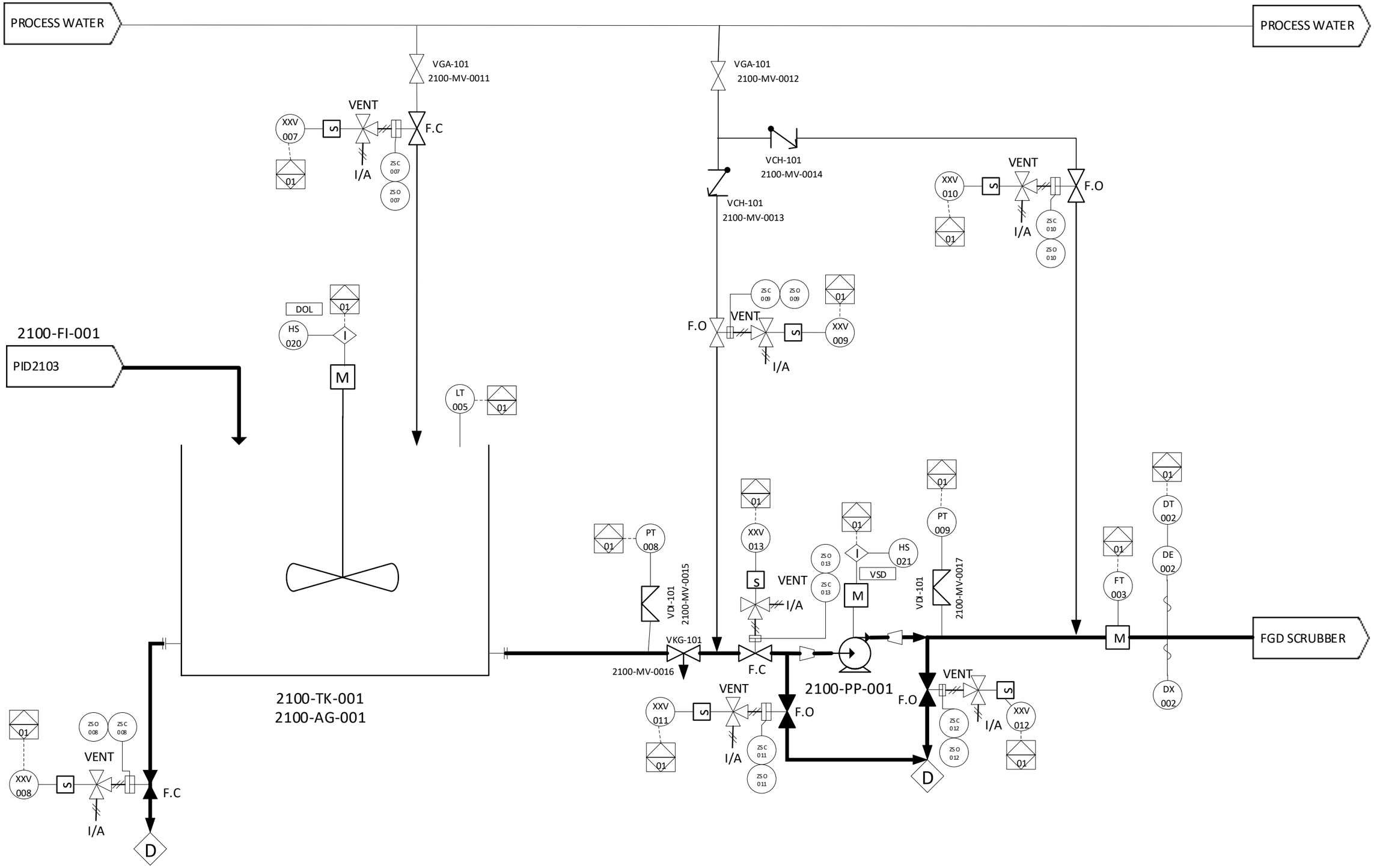

Figure D-8: PID2204 – Dry Milling Loesche VRM Piping and Instrumentation Diagram Page 4

Appendix E: Mechanical Equipment List

Table E-1: MEL1101 – Ball Mill Circuit Mechanical Equipment List

AREA	CODE	#	P&ID	DESCRIPTION	SIZE	INSTALLED POWER	ABSORBED POWER	COST
1101	SI	001	PID1101	SILO	Not Included	-	-	not incl.
1101	CH	001	PID1101	CHUTE	Platework=282.6kg; Support Steelwork=353.25kg; Liner Type=VRN 400; Liner=4.5m2	-	-	R 41,012.33
1101	FE	001	PID1101	BELT FEEDER	36"x5, 115 t/h design capacity, 900 mm width, 5 m between pulleys	22	17	R 2,502,177.30
1100	CH	002	PID1101	FEEDER DISCHARGE CHUTE	Platework=565.2kg; Support Steelwork=706.5kg; Liner Type=VRN 400; Liner=9m2	-	-	R 82,024.65
1100	CV	001	PID1101	CONVEYOR	600 mm width, 10 m length, horizontal, 3 kW motor drive, 1262 kg	3	3	R 157,200.63
1100	CH	003	PID1101	CONVEYOR DISCHARGE CHUTE	Platework=565.2kg; Support Steelwork=706.5kg; Liner Type=VRN 400; Liner=9m2	-	-	R 82,024.65
1100	WT	001	PID1101	WEIGHTOMETER	6 idler, 3 roll, 600 mm belt width	-	-	R 288,930.00
1100	ML	001	PID1102	BALL MILL	Ø 4.8 x 9.75 M	3700	2649	R 38,020,500.00
1100	CH	004	PID1102	MILL DISCHARGE CHUTE	Platework=2260.8kg; Support Steelwork=2826kg; Liner Type=VRN 400; Liner=36m2	-	-	R 328,098.60
1100	SC	001	PID1102	TROMMEL SCREEN	Included in ball mill supplier scope	-	-	incl.
1100	SU	001	PID1102	MILL DISCHARGE UNDERFLOW SUMP	12.5 m³ Cylindrical SB 1 min Residence Time with Epoxy Coating 250 mm Freeboard (1,612 kg Steel)	-	-	R 103,974.00
1100	PP	001	PID1102	MILL DISCHARGE PUMP	8/6 pump size, 62.4% pump efficiency, 10.6 m TDH, 13.7 m/s impeller tip speed	15	11	R 126,937.12
1100	HD	001	PID1102	HYDRAULIC POWER PACK	Included in ball mill supplier scope	incl.	incl.	incl.

1100	ZM	001	PID1102	MILL RELINING MACHINE	Included in ball mill supplier scope	50	39	R 4,987,623.00
1100	CY	001	PID1103	CYCLONE CLUSTER	24-way cluster, 20 operating @ 65 kPa, 50 mm spigot size	-	-	R 946,723.50
1100	TK	001	PID1104	REAGENT FEED TANK	62 m³ Cylindrical FB 10 min Residence Time with Epoxy Coating 250 mm Freeboard (3,760 kg Steel)	-	-	R 242,520.00
1100	AG	001	PID1104	REAGENT FEED TANK AGITATOR		15		R 159,799.00
1100	PP	002	PID1104	REAGENT FEED PUMP	8/6 pump size, 72.7% pump efficiency, 10.9 m TDH, 14.2 m/s impeller tip speed	22	16	R 257,983.59
					TOTAL	**3802**	**2734**	**R 48,327,528.37**

Table E-2: MEL2102 – VRM Mechanical Equipment List

AREA	CODE	#	P&ID	DESCRIPTION	SIZE	INSTALLED POWER	ABSORBED POWER	COST
2100	SI	001	PID1101	FEED SILO	NOT INCLUDED	-	-	NOT INCLUDED
2100	CH	001	PID1101	FEED SILO DISCHARGE CHUTE	Platework=282.6kg; Support Steelwork=353.25kg; Liner Type=VRN 400; Liner=4.5m2	-	-	R 41,012.33
2100	FE	001	PID1101	BELT FEEDER	36"x5, 115 t/h design capacity, 900 mm width, 5 m between pulleys	22	16.50	R 2,502,177.30
2100	CH	002	PID1101	FEEDER DISCHARGE CHUTE	Platework=565.2kg; Support Steelwork=706.5kg; Liner Type=VRN 400; Liner=9m2	-	-	R 82,024.65
2100	CV	001	PID1101	FEED CONVEYOR	600 mm width, 10 m length, horizontal, 3 kW motor drive, 1262 kg	3	2.69	R 157,200.63
2100	CH	003	PID1101	FEED CONVEYOR DISCHARGE CHUTE	Platework=565.2kg; Support Steelwork=706.5kg; Liner Type=VRN 400; Liner=9m2	-	-	R 82,024.65
2100	WT	001	PID1101	WEIGHTOMETER	6 idler, 3 roll, 600 mm belt width	-	-	R 288,930.00
2100	MA	001	PID1101	OVERHEAD MAGNET	Provided by vendor	7.5	6.11	R 2,456,736.30
2100	MD	001	PID1101	METAL DETECTOR	Provided by vendor	4.0	2.84	R 264,500.00

2100	CH	004	PID1101	DIVERTER CHUTE	Platework=1130.4kg; Support Steelwork=1413kg; Liner Type=VRN 400; Liner=18m2	-	-	R 164,049.30
2100	CV	002	PID1101	VRM FEED CONVEYOR	600 mm width, 7 m length, horizontal, 3 kW motor drive, 940 kg	3	1.88	R 110,040.44
2100	CH	005	PID1101	VRM FEED CONVEYOR DISCHARGE CHUTE	Platework=565.2kg; Support Steelwork=706.5kg; Liner Type=VRN 400; Liner=9m2	-	-	R 82,024.65
2100	ML	001	PID1102	VRM	LM31.3 Loesche VRM (1 grinding table, 3 grinding rollers)	see VRM motor	1370.00	R 40,811,403.60
2100	CH	006	PID1102	VRM FEED CHUTE	Platework=282.6kg; Support Steelwork=353.25kg; Liner Type=VRN 400; Liner=4.5m2	-	-	R 41,012.33
2100	FE	002	PID1102	LIMESTONE SCREW FEEDER	Included in Loesche scope	incl.	incl.	incl.
2100	FE	003	PID1102	MILL FEED SCREW FEEDER	Included in Loesche scope	incl.	incl.	incl.
2100	CH	007	PID1102	MILL DISCHARGE CHUTE	Platework=131.88kg; Support Steelwork=164.85kg; Liner Type=VRN 400; Liner=2.1m2	-	-	R 19,139.09
2100	CH	008	PID1102	REJECTS CONVEYOR DISCHARGE CHUTE	Platework=131.88kg; Support Steelwork=164.85kg; Liner Type=VRN 400; Liner=2.1m2	-	-	R 19,139.09
2100	CV	003	PID1102	REJECTS CONVEYOR	600 mm width, 10 m length, horizontal, 3 kW motor drive, 1262 kg	3	2.69	R 157,200.63
2100	WT	002	PID1102	REJECTS WEIGHTOMETER	6 idler, 3 roll, 450 mm belt width	-	-	R 269,890.00
2100	CL	001	PID1102	CHILLER (INCL. HEAT EXCHANGER AND PUMP)	5.5 kW single speed	5.5	4.01	R 2,864,597.00
2100	ZM	001	PID1102	HYDRAULIC UNIT	Included in Loesche scope	incl.	incl.	incl.
2100	ZM	002	PID1102	LUBE OIL UNIT	Included in Loesche scope	incl.	incl.	incl.
2100	DC	001	PID1103	MILL FUEL BAG HOUSE	Included in Loesche scope	-	-	incl.
2100	FL	001	PID1103	SAMPLE FILTER BAG HOUSE	Included in Loesche scope	-	-	incl.

2100	CV	004	PID1103	CONVEYOR	600 mm width, 16 m length, horizontal, 4 kW motor drive, 1660 kg	4	3.71	R 185,044.38
2100	CH	009	PID1103	CONVEYOR DISCHARGE CHUTE	Platework=565.2kg; Support Steelwork=706.5kg; Liner Type=VRN 400; Liner=9m2	-	-	R 82,024.65
2100	WT	003	PID1103	WEIGHTOMETER	6 idler, 3 roll, 600 mm belt width	-	-	R 288,930.00
2100	BE	001	PID1103	BUCKET ELEVATOR	150 bucket elevator	11.00	9.00	R 214,444.44
2100	FA	001	PID1103	FILTER FAN	Included in Loesche scope	-	-	incl.
2100	FE	004	PID1103	BAG HOUSE PRODUCT SCREW FEEDER 1		11.00	8.25	R 1,662,987.60
2100	FE	005	PID1103	BAG HOUSE PRODUCT SCREW FEEDER 2		11.00	8.25	R 1,662,987.60
2100	SX	001	PID1103	STACK (AND DUCT)	Reference Project - Provided by Loesche	-	-	R 2,350,000.00
2100	TK	001	PID1104	REAGENT FEED TANK	62 m³ Cylindrical FB 10 min Residence Time with Epoxy Coating 250 mm Freeboard (3,760 kg Steel)	-	-	R 242,520.00
2100	AG	001	PID1104	REAGENT FEED TANK AGITATOR		15	11.21	R 159,799.00
2100	PP	001	PID1104	REAGENT FEED PUMP	8/6 pump size, 72.7% pump efficiency, 10.9 m TDH, 14.2 m/s impeller tip speed	22	15.71	R 257,983.59
2100			PID1102	MILL MOTOR	1200 kW, 990 rpm, 380 V, 50 Hz (not included in Loesche price)	1200	see VRM	R 1,210,278.00
2100			PID1102	CLASSIFIER MOTOR	110 kW, 990 rpm, 380 V, 50 Hz (not included in Loesche price)	100	see VRM	R 379,053.00
2100			PID1102	FAN MOTOR	500 kW, 990 rpm, 380 V, 50 Hz (not included in Loesche price)	500	see VRM	R 75,531.00
2200	*HG*	*001*	*NO DRAWING*	*HOT GAS GENERATOR SYSTEM*	*6.02 MW Hot Gas Generator*			*R 4,743,000.00*
						1893	**1463**	**R 59,184,685.23**

Appendix F: Equipment Sizing

The volume of the steel for the cylindrical (or "straight") part of a tank ($V_{Straight,Steel}$) is calculated using Equation 54. The steel volume required for the full cone ($V_{Full\ Cone,Steel}$) and small cone ($V_{Small\ Cone,Steel}$) section of the tank is calculated using Equations 55 and 56, respectively. The cone nozzle steel volume ($V_{Nozzle,Steel}$) is calculated using Equation 57.

$$V_{Straight,Steel} = (D + T_{plate})\pi h \quad (54)$$

$$V_{Full\ Cone,Steel} = D \times L_{Face} \times \pi \quad (55)$$

$$V_{Small\ Cone,Steel} = d \times l_{Face} \times \pi \quad (56)$$

$$V_{Nozzle,Steel} = (d_{i,Nozzle} + T_{Plate}) \times 100\pi \quad (57)$$

where:

$D =$ diameter of the cylinder

$T_{Plate} =$ thickness of the plate

$h =$ height of the cylinder

$L_{Face} =$ diagonal length of the full cone section

$l_{Face} =$ diagonal length of the small cone section

$d_{i,Nozzle} =$ inside diameter of the nozzle

The total mass of steelwork required for platework ($m_{Platework,Steel}$) is calculated with Equation 58. The specific gravity of steel (ρ_{Steel}) is 7.85. Finally, the total tank steel mass is calculated by adding the mass of steel required for platework, tank legs, flanges, nozzles, plate cover and extras.

$$m_{Platework,Steel} = (V_{Straight,steel} + V_{Full\ Cone,Steel} - V_{Small\ Cone,Steel} + V_{Nozzle,Steel}) \times \rho_{Steel} \times T_{Plate} \quad (58)$$

Table F-1: Tank Schedule for the Wet Ball Mill Circuit

		Units	Wet Ball Mill Circuit	
Parameters	Tag Number	Text	1100-SU-001	1100-TK-001
	Title	Text	Ball Mill Underflow Sump	Reagent Feed Tank
	Stream out	#	5	8
	Flow Rate	m³/h	597.0	290.1
	Design Flow Rate	m³/h	686.6	333.6
		m³/s	0.2	0.1
	Solids SG	-	2.79	2.79
	Residence Time	s	60	600
	Volume Required	m³	11.4	55.6
	Tank Freeboard	mm	250	250
Cylinder	Vessel Diameter	mm	2272	3759
	Vessel Height	mm	1893	5011
	D/h ratio	-	1.2	0.75
	Vessel Volume	m³	7.7	55.6
Sloped Bottom	Angle	°	60	N/A
	Sloped Height	mm	1837	N/A
	Volume	m³	3.7	N/A
	Total Volume	m³	11.4	N/A
Steel	Tank Steelwork	kg	1493	3621
	Platework Area	m²	18.3	59.3
Liner Type	Type	text	Epoxy Coating	Epoxy Coating
	Thickness	mm	6	6

Table F-2: Chute Schedule for the Wet Ball Mill Circuit

Tag Number		1100-CH-001	1100-CH-002	1100-CH-003	1100-CH-004
Chute Description		Silo Discharge Chute	Belt Feeder Discharge Chute	Ball Mill Feed Conveyor Discharge Chute	Trommel Screen Undersize Chute
Platework Area	m²	6	12	12	48
Platework Thickness	mm	6	6	6	6
Platework Mass	kg	282.6	565.2	565.2	2260.8
Support Steelwork Mass	kg	353.25	706.5	706.5	2826
Type of Liner	test	VRN 400	VRN 400	VRN 400	VRN 400
Liner	m²	4.5	9	9	36
Liner Thickness	mm	12	12	12	12
Liner Mass	kg	423.9	847.8	847.8	3391.2
Total Mass	kg	777.15	1554.3	1554.3	6217.2

Equipment Specification/Model		Platework=282.6kg; Support Steelwork=353.25kg; Liner Type=VRN 400; Liner=4.5m2	Platework=565.2kg; Support Steelwork=706.5kg; Liner Type=VRN 400; Liner=9m2	Platework=565.2kg; Support Steelwork=706.5kg; Liner Type=VRN 400; Liner=9m2	Platework=2260.8kg; Support Steelwork=2826kg; Liner Type=VRN 400; Liner=36m2

Table F-3: Tank Schedule for the Dry VRM Circuit

		Units	VRM Circuit
Parameters	**Tag Number**	Text	2100-TK-001
	Title	Text	Reagent Feed Tank
	Stream out	#	8
	Flow Rate	m^3/h	290.2
	Design Flow Rate	m^3/h	333.7
		m^3/s	0.1
	Solids SG	-	2.79
	Residence Time	s	600
	Volume Required	m^3	55.6
	Tank Freeboard	mm	250
Cylinder	**Vessel Diameter**	mm	3759
	Vessel Height	mm	5011
	D/h ratio	-	0.75
	Vessel Volume	m^3	55.6
Sloped Bottom	**Angle**	°	N/A
	Sloped Height	mm	N/A
	Volume	m^3	N/A
	Total Volume	m^3	N/A
Steel	**Tank Steelwork**	kg	3621
	Platework Area	m^2	59.3
Liner Type	**Type**	text	Epoxy Coating
	Thickness	mm	6

Table F-4: Chute Schedule for the Dry VRM Circuit

Tag Number		2100-CH-001	2100-CH-002	2100-CH-003	2100-CH-004	2100-CH-005
Chute Description		Silo Discharge Chute	Belt Feeder Discharge Chute	Feed Conveyor Discharge Chute	Diverter Chute	VRM Feed Conveyor Discharge Chute
Platework Area	m^2	6	12	12	24.0	12
Platework Thickness	mm	6	6	6	6	6
Platework Mass	kg	282.6	565.2	565.2	1130.4	565.2
Support Steelwork Mass	kg	353.25	706.5	706.5	1413	706.5
Type of Liner	test	VRN 400	VRN 400	VRN 400	VRN 400	VRN 400
Liner	m^2	4.5	9	9	18	9
Liner Thickness	mm	12	12	12	12	12
Liner Mass	kg	423.9	847.8	847.8	1695.6	847.8
Total Mass	kg	777.15	1554.3	1554.3	3108.6	1554.3

Equipment Specification/Model		Platework=282.6kg; Support Steelwork=353.25kg; Liner Type=VRN 400; Liner=4.5m2	Platework=565.2kg; Support Steelwork=706.5kg; Liner Type=VRN 400; Liner=9m2	Platework=565.2kg; Support Steelwork=706.5kg; Liner Type=VRN 400; Liner=9m2	Platework=1130.4kg; Support Steelwork=1413kg; Liner Type=VRN 400; Liner=18m2	Platework=565.2kg; Support Steelwork=706.5kg; Liner Type=VRN 400; Liner=9m2

Tag Number		2100-CH-006	2100-CH-007	2100-CH-008	2100-CH-009
Chute Description		VRM Feed Chute	VRM Rejects Chute	Rejects Conveyor Discharge Chute	Product Conveyor Discharge Chute
Platework Area	**m²**	6	2.8	2.8	12
Platework Thickness	**mm**	6	6	6	6
Platework Mass	**kg**	282.6	131.88	131.88	565.2
Support Steelwork Mass	**kg**	353.25	164.85	164.85	706.5
Type of Liner	**test**	VRN 400	VRN 400	VRN 400	VRN 400
Liner	**m²**	4.5	2.1	2.1	9
Liner Thickness	**mm**	12	12	12	12
Liner Mass	**kg**	423.9	197.82	197.82	847.8
Total Mass	**kg**	777.15	362.67	362.67	1554.3
Equipment Specification/Model		Platework=282.6kg; Support Steelwork=353.25kg; Liner Type=VRN 400; Liner=4.5m2	Platework=131.88kg; Support Steelwork=164.85kg; Liner Type=VRN 400; Liner=2.1m2	Platework=131.88kg; Support Steelwork=164.85kg; Liner Type=VRN 400; Liner=2.1m2	Platework=565.2kg; Support Steelwork=706.5kg; Liner Type=VRN 400; Liner=9m2

Appendix G: CAPEX Calculations

Table G-1: Constituents of the Fixed Capital Investment

Direct Costs		Indirect Costs
• Site Development	• Mechanical/Process Equipment	• Owner's Cost
• Concrete	• Platework	• EPCM Costs
• Roads	• Piping	• Sub-Consultants
• Bulk Earthworks	• Cable ladder, Tray and Conduit	• Construction Indirect Costs
• Architectural	• Structural Steel	• Contingency
• Electrical Equipment	• Wire and Cable	• Forex Variation
• Control and Instrumentation		

Table G-2: Percentages for Estimating Capital-Investment Items based on Mechanical Equipment Cost

Component	Range%
Purchased Equipment	15-40
Purchased Equipment Installation	6-14
Control and Instrumentation (installed)	2-8
Piping (installed)	3-20
Electrical (installed)	2-10
Buildings (including services)	3-18
Yard improvements	2-5
Service facilities (installed)	8-20
Land	1-2
Total Direct Costs	
Engineering and Supervision	4-21
Construction Expense	4-16
Contractor's Fee	2-6
Contingency	5-15
Total Indirect Costs	

Table G-3: Percentages for Estimating Capital-Investment Items based on Mechanical Equipment Cost (Peters and Timmerhaus, 1991)

	Percentage Delivered Equipment Cost for:		
Component	**Solid Processing Plant**	**Slurry Processing Plant**	**Fluid Processing Plant**
Purchased Equipment	**E**	**E**	**E**
Purchased Equipment Installation	40% x E	39% x E	47% x E
Control and Instrumentation (installed)	9% x E	13% x E	18% x E
Piping (installed)	16% x E	31% x E	66% x E
Electrical (installed)	10% x E	10% x E	11% x E
Buildings (including services)	25% x E	29% x E	18% x E
Yard improvements	13% x E	10% x E	10% x E
Service facilities (installed)	40% x E	55% x E	70% x E
Land	6% x E	6% x E	6% x E
Total Direct Costs	**D**	**D**	**D**
Engineering and Supervision	33% x E	33% x E	33% x E
Construction Expense	39% x E	41% x E	41% x E
Total Direct and Indirect	**D + I**	**D + I**	**D + I**
Contractor's Fee (CF)	5% x (D + I)	5% x (D + I)	5% x (D + I)
Contingency (C)	10% x (D + I)	10% x (D + I)	10% x (D + I)
Fixed Capital Investment (FCI)	**D + I + CF + C**	**D + I + CF + C**	**D + I + CF + C**
Working Capital Investment (WCI)	15% x TCI	15% x TCI	15% x TCI
Total Capital Investment (TCI)	**FCI + WCI**	**FCI + WCI**	**FCI + WCI**

Table G-4: Total Capital Investment (TCI) for the Wet Ball Mill Circuit

COMPONENT	AMOUNT	COMMENT	% OF DIRECT COST	% OF INDIRECT COST	% OF PROJECT TOTAL
DIRECT COSTS	**R141,599,658.11**	**D**	**100%**	**-**	**59.0%**
Purchased Equipment	R 48,327,528.37	E	34.1%	-	20.1%
Purchased Equipment Installation	R 18,847,736.06	39% x E	13.3%	-	7.9%
Control and Instrumentation (installed)	R 6,282,578.69	13% x E	4.4%	-	2.6%
Piping (installed)	R14,981,533.79	31% x E	10.6%	-	6.2%
Electrical (installed)	R 4,832,752.84	10% x E	3.4%	-	2.0%
Buildings (including services)	R14,014,983.23	29% x E	9.9%	-	5.8%
Yard improvements	R 4,832,752.84	10% x E	3.4%	-	2.0%
Service facilities (installed)	R 26,580,140.60	55% x E	18.8%	-	11.1%
Land	R 2,899,651.70	6% x E	2.0%	-	1.2%
TOTAL INDIRECT COSTS	**R 35,762,370.99**	**I**	**-**	**100%**	**14.9%**
Engineering and Supervision	R 15,948,084.36	33% x E	-	44.6%	6.6%
Construction Expense	R 19,814,286.63	41% x E	-	55.4%	8.3%
Contractor's Fee (CF)	R 8,868,101.45	5% x (D + I)	-	-	3.7%
Contingency (C)	R 17,736,202.91	10% x (D + I)	-	-	7.4%
Fixed Capital Investment	R203,966,333.46	D + I + CF + C	-	-	85.0%
Working Capital (WC)	**R 35,994,058.85**	**15% x TCI**	**-**	**-**	**15.0%**
TOTAL CAPITAL INVESTMENT (TCI)	**R239,960,392.31**	**FCI + WC**	**-**	**-**	**100.0%**

Table G-5: Total Capital Investment (TCI) for the Dry Loesche VRM Circuit

COMPONENT	AMOUNT	REF	% OF DIRECT COST	% OF INDIRECT COST	% OF PROJECT TOTAL
DIRECT COSTS	**R153,288,334.75**	**D**	**100%**	**-**	**57.8%**
Purchased Equipment	R 59,184,685.23	E	38.6%	-	22.3%
Purchased Equipment Installation	R 3,673,874.09	40% x E	15.4%	-	8.9%
Control and Instrumentation (installed)	R 5,326,621.67	9% x E	3.5%	-	2.0%
Piping (installed)	R 9,469,549.64	16% x E	6.2%	-	3.6%
Electrical (installed)	R 5,918,468.52	10% x E	3.9%	-	2.2%
Buildings (including services)	R 14,796,171.31	25% x E	9.7%	-	5.6%
Yard improvements	R 7,694,009.08	13% x E	5.0%	-	2.9%
Service facilities (installed)	R 23,673,874.09	40% x E	15.4%	-	8.9%
Land	R 3,551,081.11	6% x E	2.3%	-	1.3%
TOTAL INDIRECT COSTS	**R 42,612,973.37**	**I**	**-**	**100%**	**16.1%**
Engineering and Supervision	R 19,530,946.13	33% x E	-	45.8%	7.4%
Construction Expense	R 23,082,027.24	39% x E	-	54.2%	8.7%
Contractor's Fee (CF)	R 9,795,065.41	5% x (D + I)	-	-	3.7%
Contingency (C)	R 19,590,130.81	10% x (D + I)	-	-	7.4%
Fixed Capital Investment	R 225,286,504.33	D + I + CF + C	-	-	85.0%
Working Capital (WC)	**R 39,756,441.94**	**15% x TCI**	**-**	**-**	**15.0%**
TOTAL CAPITAL INVESTMENT (TCI)	**R 265,042,946.27**	**FCI + WC**	**-**	**-**	**100.0%**

Appendix H: OPEX Calculations

Table H-1: Distribution Network Charges (Eskom 2019/2020 Tariff Book)

	Network Capacity Charge R/kVA/month		Network Demand Charge R/kVA/month	
Voltage	**VAT excl.**	**VAT Incl.**	**VAT excl.**	**VAT Incl.**
< 500 V	R 18.96	R21.80	R35.95	R41.34
≥ 500 V & < 66 kV	R17.39	R20.00	R32.98	R37.93
≥ 66 kV & < 132 kV	R6.21	R7.14	R11.50	R13.23

Table H-2: Annual Cost of Limestone

Parameter	Units	Wet Ball Mill Circuit	Dry Loesche VRM Circuit
Cost of Limestone	R/t	R 219	R 219
Throughput	t/h	100	100
Operating Factor	%	89.8	89.8
Annual Throughput	t/a	786,648	786,648
ANNUAL LIMESTONE COST	**R/a**	**R 172,275,900**	**R 172,275,900**

Table H-3: Water Cost for Wet Ball Mill Circuit versus Dry Loesche VRM Circuit

Parameter	Units	Wet Ball Mill Circuit	Dry Loesche VRM Circuit
Cost of water	R/m³	R 20.0	R 20.0
Water consumption	m³/h	251.2	251.2
Operating Factor	%	89.8	89.8
Annual Water Consumption	m³/a	1,975,700	1,975,700
COST PER ANNUM	**R/a**	**R 39,514,900**	**R 39,514,900**

Table H-4: Spare Parts Cost for Wet Ball Mill Circuit

Spares	Tag	Spare Type	Spare Description	Unit Price	Qty PA	Total PA
Belt Feeder	1100-FE-001	Operational	center carry rollers/center impact rollers/return rollers	R 17,038.6	1	R 17,038.6
		Strategic/ Critical	pulley drive/motor 7,5kW/motor 11,2kW	R 10,431.8	1	R 10,431.8
Conveyors	1100-CV-001	Operational	Ø 108/200 idler (BB500) - 10151	R 2,677.50	6	R16,065.0
		Operational	Ø 108/600 return roller (BB500) - 10231	R 6,028.20	3	R 16,745.0
		Strategic/ Critical	Ø 220/750/60 drive drum w/rubber - 21532	R 113,740.20	0	R 4,212.6
Ball Mill	1100-ML-001	Strategic /Critical	Girth gear	R 1,253,070.00	1	R 1,253,070
		Strategic /Critical	Pinion (with bearings & housings)	R 593,609.40	1	R 593,609
		Strategic /Critical	Gearbox box & mounted half couplings	R 714,984.30	1	R 714,984
		Strategic /Critical	Feed sprout with trolley	R 608,404.50	1	R 608,404
		Strategic /Critical	Roller bearing	R 459,000.00	1	R 459,000
		Strategic /Critical	Trommel screen	R 363,650.40	1	R 363,650
		Strategic /Critical	Full set of liners	R 2,721,961.80	1	R 2,721,962

		Strategic /Critical	Motor	R 1,560,600.00	1	R 1,560,600
		Operational	Gearbox lube system spares	R 167,841.00	1	R 167,841
		Operational	Feed sprout seals	R 45,180.90	1	R 45,181
		Operational	Gear spray and trunnion bearing lube system spares	R 71,007.30	1	R 71,007
		Operational	Ball mill wear cost	R 7,172,640.00	1	R 7,235,125
Centrifugal Pumps	1100-PP-001	Operational	Casing Liner	R 104,958.00	1	R 104,958
		Operational	Suction Liner	R 42,993.00	1	R 42,993
		Operational	Gasket Suction	R 1,728.90	1	R 1,728.90
		Operational	Gasket Discharge	R 1,300.50	1	R 1,300.50
		Operational	Impeller - 4 Vane	R 82,773.00	1	R 82,773.00
		Operational	Impeller Gasket	R 91.80	1	R 91.80
		Operational	Sleeve Spacer Gasket	R 244.80	1	R 244.80
		Operational	Wear Ring	R 18,972.00	1	R 18,972.00
		Operational	Packing	R 4,957.20	1	R 4,957.20
		Operational	Shaft Sleeve	R 11,123.10	1	R 11,123.10
		Operational	Expeller Ring Gasket	R 1,361.70	1	R 1,361.70
		Operational	Wear Ring Carrier	R 10,358.10	1	R 10,358.10
		Operational	Wear Ring Screw	R 780.30	1	R 780.30
		Operational	Expeller	R 23,256.00	1	R 23,256.00
		Operational	Expeller Ring	R 29,070.00	1	R 29,070.00
		Operational	Lantern Ring	R 5,064.30	1	R 5,064.30
		Operational	Shaft Sleeve Gasket	R 198.90	1	R 198.90
		Operational	Grease Nipple	R 1,254.60	1	R 1,254.60
		Strategic /Critical	Bearing Assembly	R 88,893.00	1	R 88,893.00
	1100-PP-002	Operational	Casing Liner	R 70,380.00	4	R 281,520.00
		Operational	Suction Liner	R 24,327.00	4	R 97,308.00
		Operational	Gasket Suction	R 1,009.80	4	R 4,039.20
		Operational	Gasket Discharge	R 1,468.80	4	R 5,875.20
		Operational	Release Collar	R 1,239.30	1	R 1,239.30
		Operational	Impeller - 4 Vane	R 45,594.00	4	R 182,376.00
		Operational	Impeller Gasket	R 183.60	12	R 2,203.20
		Operational	Shaft Seal O-Ring	R 183.60	12	R 2,203.20
		Operational	Wear Ring	R 11,872.80	4	R 47,491.20
		Operational	Packing	R 3,197.70	4	R 12,790.80
		Operational	Shaft Sleeve	R 6,594.30	4	R 26,377.20
		Operational	Expeller Ring Gasket	R 1,239.30	4	R 4,957.20
		Operational	Wear Ring Carrier	R 8,981.10	4	R 35,924.40
		Operational	Wear Ring Screw	R 153.00	24	R 3,672.00
		Operational	Expeller	R 16,524.00	4	R 66,096.00
		Operational	Expeller Ring	R 27,387.00	4	R 109,548.00
		Operational	Lantern Ring	R 3,947.40	4	R 15,789.60
		Operational	Shaft Sleeve Gasket	R 198.90	6	R 1,193.40
		Operational	Grease Nipple	R 1,254.60	1	R 1,254.60
		Strategic /Critical	Bearing Assembly	R 65,178.00	1	R 65,178.00

Classifier Cyclone	1100-CY-001	Operational	Overflow Elbow Full	R 2,704.00	1	R 1,352.00
		Operational	Overflow Elbow Sleeve	R 165.00	2	R 247.50
		Operational	Vortex Finder	R 5,817.00	3	R 17,451.00
		Operational	Inlet Head Shell	R 10,762.00	2	R 21,524.00
		Operational	Inlet Head Liner	R 9,801.00	1	R 4,900.50
		Operational	Barrel Shell	R 4,965.00	1	R 4,965.00
		Operational	Barrel Liner	R 4,346.00	1	R 2,173.00
		Operational	Cone Shell 15 Deg	R 6,177.00	1	R 6,177.00
		Operational	Cone Liner 15 Deg	R 5,394.00	2	R 8,091.00
		Operational	Spigot - selected	R 820.00	3	R 2,460.00
		Operational	Spigot housing	R 2,007.00	1	R 2,007.00
TOTAL						R 17,326,692

Table H-5: Spare Parts Cost for Dry Loesche VRM Circuit

SPARES	Tag	Spare Type	Spare Description	Unit Price	Qty PA	Total PA
Belt Feeder	2100-FE-001	Operational	center carry rollers/center impact rollers/return rollers	R 17,038.6	1	R 17,038.6
		Strategic/ Critical	pulley drive/motor 7,5kW/motor 11,2kW	R 10,431.8	1	R 10,431.8
Conveyors	2100-CV-001	Operational	Ø 108/200 idler (BB500) – 10151	R 2,677.50	6	R 16,065.0
		Operational	Ø 108/600 return roller (BB500) - 10231	R 6,028.20	3	R 16,745.0
		Strategic/ Critical	Ø 220/750/60 drive drum w/rubber - 21532	R 113,740.20	0	R 4,212.6
	2100-CV-002	Operational	Ø 108/200 idler (BB500) – 10151	R 2,677.50	6	R 16,065.0
		Operational	Ø 108/600 return roller (BB500) - 10231	R 6,028.20	3	R 16,745.0
		Strategic/ Critical	Ø 220/750/60 drive drum w/rubber - 21532	R 113,740.20	0	R 4,212.6
	2100-CV-003	Operational	Ø 108/200 idler (BB500) – 10151	R 2,677.50	6	R 16,065.0
		Operational	Ø 108/600 return roller (BB500) - 10231	R 6,028.20	3	R 16,745.0
		Strategic/ Critical	Ø 220/750/60 drive drum w/rubber - 21532	R 113,740.20	0	R 4,212.6
	2100-CV-004	Operational	Ø 108/200 idler (BB500) – 10151	R 2,677.50	6	R 16,065.0
		Operational	Ø 108/600 return roller (BB500) - 10231	R 6,028.20	3	R 16,745.0
		Strategic/ Critical	Ø 220/750/60 drive drum w/rubber - 21532	R 113,740.20	0	R 4,212.6
Screw Feeders	2100-FE-002	Operational		R 17,038.6	1	R 17,038.6
		Strategic/ Critical	Motor	R 10,431.8	1	R 10,431.8
	2100-FE-003	Operational		R 17,038.6	1	R 17,038.6
		Strategic/ Critical	Motor	R 10,431.8	1	R 10,431.8
	2100-FE-004	Operational		R 17,038.6	1	R 17,038.6
		Strategic/ Critical	Motor	R 10,431.8	1	R 10,431.8
	2100-FE-005	Operational		R 17,038.6	1	R 17,038.6
		Strategic/ Critical	Motor	R 10,431.8	1	R 10,431.8
VRM	2100-ML-001	Strategic / Critical	Mill motor (1200 kW)	R 1,210,278.00	1	R 1,210,278.00
		Strategic / Critical	Fan motor (100 kW)	R 379,053.00	1	R 379,053.00
		Strategic / Critical	Classifier motor (500 kW)	R 75,531.00	1	R 75,531.00

		Strategic / Critical	VRM additional spares	R 1,952,638.00	1	R 1,952,638.00
		Strategic / Critical	Full set of liners (including grinding table and grinding roll)	R 3,975,031.80	1	R 3,975,031.80
		Strategic / Critical	Gear spares	R 1,560,600.00	1	R 1,560,600.00
		Operational	Lube system spares	R 167,841.00	1	R 167,841.00
		Operational	Water nozzle spares	R 45,180.90	1	R 45,180.90
Centrifugal Pumps	2100-PP-001	Operational	Casing Liner	R 70,380.00	4	R 281,520.00
		Operational	Suction Liner	R 24,327.00	4	R 97,308.00
		Operational	Gasket Suction	R 1,009.80	4	R 4,039.20
		Operational	Gasket Discharge	R 1,468.80	4	R 5,875.20
		Operational	Release Collar	R 1,239.30	1	R 1,239.30
		Operational	Impeller - 4 Vane	R 45,594.00	4	R 182,376.00
		Operational	Impeller Gasket	R 183.60	12	R 2,203.20
		Operational	Shaft Seal O-Ring	R 183.60	12	R 2,203.20
		Operational	Wear Ring	R 11,872.80	4	R 47,491.20
		Operational	Packing	R 3,197.70	4	R 12,790.80
		Operational	Shaft Sleeve	R 6,594.30	4	R 26,377.20
		Operational	Expeller Ring Gasket	R 1,239.30	4	R 4,957.20
		Operational	Wear Ring Carrier	R 8,981.10	4	R 35,924.40
		Operational	Wear Ring Screw	R 153.00	24	R 3,672.00
		Operational	Expeller	R 16,524.00	4	R 66,096.00
		Operational	Expeller Ring	R 27,387.00	4	R 109,548.00
		Operational	Lantern Ring	R 3,947.40	4	R 15,789.60
		Operational	Shaft Sleeve Gasket	R 198.90	6	R 1,193.40
		Operational	Grease Nipple	R 1,254.60	1	R 1,254.60
		Strategic / Critical	Bearing Assembly	R 65,178.00	1	R 65,178.00
Bucket Elevator	2100-BE-001	Operational	145 Buckets - Mille 140	R 145.00	7	R 966.67
		Operational	Conveyor belting with Matching holes for buckets - 200mm wide	R 165.00	7	R 1,100.00
		Operational	Bucket bolts and nuts with domed washer - M8	R 6.50	17	R 108.33
		Strategic / Critical	SEW R77 gearbox with 4kW motor - SEW R77 - 22:1	R 22,500.00	0	R 3,000.00
		Strategic / Critical	SEW R67 gearbox with 3kW motor - SEW R67 - 22:1	R 19,990.00	0	R 2,665.33
		Strategic / Critical	Bearings 4 hole flange bearing - Dia 40	R 450.00	0	R 120.00
		Strategic / Critical	Bearing plumber block - Dia 50	R 650.00	0	R 173.33
		Strategic / Critical	Shaft coupling - HRC 170	R 2,400.00	0	R 800.00
						R 10,627,566.50

Appendix I: Profitability Evaluation

Table I-1: Net Present Value (NPV) Calculation for the Wet Ball Mill Circuit

Year	Gross Profit	Depreciation Charge	Taxable Income	Taxes Paid	Cash Flow	Cumul CF	Discount factor	PV of CF	Cumul. CF
0	0.00	0.00	0.00	0.00	-239,961,000.00	-239,961,000.00	1.00	-239,961,000.00	-R239,961,000.00
0.5	106,484,988.68	56,639,863.24	49,845,125.44	17,445,793.90	89,039,194.78	-150,921,805.22	0.94	84,134,130.83	-R155,826,869.17
1.5	106,484,988.68	28,319,931.62	78,165,057.06	27,357,769.97	79,127,218.71	-71,794,586.51	0.84	66,757,315.89	-R 89,069,553.28
2.5	106,484,988.68	28,319,931.62	78,165,057.06	27,357,769.97	79,127,218.71	7,332,632.20	0.75	59,604,746.33	-R 29,464,806.95
3.5	106,484,988.68	28,319,931.62	78,165,057.06	27,357,769.97	79,127,218.71	86,459,850.91	0.67	53,218,523.51	R 23,753,716.57
4.5	106,484,988.68	0.00	106,484,988.68	37,269,746.04	69,215,242.64	155,675,093.55	0.60	41,564,316.55	R 65,318,033.11
5.5	106,484,988.68	0.00	106,484,988.68	37,269,746.04	69,215,242.64	224,890,336.19	0.54	37,110,996.92	R102,429,030.03
6.5	106,484,988.68	0.00	106,484,988.68	37,269,746.04	69,215,242.64	294,105,578.83	0.48	33,134,818.68	R135,563,848.71
7.5	106,484,988.68	0.00	106,484,988.68	37,269,746.04	69,215,242.64	363,320,821.47	0.43	29,584,659.53	R165,148,508.24
8.5	106,484,988.68	0.00	106,484,988.68	37,269,746.04	69,215,242.64	432,536,064.12	0.38	26,414,874.58	R191,563,382.82
9.5	106,484,988.68	0.00	106,484,988.68	37,269,746.04	69,215,242.64	501,751,306.76	0.34	23,584,709.45	R215,148,092.27
10.5	106,484,989.68	0.00	106,484,989.68	37,269,746.39	69,215,243.29	570,966,550.05	0.30	21,057,776.49	R236,205,868.77
11.5	106,484,989.68	0.00	106,484,989.68	37,269,746.39	69,215,243.29	640,181,793.34	0.27	18,801,586.15	R255,007,454.92
12.5	106,484,989.68	0.00	106,484,989.68	37,269,746.39	69,215,243.29	709,397,036.63	0.24	16,787,130.49	R271,794,585.41
13.5	106,484,989.68	0.00	106,484,989.68	37,269,746.39	69,215,243.29	778,612,279.93	0.22	14,988,509.37	R286,783,094.78
14.5	106,484,989.68	0.00	106,484,989.68	37,269,746.39	69,215,243.29	847,827,523.22	0.19	13,382,597.65	R300,165,692.43
15.5	106,484,989.68	0.00	106,484,989.68	37,269,746.39	69,215,243.29	917,042,766.51	0.17	11,948,747.90	R312,114,440.34
16.5	106,484,989.68	0.00	106,484,989.68	37,269,746.39	69,215,243.29	986,258,009.80	0.15	10,668,524.91	R322,782,965.25
17.5	106,484,989.68	0.00	106,484,989.68	37,269,746.39	69,215,243.29	1,055,473,253.09	0.14	9,525,468.67	R332,308,433.92
18.5	106,484,989.68	0.00	106,484,989.68	37,269,746.39	69,215,243.29	1,124,688,496.39	0.12	8,504,882.74	R340,813,316.67
19.5	106,484,989.68	0.00	106,484,989.68	37,269,746.39	69,215,243.29	1,193,903,739.68	0.11	7,593,645.31	R348,406,961.97
					Interest Rate		12%		
					Total NPV			**R 348,406,961.97**	

Table I-2: Net Present Value (NPV) Calculation of the Dry VRM Circuit

Year	Gross Profit	Depreciation Charge	Taxable Income	Taxes Paid	Cash Flow		Discount factor	PV of CF	Cumul. CF
0	R -	0	R -	R -	-R265,043,000.00	-R 265,043,000	1.00	-R265,043,000.00	-R265,043,000.00
0.5	R122,413,512.78	R61,315,333.90	R 61,098,178.88	R21,384,362.61	R101,029,150.17	-R 164,013,850	0.94	R 95,463,573.76	-R169,579,426.24
1.5	R122,413,512.78	R30,657,666.95	R 91,755,845.83	R32,114,546.04	R 90,298,966.74	-R 73,714,883	0.84	R 76,182,592.36	-R 93,396,833.89
2.5	R122,413,512.78	R30,657,666.95	R 91,755,845.83	R32,114,546.04	R 90,298,966.74	R 16,584,084	0.75	R 68,020,171.75	-R 25,376,662.14
3.5	R122,413,512.78	R30,657,666.95	R 91,755,845.83	R32,114,546.04	R 90,298,966.74	R 106,883,050	0.67	R 60,732,296.20	R 35,355,634.06
4.5	R122,413,512.78	R -	R122,413,512.78	R42,844,729.47	R 79,568,783.30	R 186,451,834	0.60	R 47,781,701.98	R 83,137,336.05
5.5	R122,413,512.78	R -	R122,413,512.78	R42,844,729.47	R 79,568,783.30	R 266,020,617	0.54	R 42,662,233.91	R125,799,569.96
6.5	R122,413,512.78	R -	R122,413,512.78	R42,844,729.47	R 79,568,783.30	R 345,589,400	0.48	R 38,091,280.28	R163,890,850.24
7.5	R122,413,512.78	R -	R122,413,512.78	R42,844,729.47	R 79,568,783.30	R 425,158,184	0.43	R 34,010,071.68	R197,900,921.92
8.5	R122,413,512.78	R -	R122,413,512.78	R42,844,729.47	R 79,568,783.30	R 504,726,967	0.38	R 30,366,135.43	R228,267,057.35
9.5	R122,413,512.78	R -	R122,413,512.78	R42,844,729.47	R 79,568,783.30	R 584,295,750	0.34	R 27,112,620.92	R255,379,678.26
10.5	R122,413,512.78	R -	R122,413,512.78	R42,844,729.47	R 79,568,783.30	R 663,864,534	0.30	R 24,207,697.25	R279,587,375.51
11.5	R122,413,512.78	R -	R122,413,512.78	R42,844,729.47	R 79,568,783.30	R 743,433,317	0.27	R 21,614,015.40	R301,201,390.91
12.5	R122,413,512.78	R -	R122,413,512.78	R42,844,729.47	R 79,568,783.30	R 823,002,100	0.24	R 19,298,228.04	R320,499,618.94
13.5	R122,413,512.78	R -	R122,413,512.78	R42,844,729.47	R 79,568,783.30	R 902,570,883	0.22	R 17,230,560.75	R337,730,179.69
14.5	R122,413,512.78	R -	R122,413,512.78	R42,844,729.47	R 79,568,783.30	R 982,139,667	0.19	R 15,384,429.24	R353,114,608.93
15.5	R122,413,512.78	R -	R122,413,512.78	R42,844,729.47	R 79,568,783.30	R1,061,708,450	0.17	R 13,736,097.53	R366,850,706.46
16.5	R122,413,512.78	R -	R122,413,512.78	R42,844,729.47	R 79,568,783.30	R1,141,277,233	0.15	R 12,264,372.80	R379,115,079.26
17.5	R122,413,512.78	R -	R122,413,512.78	R42,844,729.47	R 79,568,783.30	R1,220,846,017	0.14	R 10,950,332.85	R390,065,412.11
18.5	R122,413,512.78	R -	R122,413,512.78	R42,844,729.47	R 79,568,783.30	R1,300,414,800	0.12	R 9,777,082.91	R399,842,495.02
19.5	R122,413,512.78	R -	R122,413,512.78	R42,844,729.47	R 79,568,783.30	R1,379,983,583	0.11	R 8,729,538.31	R408,572,033.33
					Interest Rate		12%		
					Total NPV			**R408,572,033.33**	

Appendix J: Testwork Photographs

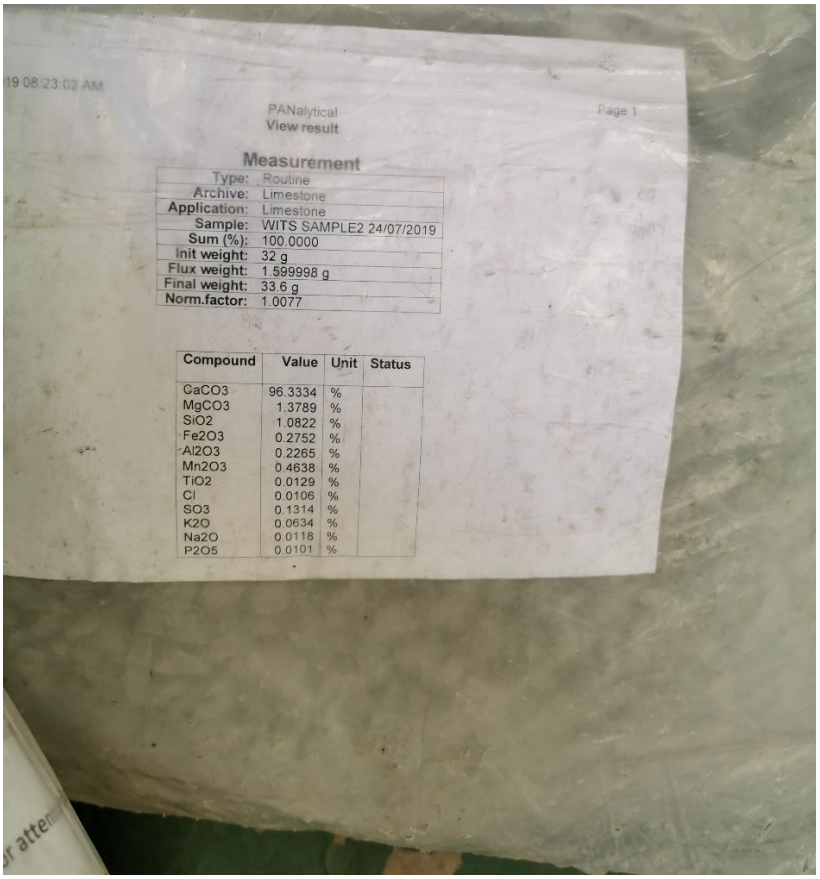

19 08:23:02 AM

PANalytical
View result

Page 1

Measurement

Type:	Routine
Archive:	Limestone
Application:	Limestone
Sample:	WITS SAMPLE2 24/07/2019
Sum (%):	100.0000
Init weight:	32 g
Flux weight:	1.599998 g
Final weight:	33.6 g
Norm.factor:	1.0077

Compound	Value	Unit	Status
CaCO3	96.3334	%	
MgCO3	1.3789	%	
SiO2	1.0822	%	
Fe2O3	0.2752	%	
Al2O3	0.2265	%	
Mn2O3	0.4638	%	
TiO2	0.0129	%	
Cl	0.0106	%	
SO3	0.1314	%	
K2O	0.0634	%	
Na2O	0.0118	%	
P2O5	0.0101	%	

Figure J-1: Chemical Composition of Limestone Sample delivered from Danielskuil Idwala Lime

Figure J-2: Limestone Sample -19+8 mm from Danielskuil Idwala Lime

Figure J-3: Rotary Splitter used to divide Sample in Equal Fractions (Mintek)

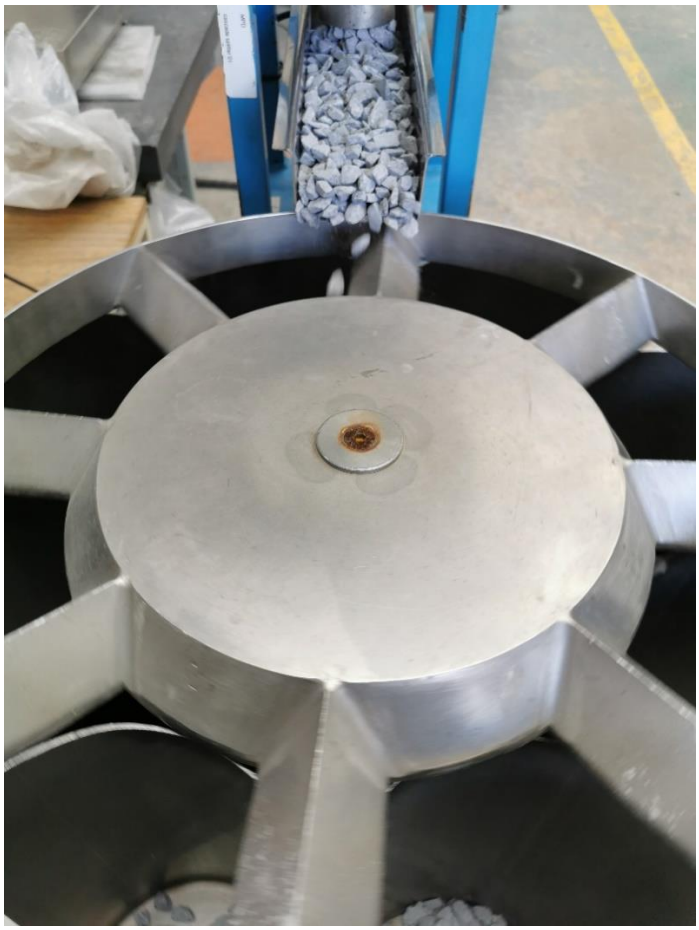

Figure J-4: Rotary Splitter separating Limestone in Equal Fractions (Mintek)

Figure J-5: Sieves used for Particle Size Distribution (PSD) Analysis (Mintek)

Figure J-6: Laboratory Scale Used for Weighing Limestone during PSD Analysis (Mintek)

Figure J-7: 6 Pot Swing Mill to Pulverize the Limestone (Mintek)

Figure J-8: Grinding Vessels for the 6 Pot Swing Mill (Mintek)

Figure J-9: Pulverized Limestone from the 6 Pot Swing Mill

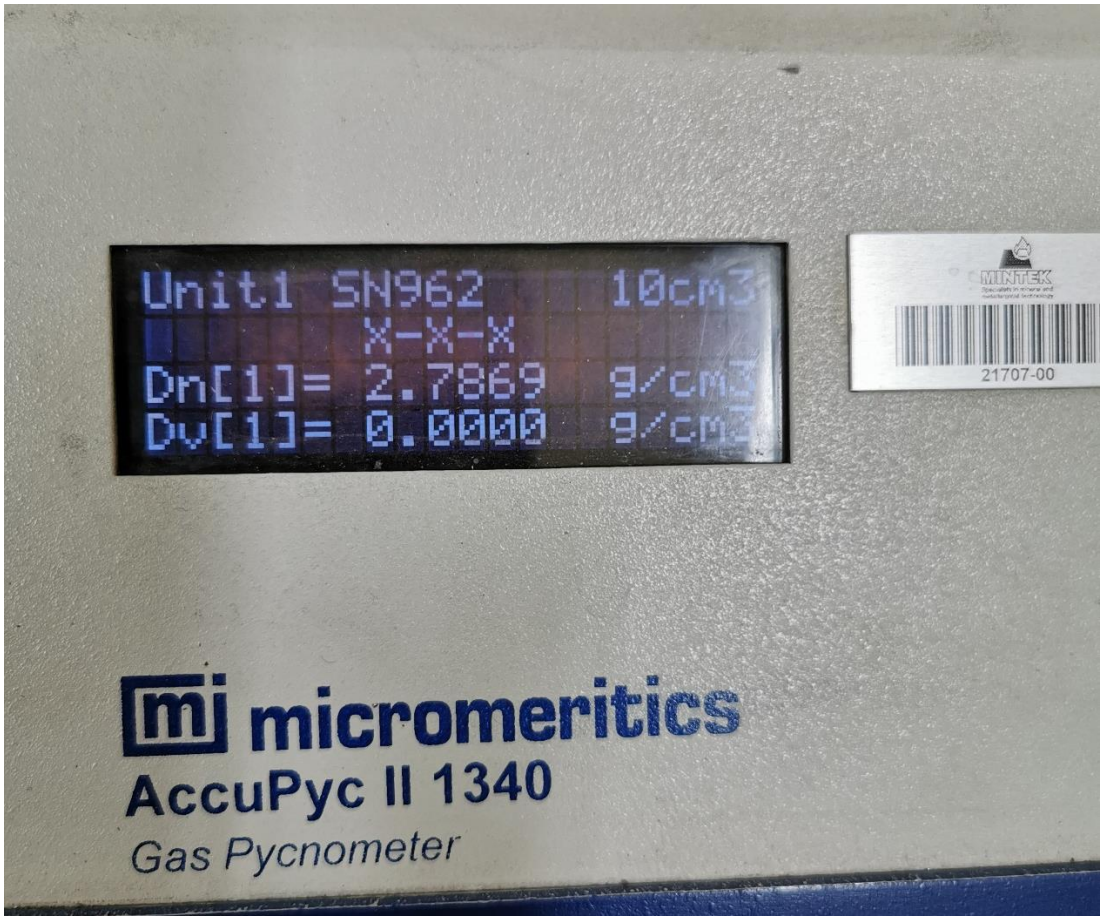

Figure J-10: Gas Pycnometer used for Solids Specific Gravity Analysis

Figure J-11: Laboratory Scale Ball Mill Set-Up Position (Mintek)

Figure J-12: Ball Mill Filled with (i) Grinding Media, (ii) Grinding Media and Limestone, and (iii) Grinding Media, Limestone and Water (Mintek)

Figure J-13: Ball Mill in Grinding Position (Mintek)

Figure J-14: Ball Mill Software to track Specific Energy, Mill Speed, and Mill Power

Figure J-15: Roligan with 53 µm Aperture Sieve (Mintek)

Appendix K: Sizing Charts and Tables

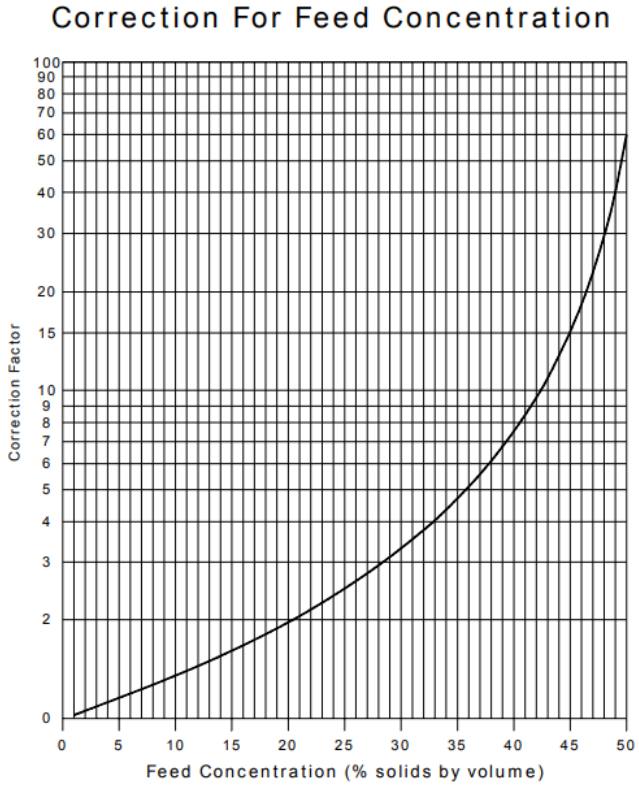

Figure K-1: Correction for Feed Solids Concentration – Cyclone Sizing (Arterburn, 2001)

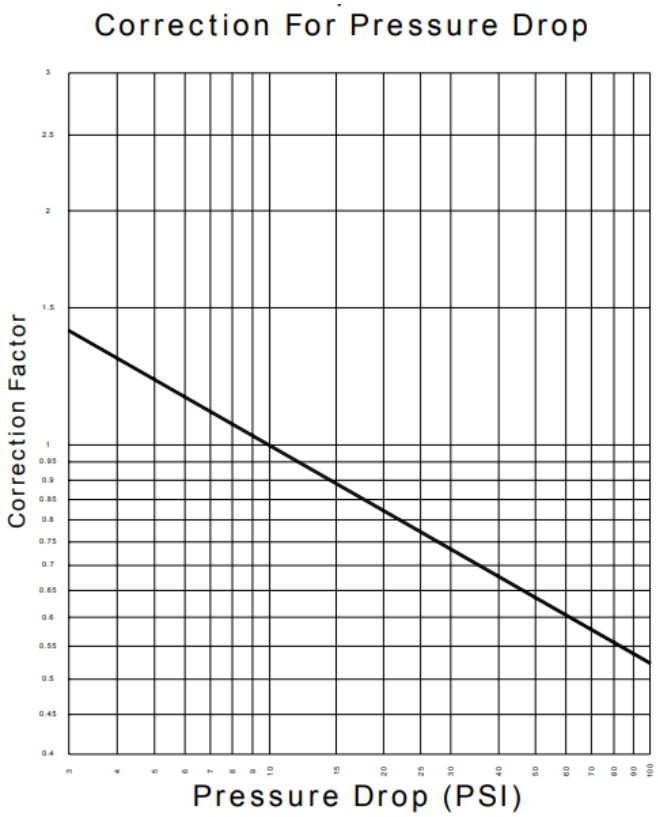

Figure K-2: Correction Factor for Pressure Drop – Cyclone Sizing (Arterburn, 2001)

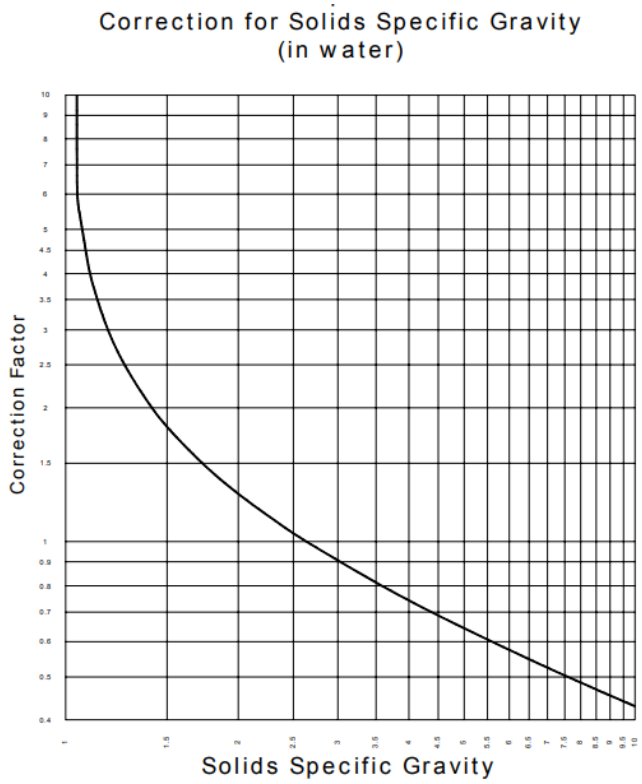

Figure K-3: Correction for Solids Specific Gravity – Cyclone Sizing (Arterburn, 2001)

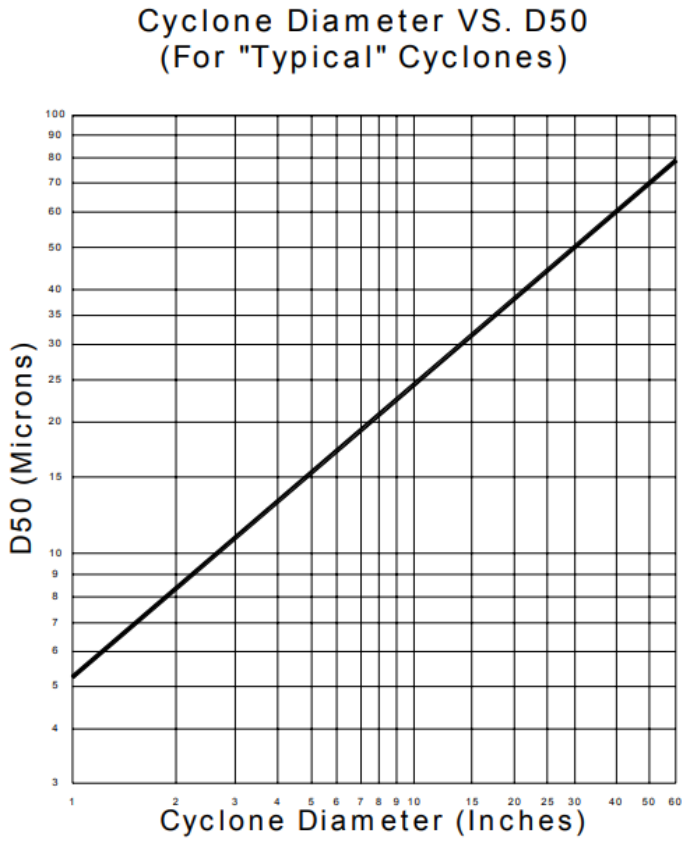

Figure K-4: Cyclone Diameter versus D_{50} for Typical Cyclones (Arterburn, 2001)

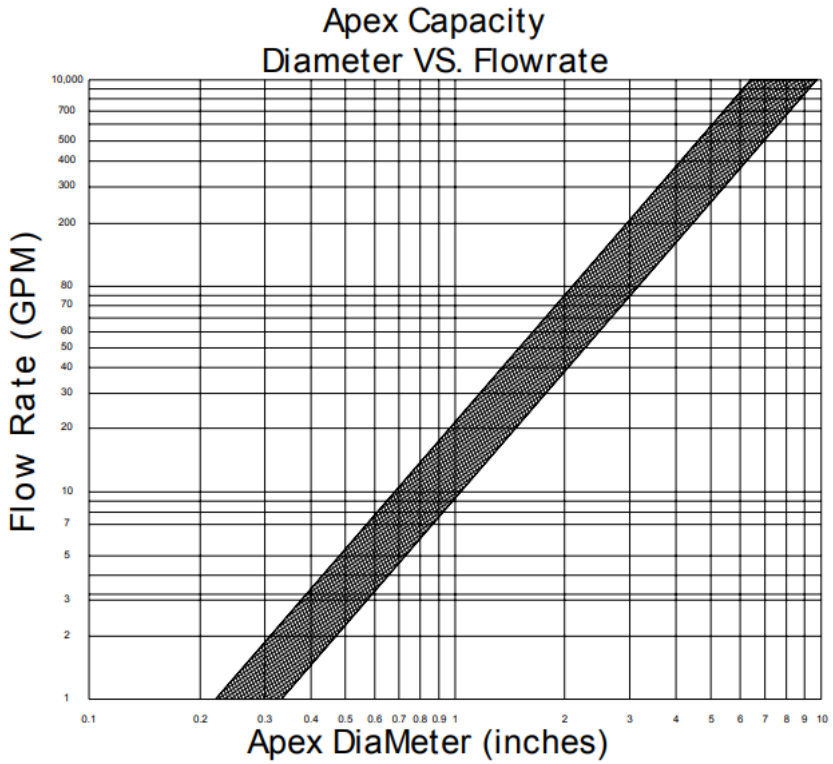

Figure K-5: Apex Capacity Diameter versus Flowrate (Arterburn, 2001)

Table K-1: Relationship of D_{50} to Overflow Size Distribution

Required Overflow Size Distribution of Specified Micron Size (%)	Multiplier
98.8	0.54
95	0.73
90	0.91
80	1.25
70	1.67
60	2.08
50	2.78

Table K-2: Durand Settling Velocity Parameter

F_L from Durand						
	Concentration Volume, Cv (%)					
d 50 Particle Size (µm)		5	10	20	30	40
	10	0.474026	0.474026	0.474026	0.474026	0.474026
	20	0.584416	0.592532	0.599026	0.61526	0.599026
	40	0.704545	0.722403	0.738636	0.75974	0.738636
	60	0.772727	0.793831	0.818182	0.842532	0.818182
	80	0.824675	0.849026	0.875	0.900974	0.875
	100	0.862013	0.886364	0.917208	0.949675	0.917208
	200	0.975649	1.00974	1.047078	1.092532	1.047078
	400	1.094156	1.137987	1.186688	1.23539	1.186688
	600	1.159091	1.209416	1.266234	1.300325	1.266234
	800	1.211039	1.261364	1.308442	1.340909	1.308442
	1000	1.248377	1.295455	1.332792	1.36039	1.332792
	2000	1.336039	1.363636	1.381494	1.404221	1.381494
	3000	1.362013	1.381494	1.391234	1.404221	1.391234

Table K-3: k-Values for Fittings and Valves

Fitting	Types	k
45° Elbow	Standard (R/D = 1)	0.35
	Long Radius (R/D = 1.5)	0.2
90° Elbow Curved	Standard (R/D = 1)	0.75
	Long Radius (R/D = 1.5)	0.45
90° Elbow Square or Mitred		1.3
180° Bend	Close Return	1.5
Tee, Run Through	Branch Blanked	0.4
Tee, as Elbow	Entering in run	1
Tee, as Elbow	Entering in branch	1
Tee, Branching Flow		1
Coupling		0.04
Union		0.04
Gate valve	Fully Open	0.17
	3/4 Open	0.9
	1/2 Open	4.5
	1/4 Open	24
Diaphragm valve	Fully Open	2.3
	3/4 Open	2.6
	1/2 Open	4.3
	1/4 Open	21
Globe valve, Bevel Seat	Fully Open	6
	1/2 Open	9.5

Globe Valve, Composition seat	Fully Open	6
	1/2 Open	8.5
Plug disk	Fully Open	9
	3/4 Open	13
	1/2 Open	36
	1/4 Open	112
Angle valve	Fully Open	2
Y valve or blowoff valve	Fully Open	3
Plug cock	$\theta = 5°$	0.05
	$\theta = 10°$	0.29
	$\theta = 20°$	1.56
	$\theta = 40°$	17.3
	$\theta = 60°$	206
Butterfly valve	$\theta = 5°$	0.24
	$\theta = 10°$	0.52
	$\theta = 20°$	1.54
	$\theta = 40°$	10.8
	$\theta = 60°$	118
Check valve	Swing	2
	Disk	10
	Ball	70
Foot valve		15
Water meter	Disk	7
	Piston	15
	Rotary (star-shaped disk)	10
	Turbine-wheel	6

Table K-4: Standard Motor Sizes

STANDARD MOTOR SIZES, kW					
0.18	0.37	0.55	0.75	1.1	1.5
2.2	3	4	5.5	7.5	11
15	18.5	22	30	37	45
55	75	90	110	132	150
185	220	250	300	355	400
450	500	560	630	710	750
800	900	1000			

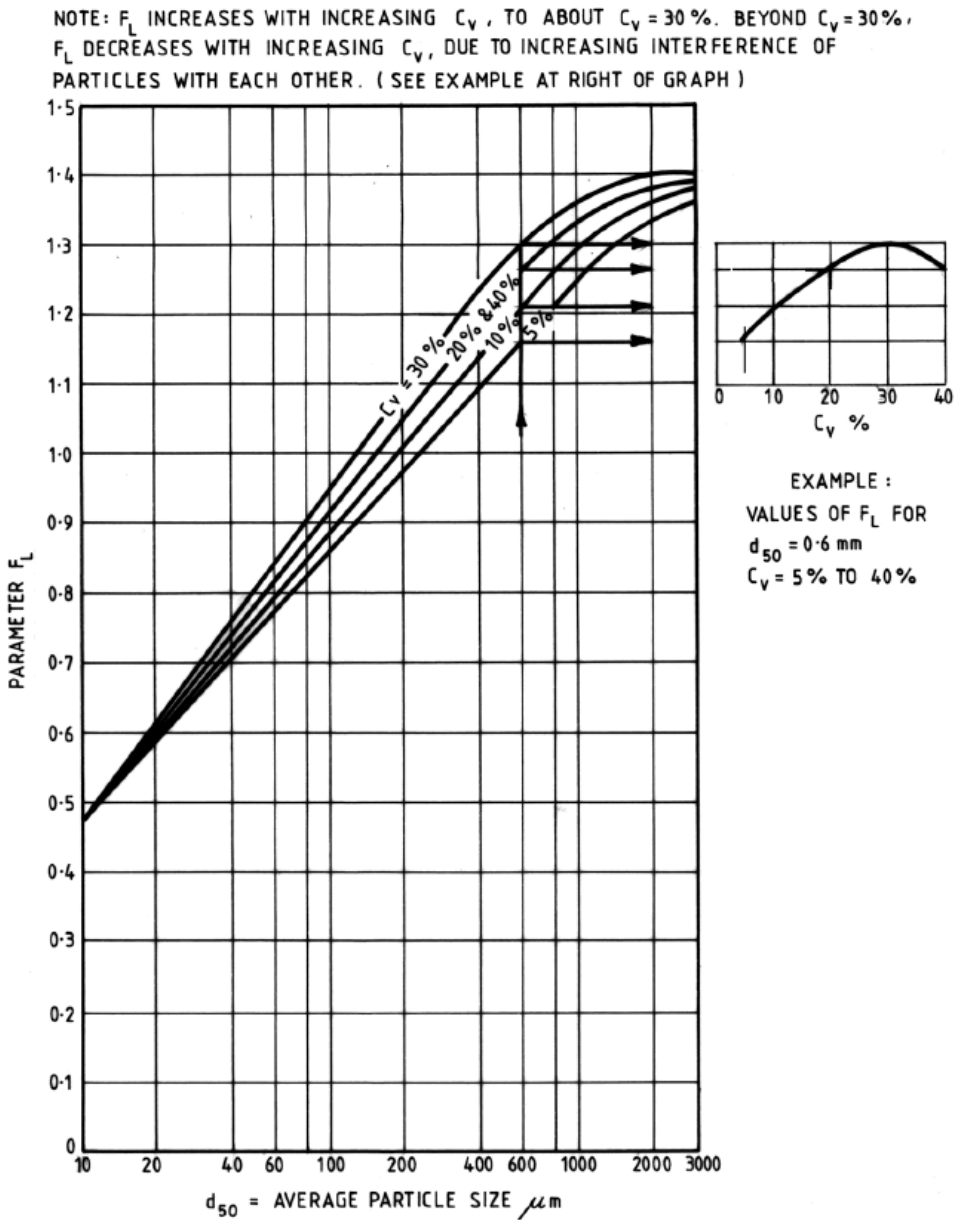

Figure K-6: Modified Durand's Limiting Settling Velocity Parameter (Warman Slurry Pumping Handbook, 2000)

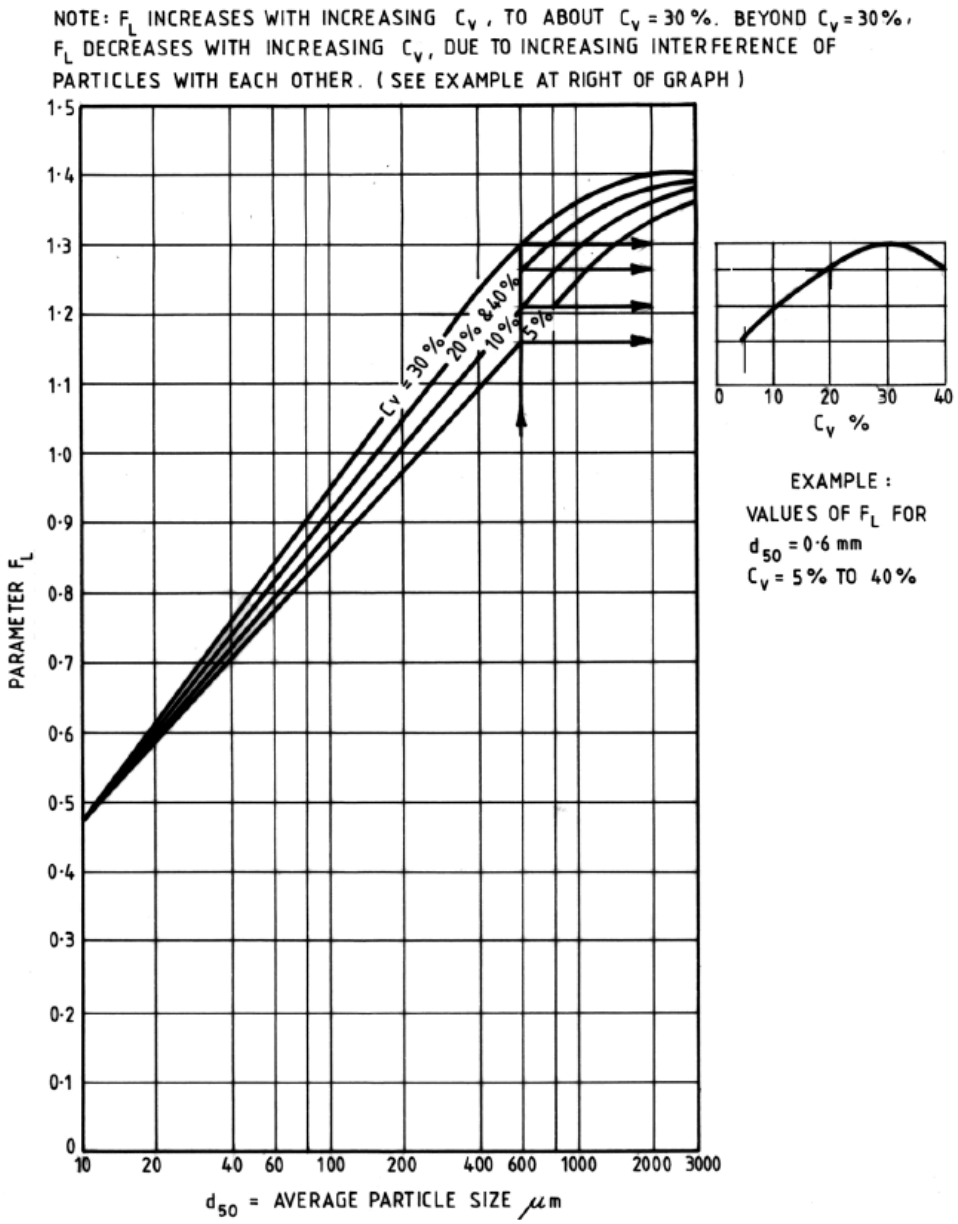

Figure K-7: Modified Durand's Limiting Settling Velocity Parameter (Warman Slurry Pumping Handbook, 2000)

Appendix L: Pump Sizing

Table L-1: Steps for Sizing a Centrifugal Pump

Step 1: Determination of Durand Settling Velocity - Schiller Correction				
#	Parameter	Equation	Units	Equation #
1	Schiller Correction Factor	$f_L = 1.3 \times \left(\frac{C_v}{100}\right)^{0.125} \times \left[1 - e^{(-6.9 \times s50)}\right]$	-	59
2	Durand Settling Velocity (corrected)	$V_{D(Schiller)} = f_L \times \sqrt{\frac{2gd_i}{1000} \times \frac{\rho_S - \rho_l}{\rho_l}}$	m/s	60
Step 2: Turton Levenspiel Iteration				
#	Parameter	Equation	Units	Equation #
1	Preliminary Drag Co-Efficient	Select C_D	-	
2	Particle Terminal Velocity	$V_{T1} = \sqrt{\frac{4gd_{50}}{1000} \times \frac{\rho_S - \rho_l}{3C_{D1}\rho_l}}$	m/s	61
3	Particle Reynolds Number	$Re_{p1} = \frac{\rho_l d_{50}}{1000} \times \frac{V_{T1}}{\mu}$	-	62
4	Particle Drag Co-Efficient	$C_{D2} = \left[\frac{24}{Re_{P1}} \times (1 + 0.173 Re_{P1}^{0.657})\right] + \left[\frac{0.413}{1+16300 Re_{P1}^{-1.09}}\right]$	-	63
5	Complete 3 iterations			
Step 3: Determination of Darcy Friction Factor				
#	Parameter	Equation	Units	Equation #
1	Reynolds Number	$Re = V \times \frac{d_i}{1000} \times \frac{\rho}{\mu}$	-	64
2	Relative Roughness	$\frac{e}{D} = \frac{e}{d_i}$	-	65
3	Preliminary Friction Factor - Swamee-Jain	$f_j = \frac{1}{\left[1.14 - \left(2\log\left(\frac{e}{D} + \left(\frac{21.25}{Re^{0.9}}\right)\right)\right)\right]^2}$	-	66
4	Darcy Friction Factor - Colebrook White (iterative)	$f_D = \frac{1}{\left[-2\log\left(\frac{\frac{e}{D}}{3.7} + \frac{2.51}{Re \times 0.013569^{0.5}}\right)\right]^2}$	-	67
5	Darcy Friction Factor - Fully Turbulent Region	$f_T = \frac{1}{\left[-2\log\left(\frac{\frac{e}{D}}{3.7} + \frac{2.51}{10^8 \times f_D^{0.5}}\right)\right]^2}$	-	68
Step 4: Determination of Minor Head Loss				
#	Parameter	Equation	Units	Equation #
1	Discharge Line Equivalent Length	$\sum(n_{fittings\ and\ valves} \times k)$	m	69
2	Suction Line Equivalent Length	$\sum(n_{fittings\ and\ valves} \times k)$	m	70
3	Head Loss due to Length of Pipe	$h_{f1} = \frac{f_D L V^2}{2g\left(\frac{d_i}{1000}\right)}$	m	71
4	K Factor for Fittings & Valves	$\sum K = \sum L/D \times f_T$	-	72
5	Head Loss due to Fittings	$h_{f2} = \frac{\sum K V^2}{2g}$	m	73
6	Combined Head Loss due to Friction	$h_f = h_{f1} + h_{f2}$	m	74
Step 5: Determination of Total Dynamic Head - Clear Water				
#	Parameter	Equation	Units	Equation #
1	Potential Head	$h_Z = Z_2 - Z_1$	m	75
2	Pressure Head	$h_p = 1000 \times \frac{P}{\rho g}$	m	76

3	Velocity Head	$h_v = \frac{V^2}{2g}$	m	77
4	Total Dynamic Head	$h_{td} = h_z + h_p + h_v + h_f$	m	78
Step 6: Head Correction				
#	**Parameter**	**Equation**	**Units**	**Equation #**
1	Froude Number	$F_r = V^2 / \left[\frac{gd_i}{1000} \times \frac{\rho_S - \rho_l}{\rho_l}\right]$	-	79
2	Excess Pressure Correlation	$\phi = 1 + \frac{82C_v}{100}\left(\sqrt{C_{D4}} \times Fr\right)^{-1.5}$	-	80
3	Slurry System Head	$H_{Sys} = h_z + h_p + h_v + (h_f \phi)$	m	81
Step 7: NPSH				
#	**Parameter**	**Equation**	**Units**	**Equation #**
1	Atmospheric Head	$h_a = \frac{P_{atm}1000}{\rho g}$	m	82
2	Vapour Pressure Head	$h_{vp} = \frac{P_{vp}1000}{\rho g}$	m	83
3	Static Head	$h_s = Z_1 - Z_p$	m	84
4	Minor Friction Losses	$h_{fs} = (f_D L_s + f_T \sum L/D) \frac{V_s^2}{2gd_{is}}$	m	85
5	Net Positive Suction Head (Available)	$NPSH_a = h_a + h_s - (h_{vp} + h_{fs} + h_i)$	m	86
Step 8: Pumping Power Requirements				
#	**Parameter**	**Equation**	**Units**	**Equation #**
1	Head Ratio Correction	$Hr = 1 - \left[\left(\frac{0.0462}{D_p^{0.8}}\right) \times \left((SG_S - 1) \times \left(1 + \frac{4}{SG_s}\right)\right) C_v \ln\left(\frac{d_{50}}{0.0227}\right)\right]$	-	87
2	Absorbed Power - Durand	$P_0 = \frac{\frac{Q}{3600}\rho_m g H_{Sys}}{Hr \times \eta_p \eta_b \eta_C \eta_m \eta_{vsd} \times 1000}$	kW	88
3	Motor Service Factor	$SF = \frac{P_i}{P0}$	-	89

References:
Warman Slurry Pump Manual
Abulnaga, 2002
King, 2002
Paterson & Cooke, 2006
Wilson & Addie, 2006

Table L-2: Pump Calculations for Mill Discharge Sump Pump and Reagent Tank Discharge Pump

Pump Number / **Pump Name**		**1100-PP-001 MILL DISCHARGE PUMP**	**1100-PP-002 / 2100-PP-001 REAGENT FEED PUMP**
	UNITS		
SOLIDS RATE	t/h	100	100
SOLIDS CONC	wt%	55	30
SLURRY RATE	t/h	181.8	333.3
SOLIDS SG	-	2.8	2.8
SLURRY FLOW	m³/h	117.7	269.2
DENSITY OF SLURRY	t/m³	1.5	1.2
SOLIDS CONC	v/v%	30.5	13.3
PARTICLE SIZE (d80)	mm	0.13	0.04
AVE PARTICLE SIZE (d50)	mm	0.08	0.03
VISCOSITY		0.00085	0.00085

PIPE MOC	TEXT	CSRL	CSRL
NOMINATED PIPE SIZE	NB	100.0	200.0
OUTSIDE DIAMETER	mm	114.3	219.1
WALL THICKNESS	mm	6.0	8.2
RUBBER LINED	mm	6.0	6.0
INSIDE DIAMETER	mm	90.3	190.7
PIPE LENGTH	mm	10.0	10.0

D_50_1	µm	60.0	20.0
D_50_2	µm	80.0	40.0
CV_1	v/v%	30.0	10.0
CV_2	v/v%	40.0	20.0
FL_11	-	0.8425	0.5925
FL_12	-	0.8182	0.5990
FL_21	-	0.9010	0.7224
FL_22	-	0.8750	0.7386

AVERAGE VELOCITY	m/s	5.1	2.6
PARAMETER FL	-	0.826	0.641
DURAND SETTLING VELOCITY	m/s	1.5	1.7
CHECK	text	CHECK	CHECK
INITIAL DRAG COEFF		11.6	11.6

ITERATION 1

PARTICLE TERMINAL VELOCITY	m/s	0.012	0.008
REYNOLDS NUMBER	-	1.1	0.3
DRAG CO-EFFICIENT	-	25.977	94.010

ITERATION 2

PARTICLE TERMINAL VELOCITY	m/s	0.008	0.003
REYNOLDS NUMBER	-	0.7	0.1
DRAG CO-EFFICIENT	-	37.442	258.252

ITERATION 3

PARTICLE TERMINAL VELOCITY	m/s	0.007	0.002
REYNOLDS NUMBER	-	0.6	0.1
DRAG CO-EFFICIENT	-	44.324	423.698

ITERATION 4

PARTICLE TERMINAL VELOCITY	m/s	0.006	0.001
REYNOLDS NUMBER	-	0.6	0.0
DRAG CO-EFFICIENT	-	47.936	540.586

CRITICAL DEPOSITION VELOCITY

PARTICLE DIMENSIONAL RATIO	-	0.00002	0.00000
VELOCITY FACTOR	-	0.57	0.04
DEPOSITION VELOCITY-WILSON	m/s	1.02	0.10

DARCY FRICTION FACTOR

REYNOLDS NUMBER	-	542589	587282
RELATIVE ROUGHNESS (e/D)	-	0.000033	0.000016
PRE-LIM FRICTION FACTOR (fj)	-	0.01343	0.01299
DARCY FRICTION FACTOR 1 (fd)	-	0.01345	0.01304
DARCY FRICTION FACTOR 2 (fd)		0.01345	0.01303
DARCY FRICTION FACTOR 3 (fd)		0.01345	0.01303
DARCY FRICTION FACTOR (ft)	-	0.00986	0.00874

MINOR HEAD LOSS DUE TO FRICTION

DISCHARGE LINE	**QUANTITY**		
PIPE ENTRANCE	0	0	0
0.75 REDUCER	1	2	2
STANDARD ELBOW 90°	2	60	60
GATE VALVE	2	16	16
STANDARD ELBOW 45°	1	16	16
SUCTION LINE			
PIPE ENTRANCE	1	0.78	0.78
0.75 REDUCER	1	2	2
GATE VALVE	2	16	16
SUM OF EQUIVALENT LENGTHS		112.78	112.78

HEAD LOSS DUE TO LENGTH OF PIPE	m	1.98	0.24
K FACTOR FOR FITTINGS	-	1.11	0.99
HEAD LOSS DUE TO FITTINGS	m	1.48	0.34
COMBINED HEAD LOSS DUE TO FRICTION	m	3.46	0.58

TOTAL DYNAMIC HEAD - CLEAR WATER

POTENTIAL HEAD	m	10	15
PRESSURE HEAD	m	0	0
VELOCITY HEAD	m	1.33	0.35
TOTAL DYNAMIC HEAD	m	14.79	15.93

HEAD CORRELATION - ZANDI & GOVATIS

INDEX NUMBER	-	1120.8	467.2
EXCESS PRESSURE CORRELATION	-	1.16	1.10
SLURRY SYTEM HEAD	m	15.35	15.99

HEAD CORRELATION - DURAND CONDOLIS WORSTER

FROUDE NUMBER	-	16.50	2.05
EXCESS PRESSURE CORRELATION	-	1.02	1.03
SLURRY SYTEM HEAD	m	14.86	15.95

HEAD CORRELATION - WILSON, ADDIE, CLIFT SIMPLIFIED APPROX. METHOD

STRATIFICATION RATIO EXPONENT	-	1.98	3.48

LINE VELOCITY @ 50% SUSPENDED SOLIDS	m/s	1.65	1.19
SOLIDS EFFECT ON PRESSURE GRADIENT	m/m	0.013	0.003
HYDRAULIC GRADIENT OF MIXTURE	m/m	0.359	0.062
SLURRY SYSTEM HEAD	m	14.92	15.97

NET POSITIVE SUCTION HEAD REQUIREMENTS

ATMOSPHERIC HEAD	m	10.33	10.33
VAPOUR PRESSURE HEAD	m	0.326	0.326
STATIC HEAD	m	0.3	0.3
LENGTH OF SUCTION LINE	m	2.7	2.7
MINOR FRICTION LOSSES	m	0.002	0.000
NET POSITIVE SUCTION HEAD (AVAILABLE)	m	9.70	9.70

PUMPING POWER REQUIREMENTS

HEAD RATIO CORRECTION	-	0.937	0.994
ABSORBED POWER (ZANDI)	kW	20.80	37.46
MOTOR SERVICE FACTOR	-	0.91	0.80
ABSORBED POWER (DURAND)	kW	20.14	37.38
MOTOR SERVICE FACTOR	-	0.94	0.80
ABSORBED POWER (WILSON-ADDIE)	kW	20.22	37.41
MOTOR SERVICE FACTOR	-	0.94	0.80

PUMP

DIAMETER OF PUMP IMPELLER	mm	386	386
PUMP EFFICIENCY	%	65	65
BELT DRIVE GEARBOX EFFICIENCY	%	95	95
COUPLING TRANSMISSION EFFICIENCY	%	95	95
MOTOR EFFICIENCY	%	95	95
MOTOR DRIVE EFFICIENCY	%	70	70
INSTALLED MOTOR POWER	kW	19	30

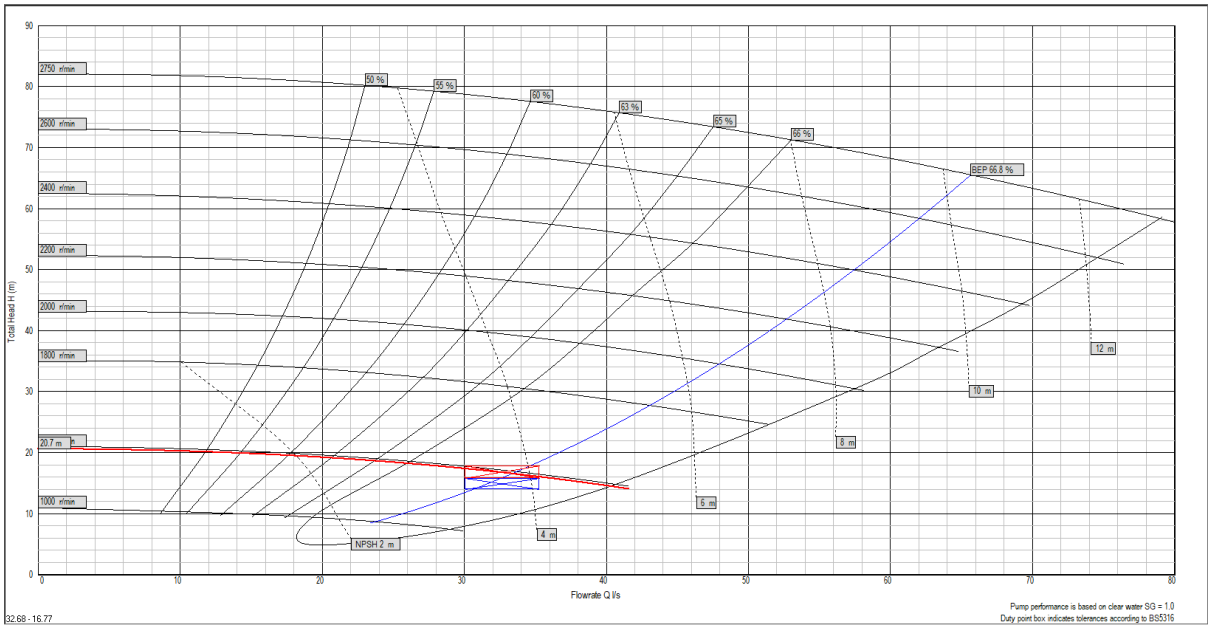

Figure L-1: Pump Curve for the Mill Discharge Underflow Sump Pump in the Wet Ball Mill Circuit

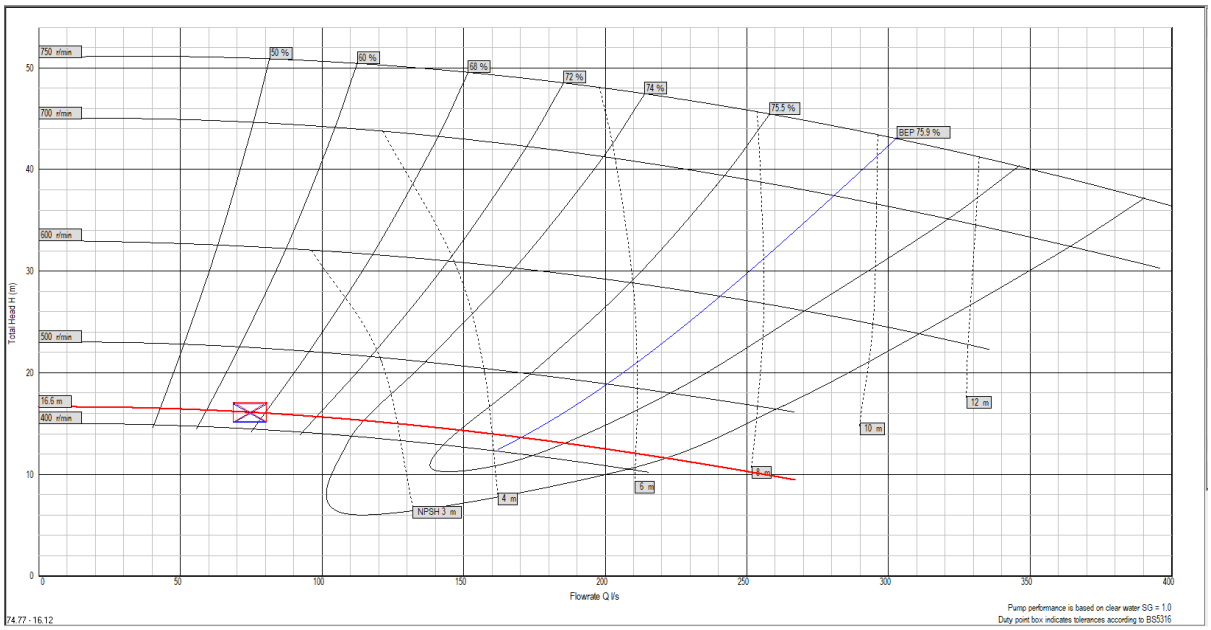

Figure L-2: Pump Curve for the Reagent Feed Tank Discharge Pump for the Wet and Dry Milling Circuit

Appendix M: Drawing Symbols and Equipment Abbreviations

Table M-1: Drawing Symbols

Equipment Names		Instrumentation - 1st Letter		Other Instrumentation	
Sym.	**Description**	**Sym.**	**Description**	**Symbol**	**Description**
FE	Feeder	L	Level	M	Motor or magnetic flowmeter
CH	Chute	T	Temperature	VSD	Variable speed drive
CV	Conveyor	X	Position	DOL	Direct on-line
WT	Weightometer	H	Motor	I	Interlock
SI	Silo	S	Alarm	FC	Fail close
SU	Sump	W	Weight	FO	Fail open
PP	Pump	P	Pressure	FL	Fail last
ML	Mill	D	Density	S	Solenoid
HD	Hydraulic power pack	F	Flow	SP	Spray water
SC	Screen	**Instrumentation - 2nd or 3rd letter**		I/A	Instrumentation air
ZM	Other equipment	**Sym.**	**Description**	**Valves**	
CY	Cyclone	T	Transmitter	**Symbol**	**Description**
TK	Tank	E	Element	VCH	Manual check valve
AG	Agitator	V	Valve	VGA	Manual ball valve
BM	Belt magnet	A	Alarm	VDI	Manual diaphragm vlave
MD	Metal detector	C	Closed	VKG	Manual knife gate valve
FA	Fan	O	Open	VBA	Manual ball valve
CL	Chiller	Q	Quantifier	VBF	Manual butterfly valve
BE	Bucket elevator	H	High		
SX	Stack	L	Low		

Appendix N: Carbon Steel Pipe Sizes

Table N-1: Carbon Steel Pipe Sizes

Nominal Bore (NB)	Outer Diameter (OD) (mm)	Wall Thickness (mm)
6	10.3	1.73
8	13.7	2.24
10	17.1	2.31
15	21.3	2.77
20	26.7	2.87
25	33.4	3.38
32.0	42.2	3.56
40	48.3	3.68
50	60.3	3.91
65	73	5.16
80	88.9	5.49
90	101.6	5.74
100	114.3	6.02
125	141.3	6.55
150.0	168.3	7.11
200	219.1	8.18
250	273	9.27
300	323.8	9.52
350	355.6	9.52
400	406.4	9.52
450	457.2	9.52
500	508	9.52
550	558.8	9.52
600	609.6	9.52

Appendix O: Gas Pycnometer SG Measurement Procedure

The procedure that was followed to determine the specific gravity of the limestone is listed below.

- 100 g of the limestone sample was split from the bulk sample using a rotary splitter (refer to Figure J-3 and Figure J-4 in Appendix J).
- The grinding vessels were cleaned and the limestone was placed in the gaps between the grinding vessel rings (refer to Figure J-8 in Appendix J)
- Once filled, the grinding vessels were placed in the 6 Pot Swing Mill (refer to Figure J-7 in Appendix J).
- The mill was switched on and left to grind for 10 minutes before the mill was switched off and the pulverized limestone was removed (refer to Figure J-9 in Appendix J).
- A sub-sample of the pulverized limestone sample was then removed and placed into the sample chamber of the Gas Pycnometer (refer to Figure J-10 in Appendix J) to determine the SG of the limestone.